A COASTAL ENGINEERING STUDY OF SHOALING IN OCEAN CITY INLET

by

Robert G. Dean, Marc Perlin and William R. Dally

Ocean Engineering Report No. 19
July 1979

DEPARTMENT OF CIVIL ENGINEERING
UNIVERSITY OF DELAWARE
NEWARK, DELAWARE

A COASTAL ENGINEERING STUDY

OF

SHOALING IN OCEAN CITY INLET

by

Robert G. Dean, Marc Perlin and William R. Dally

Ocean Engineering Report No. 19
Sponsored by Baltimore District, U.S. Army Corps of Engineers

July, 1979

TABLE OF CONTENTS

TABLE OF CONTENTS
(Continued)

TABLE OF CONTENTS
(Continued)

TABLE OF CONTENTS
(Continued)

LIST OF FIGURES

LIST OF FIGURES
(Continued)

LIST OF FIGURES
(Continued)

LIST OF FIGURES
(Continued)

LIST OF FIGURES
(Continued)

LIST OF TABLES

COASTAL ENGINEERING STUDY

OF

OCEAN CITY INLET, MARYLAND

I. ADVANCED SUMMARY

This study was conducted to determine the cause of the shoaling occurring in the navigational channel through Ocean City Inlet and to develop recommendations to alleviate the shoaling, see Figure 1 for location of shoal. The study included field and office programs and entailed hydrographic measurements and examination and interpretation of the available historical information.

The results identify the flow of sand over, around and through the inshore portion of the south jetty as a principal source of the shoal material. This transport of sand to the shoal area can be described as occurring as a combination of infrequent events (when the south jetty was flanked) and also in a more continuous manner when wave and tide conditions cause high uprush. Crude measurements have shown that the quantities transported in the more continuous mode through the jetty are of the same order of magnitude as the more recent (1972-1977) required annual dredging. It appears that if the south jetty is flanked for a period of several months, the flood currents can cause up to 250,000 yd^3 of sand to be transported around the south jetty and to be deposited in close proximity to the navigational channel. This deposit represents a source of material which is later reworked by waves propagating through the inlet and by ebb tidal currents and redeposited in the navigational channel. A portion of this material is jetted seaward by the ebb currents where a shoal of approximately 8,000,000 cubic yards volume has been built since the formation of the inlet.

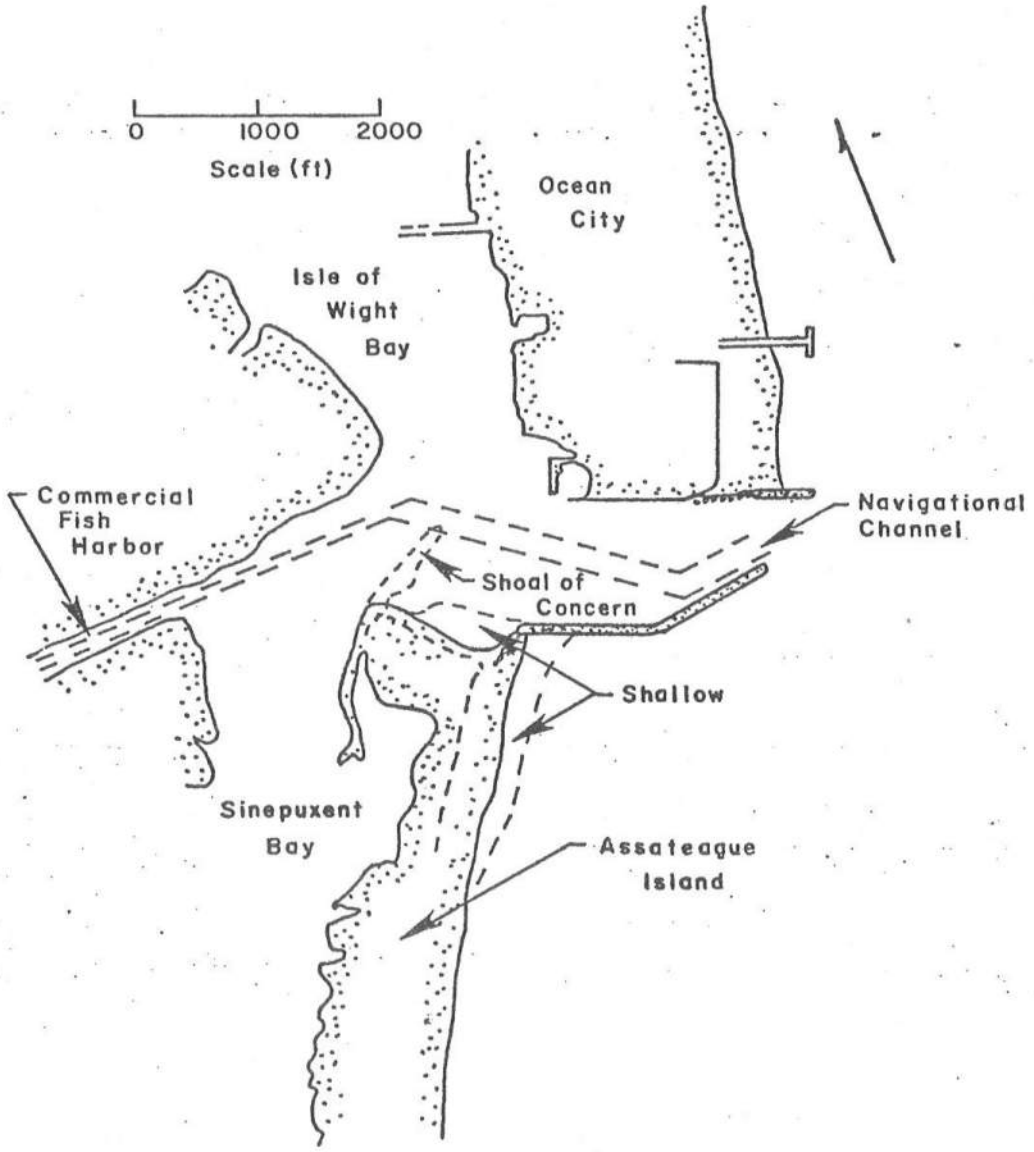

Figure 1. Ocean City Inlet, Adjacent Bays, and Shoal of Concern.

It is also important to note that material transported past the south jetty represents a loss of sand from and an associated erosion of Assateague Island.

In view of the cause of shoaling discussed above, the obvious remedial measure is to modify the inshore portion of the south jetty so that it is sand-tight. This will require a) a better tie-in of the jetty to Assateague Island, in particular extending the jetty landward, b) raising the jetty crest from the present design elevation of 4.7 ft. above Mean Sea Level (MSL) to an elevation more consistent with the natural berm elevation (approximately 7-8 ft. above MSL), and c) rendering the jetty impermeable to sand transport, especially over the inshore section where most of the sand transport is believed to be occurring. At present, the required annual dredging quantities appear to be decreasing because the volume of sand deposited in close proximity to the navigational channel during the last flanking of the jetty (1961-1962) has been diminished by erosion and dredging. It should be recognized that if the remedial action is not taken, the consequences will be a) continued erosion of Assateague Island and, b) the high probability that a major flanking of the south jetty will occur during the next ten years, leading to requirements for repair and initial extensive dredging to restore the channel followed by an increased annual dredging requirement for a number of years.

II. SCOPE OF STUDY

In December 1975, the Baltimore District of the U. S. Army Corps of Engineers contracted with the Civil Engineering Department of the University of Delaware to carry out a coastal engineering investigation to determine the cause of and identify recommended remedial measures to alleviate a shoaling problem inside Ocean City Inlet, Maryland, see Figure 1. Very briefly, the required dredging volumes have increased from approximately 7,500 yd^3/yr between 1948 to 1963 to approximately 77,000 yd^3/yr in 1973. Figure 2 presents the dredging history through 1977. In part, this increase in required dredging may be due to the trend of larger (and deeper draft) vessels requiring deeper channels which tend to shoal faster, but other factors are also considered to be of major significance. It is noteworthy that since 1973 the required dredging rate has decreased.

This report describes a combined office and field study to identify the causes of the problem and to recommend solutions. The office study consisted of evaluation of the history of the inlet from available reports, dredging records, surveys, aerial photography and current and tide measurements, discussions with Corps' personnel and other information. In addition, a numerical (computer) model was developed to represent flows and tidal elevations in the vicinity of the inlet and in Isle of Wight Bay to the North and Sinepuxent Bay to the South. The field study included concurrent tide measurements inside and outside of the inlet, current measurements, bathymetric surveys, beach profiles and sand tracer studies.

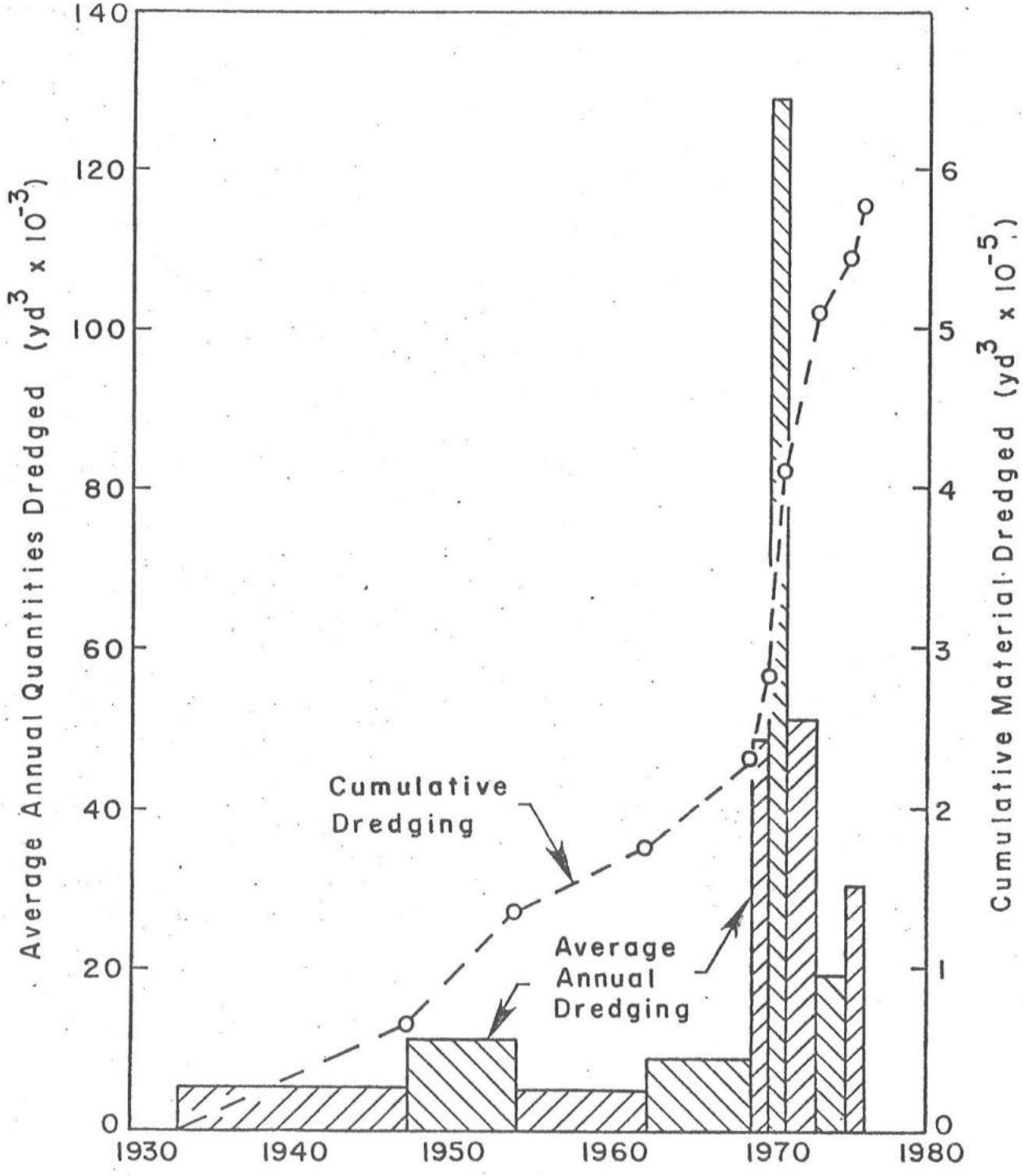

Figure 2. Average Annual and Cumulative Channel Dredging History in Area of Interest, 1933-1977.

III. BACKGROUND

Brief History of Ocean City Inlet

In August of 1933, a hurricane opened an inlet through the barrier beaches of Fenwick and Assateague Islands. Previously, inlets had been cut by other storms, but these had closed due to natural sediment processes. Congress had already authorized an inlet to be constructed approximately five miles south of the new inlet; however, this project had not begun. After reviewing the situation, Congress authorized stabilization of the new inlet.

The north jetty construction began in September of 1933 and by October of 1934, a structure 1520 ft. in length had been completed, 1100 ft. of which had a top elevation of +4 ft. mean low water (MLW). See Figure 3 for the characteristics of the inlet and jetties. The last 420 ft. of the north jetty was an "apron-like" structure which was at a lower elevation.

Construction of the south jetty was initiated in October, 1934 and completed in May, 1935. This jetty consisted of a 750 ft. section parallel to the north jetty throughout which the inlet had a width of approximately 1100 ft. Progressing seaward, the south jetty alignment trended toward the north resulting in a decrease in inlet width from 1100 ft. to a width of 600 ft. The third section of the south jetty was also constructed parallel to the north jetty but at a distance of 600 ft. with a length of 530 ft. The top elevation was +6 ft. MLW except for the seaward-most 360 ft. of which 160 ft. made the transition from +6 ft. MLW to the "apron" height. The remaining 200 ft. maintained the apron height.

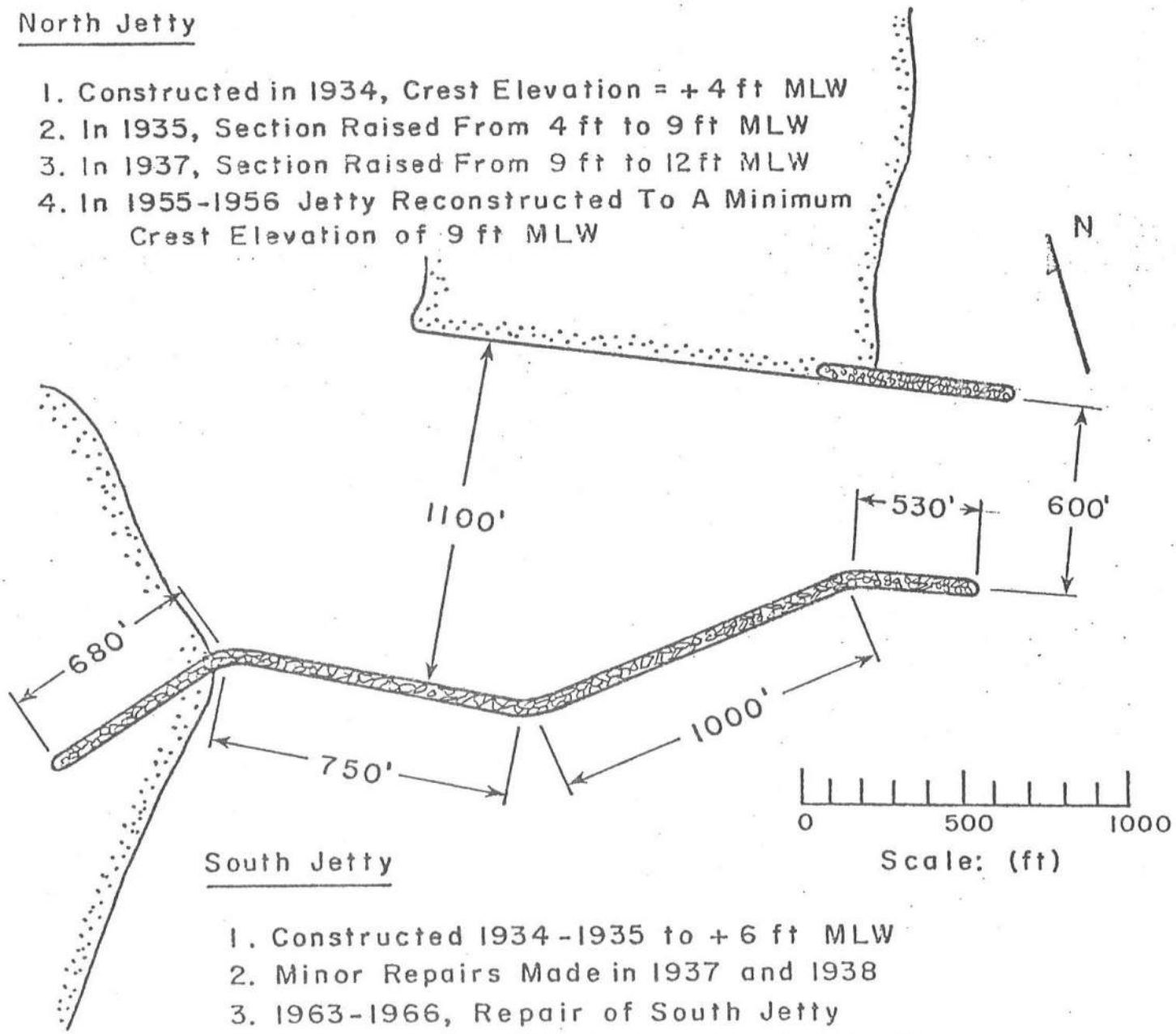

Figure 3. Dimensions and Chronology of Jetty Construction and Maintenance at Ocean City Inlet.

The dredging of the inlet was completed in August 1935 to a controlling depth of 8.5 ft. MLW. The channel was 200 ft. wide and was cut so that it was centered in the seaward portion of the inlet. In December of that same year, Commercial Fish Harbor was also dredged.

In 1935, and again in 1937, in order to prevent sand from entering the inlet from the north, it was necessary to raise the inshore portions of the north jetty. The construction in 1937 had elevated the first 100 ft. section of jetty (out from the boardwalk) to a height of 12 ft. above MLW.

Deterioration of the north jetty occurred and by 1954, the outermost section of the jetty was in such poor condition that its average height was one foot below mean low water. Reconstruction of the north jetty during 1955 and 1956 increased the elevation to +9 ft. MLW over the section which originally had been +4 ft. MLW. The first maintenance dredging of the channel was not required until 1948 even though significant deterioration of the north jetty had occurred prior to that time. However, the channel did migrate and deepen in certain sections of the inlet.

The south jetty, which was completed in 1935, required minor repairs in 1937 and 1938 and, in 1956, further work was necessitated by a breach in the inshore section of the jetty. Erosion of Assateague Island continued at an approximate rate of 35 ft/yr., and by October 1961 this erosion had resulted in flanking of the south jetty. This required an addition in 1963 to the south jetty extending landward 680 ft. in the southwest direction. Also, a 720 ft. section was repaired starting 1300 ft. seaward from the original landward jetty end.

IV. SEDIMENT TRANSPORT PROCESSES

In addressing the sediment transport processes which are relevant to Ocean City Inlet, it is helpful to first consider the section extending from Cape Henlopen, Delaware to Fishing Point, Virginia followed by an examination of the processes of importance in the immediate vicinity of Ocean City Inlet.

Cape Henlopen, Delaware to Fishing Point, Virginia

This section extends from the northern extremity at Cape Henlopen, Delaware at the entrance to Delaware Bay south to Fishing Point, Virginia at the entrance to Chincoteague Bay. This shoreline is approximately 70 miles in length and is dominantly a barrier island with several Pleistocene headlands near the northern end. The barrier is only broken by two inlets: Indian River Inlet and Ocean City Inlet approximately 13 and 33 miles south of Cape Henlopen respectively. The predominant deep-water wave energy is from the northeast (see Figure 4) and one might expect the net sediment transport to be from north to south along the entire shoreline. However, Delaware Bay and the associated shoals exert a strong influence on the waves from the northeast and result in a net northward longshore sediment transport in the Cape Henlopen-Indian River Inlet area. There are two effects, each of which diminishes the effects of the northeast waves; these are: (1) sheltering by the shoals off Cape May, and (2) refraction whereby those waves which are propagated across the shoals are refracted by the deeper channel entrance and tend to be guided into Delaware Bay. The effect of this net northward transport is evident by the northward prograding tip of Cape Henlopen[3][4] and by the accretion fillet on the south jetty of Indian River Inlet. Farther south, the

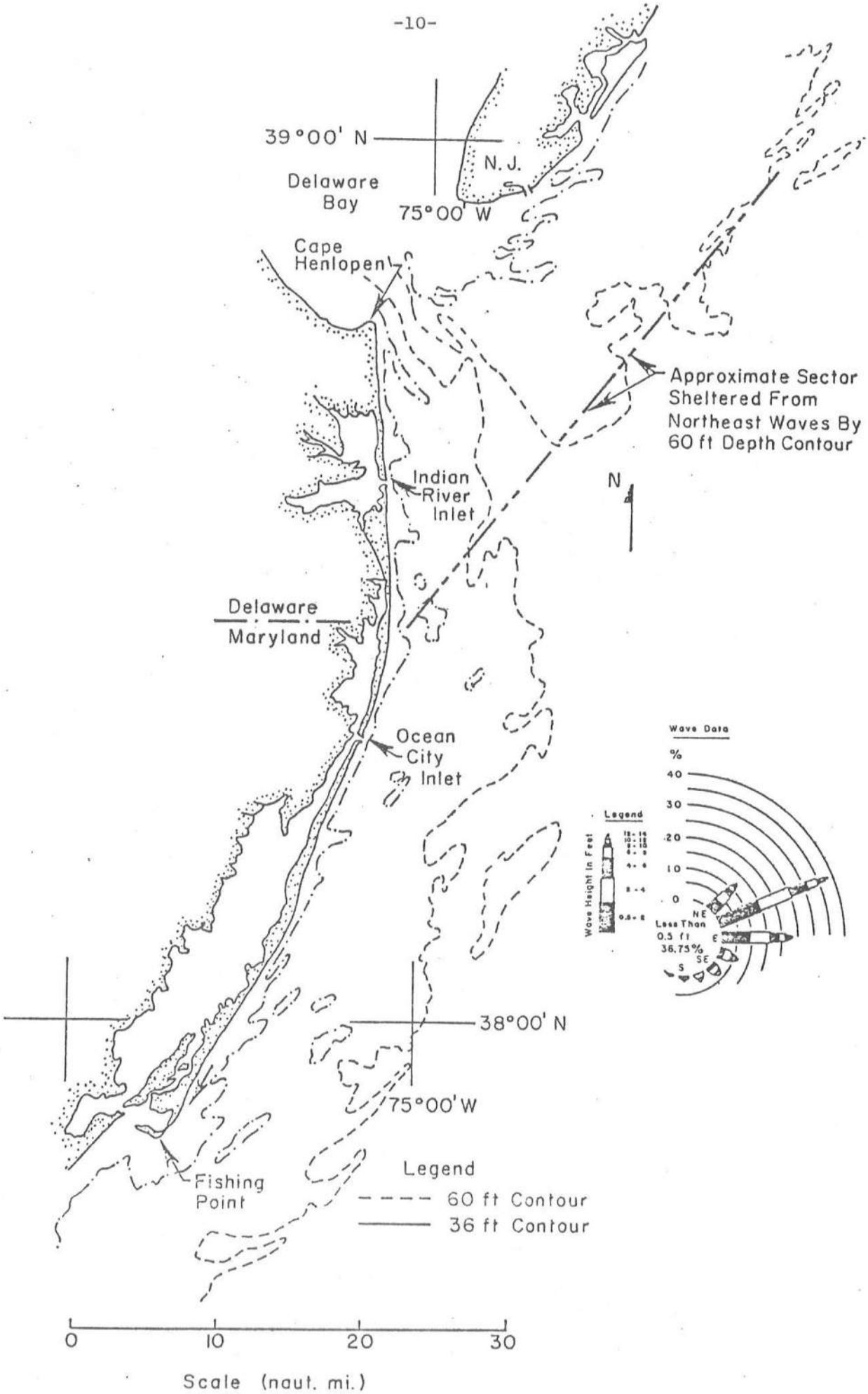

Figure 4. Influence of Shoals Off Cape May in Reducing Wave Action Along Northern Segment of Shoreline, Cape Henlopen to Fishing Point.

"sheltering" effect of Delaware Bay is reduced and the net transport is toward the south. It is interesting to question where the "balance" or "nodal" point is located for the net longshore sediment transport and Bethany Beach has been identified as the nodal point in at least one reference[8]. Actually, it would be quite surprising if the nodal point remained fixed month to month or even on a yearly basis. Rather our knowledge of the annual variability of storm directions and the amount of material that can be transported by a single major storm would suggest that the nodal point location could vary substantially on an annual basis. Moreover, trends in winds and the resulting waves could conceivably result in fairly long-term changes in the location of the nodal point. It is clear that the net annual drift is consistently toward the north at Indian River Inlet and that the net annual drift is toward the south at Fishing Point although this is to be expected since the same processes causing a net transport toward this tip of the barrier are operative as were discussed at Cape Henlopen. In the vicinity of Ocean City Inlet, there is believed to be a net southerly transport; however, the actual amount occurring in any one year or the average for a series of years could differ both in magnitude and direction.

Sediment Transport Processes in the Vicinity of Ocean City Inlet

The net longshore sediment transport is believed to be about 150,000 to 200,000 cubic yards per year to the south at Ocean City Inlet. This is based on the rate of impoundment of the north jetty following construction. Surveys conducted before the north jetty was constructed and two years later indicate that 296,000 cubic yards of material (148,000 cubic yards annually) were impounded within 1800 ft. north of the north jetty. It is also believed that a considerable quantity was being trans-

ported over the north jetty. (The jetty crest elevation at that time was 7 ft. above MLW). From December 1934 to November 1947, an annual average of 36,000 cubic yards was impounded north of the jetty. The remaining annual volume of 112,000 cubic yards was believed to be bypassing the north jetty into the inlet where it is carried bayward and landward and finally deposited. Figure 5 which shows the advancement and recession at the north and south jetties, respectively with time supports the concept that the north jetty is impounded to capacity and that any net transport now arriving at the inlet is bypassing this structure. It is not clear that in the period 1934 to 1947, an average of 76% of the net material arriving at the north jetty would be bypassed. It is plausible that some of the accreted fillet adjacent to the north jetty was due to bar material moving ashore, and sheltering (wave trapping) by the entrance channel.

The Coastal Engineering Research Center (CERC) has collected Littoral Environmental Observation (LEO) data at the Assateague State Park located some 8 miles south of Ocean City Inlet. These data, extending over the years 1973, 1974 and 1975, interpreted as longshore sediment transport, were kindly provided by CERC and are summarized as follows. The data indicate a strong net southerly longshore transport. Figure 6 presents the monthly mean net transport rates and the monthly ranges for the three years. It is seen that only in January is the average transport to the north. The average annual net transport based on these data is 264,000 yd^3 to the south. The gross transport rates are presented in Figure 7 and amount to an annual average of 649,000 yd^3. The annual southward and northward transport rates determined from these figures are 456,500 yd^3 and 192,500 yd^3, respectively. These quantities are believed to be somewhat too large for the Ocean City Inlet area and the difference may be due in part to the increasing distance south from the postulated nodal point near Bethany Beach.

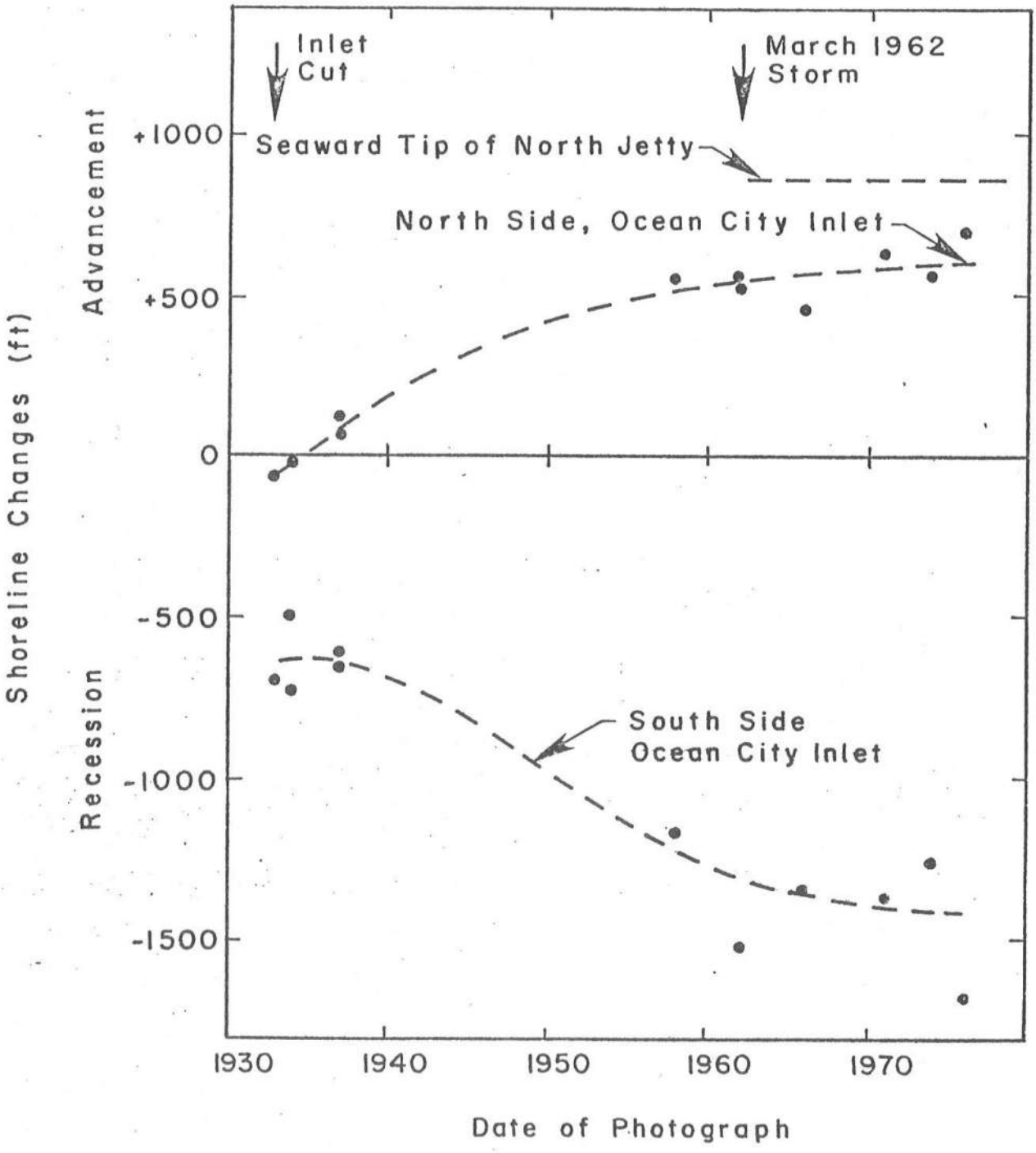

Figure 5. Variations in Locations of North and South Shorelines Immediately Adjacent to Jetties, Based on Aerial Photography.

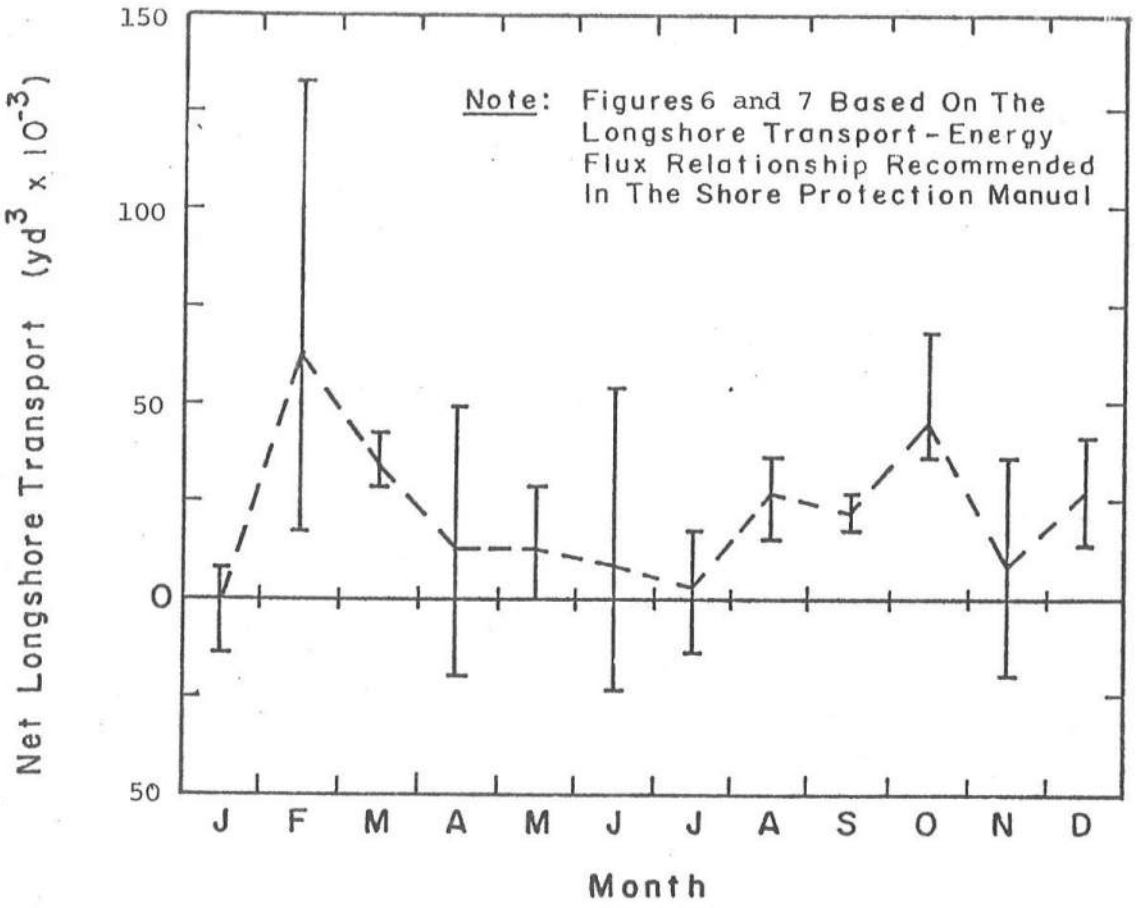

Figure 6. Averages and Ranges of Net Longshore Transport, Assateague Island, Based on LEO Data for the Years 1973, 1974 and 1975.

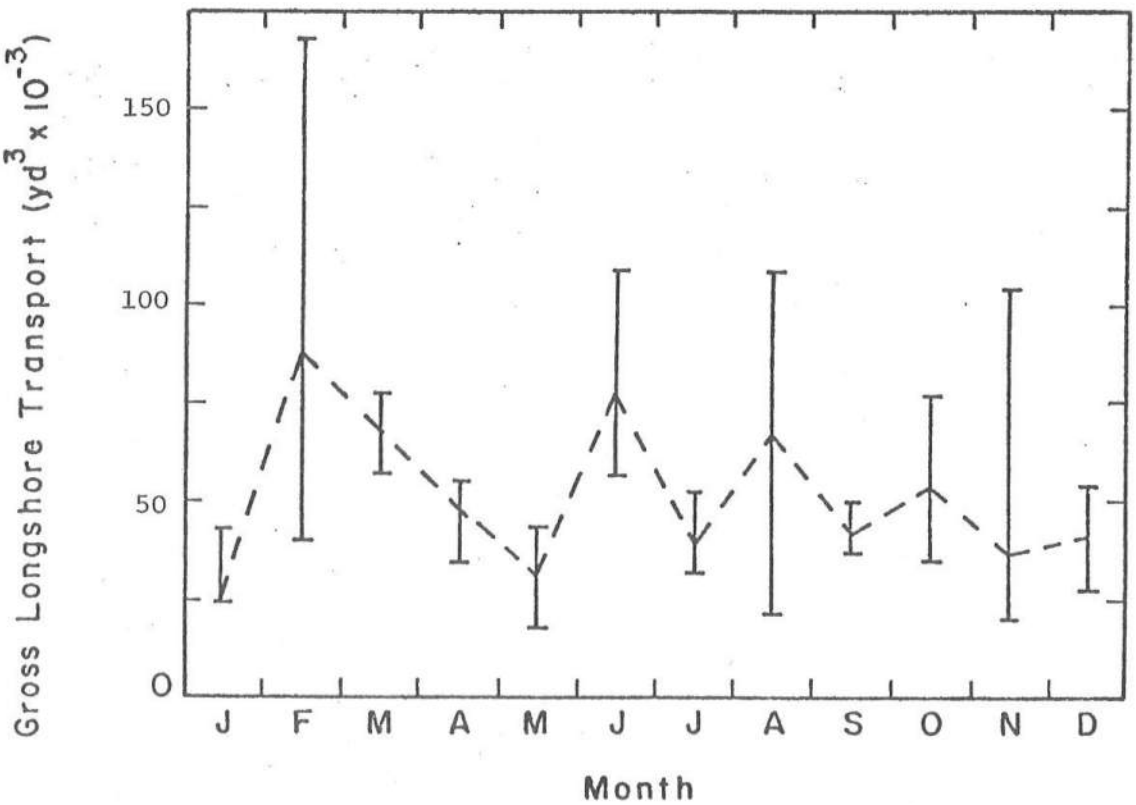

Figure 7. Averages and Ranges of Gross Longshore Transport, Assateague Island, Based on LEO Data for the Years 1973, 1974 and 1975.

Sediment Budget Analysis

In order to better understand the magnitudes of the sand transport components in the vicinity of Ocean City Inlet, an attempt was made to conduct a sediment budget analysis. This was based in part on available National Ocean Survey (formerly the U. S. Coast and Geodetic Survey) and U. S. Geological Survey Charts. The analysis included the following components: (a) The fillet impounded at the north jetty, (b) the bay shoals accumulated due to the inlet's presence, (c) the extensive ebb shoal located approximately three-quarters of a mile offshore of the inlet, (d) sediment losses associated with the recession of the ocean shore of Assateague Island, (e) sediment gain associated with the westward displacement of the bay shoreline of Assateague Island, and (f) the upward growth of Assateague Island as a result of sea level rise. The main components of the sediment budget are the recession of the ocean shoreline and associated displacement westward of the bay shoreline and the offshore shoal. A diagrammatic sketch of the sediment budget components is presented as Figure 8.

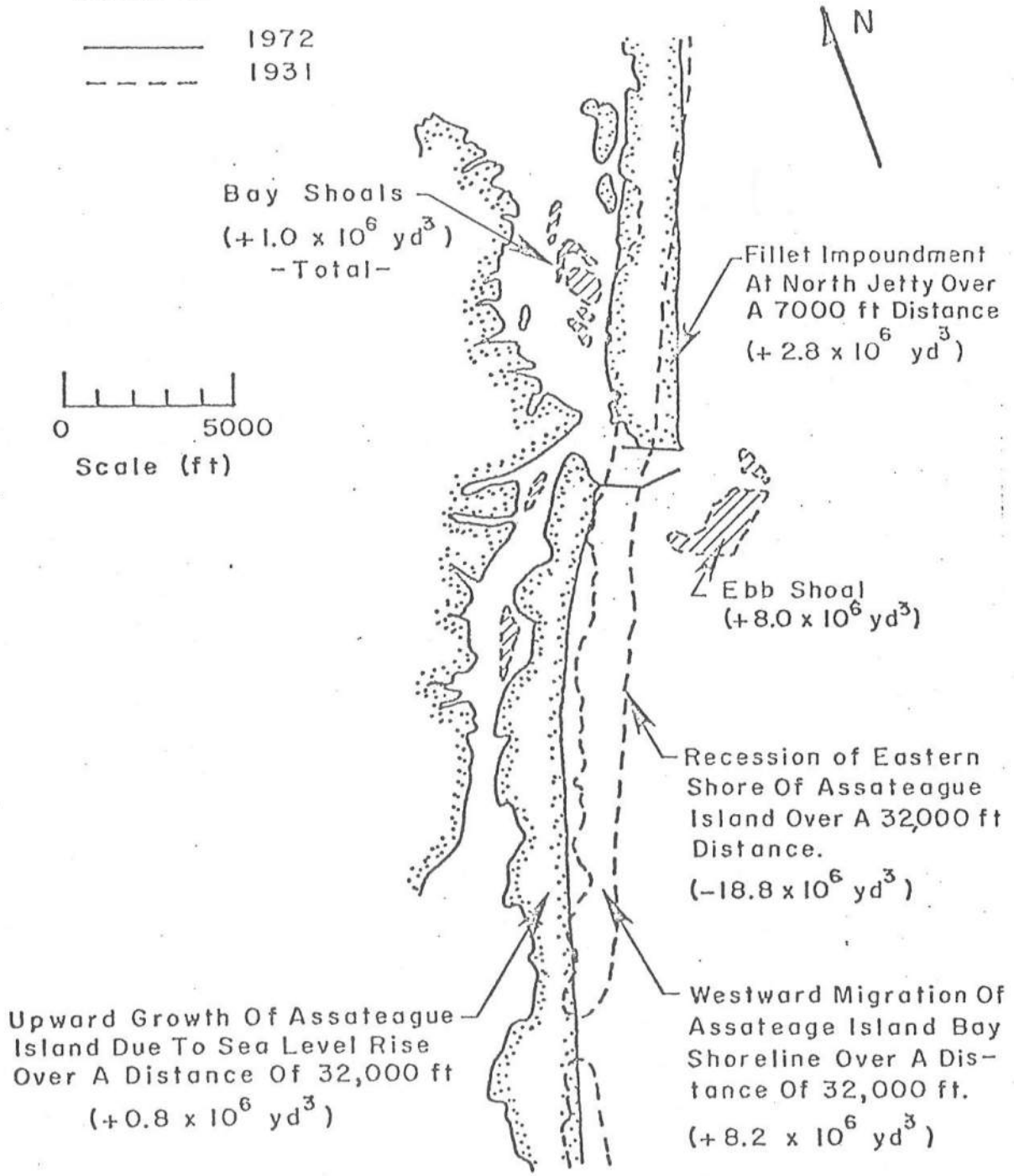

Figure 8. Components of Sediment Budget Analysis.

V. FIELD STUDIES

A number of field studies were conducted to collect the necessary data. The information obtained established the hydraulic and sedimentary processes in the vicinity of the inlet and in conjunction with the office study enabled the determination of the probable causes of shoaling of the navigation channel.

Tidal Measurements

Prior to the first major field trip, in which a bathymetric survey was to be carried out, it was necessary to install tide gages on both the ocean and the bay sides of the inlet. After securing permission, the ocean side tide gage was installed on the fishing pier which extends out approximately 350 ft. into the ocean and is situated 1200 ft. north of the north jetty. The inside tide gage was installed at the Coast Guard Station Harbor, see Figure 9. Each gage consisted of a stilling-well secured by chains to adjacent piles with a float/cable system running up the well to a Stevens strip chart recorder. The installation of these two gages was completed on June 8, 1976. Two typical tide records for the ocean and bay sides of the inlet (July 15, 1976 and August 4, 1976) are shown in Figures 10 and 11. In Figure 12, an eight day tide record is shown. This record began on July 19, 1976. Also included is a tabulation of tidal range ratios (Table I) obtained from the tide gages.

Bathymetric Survey

With the tide gages installed, the bathymetry survey was conducted on June 10-11, 1976. A fathometer was mounted on a small boat which traversed the offshore and bay areas until sufficient definition was provided

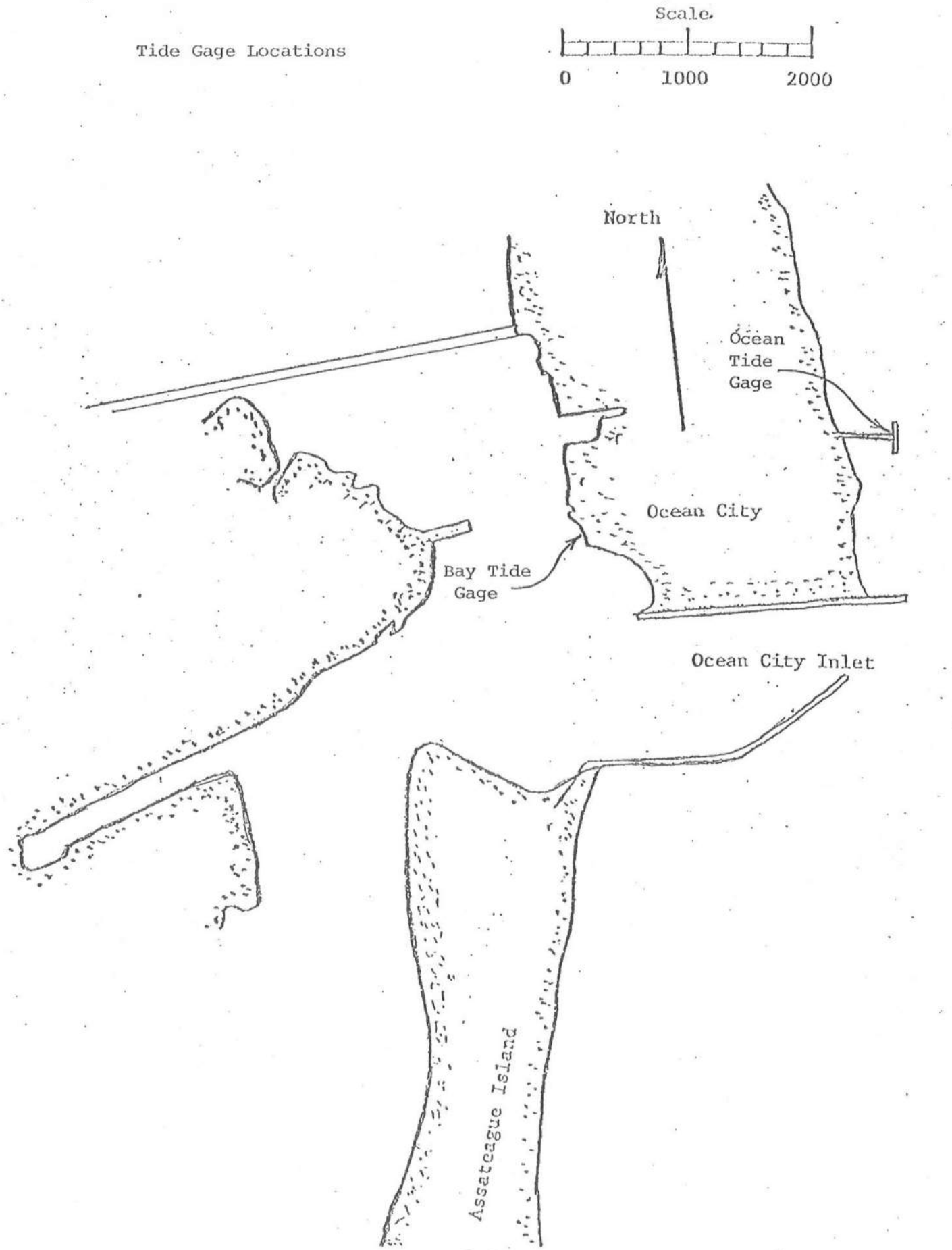

Figure 9. Locations of Tide Gage Installations.

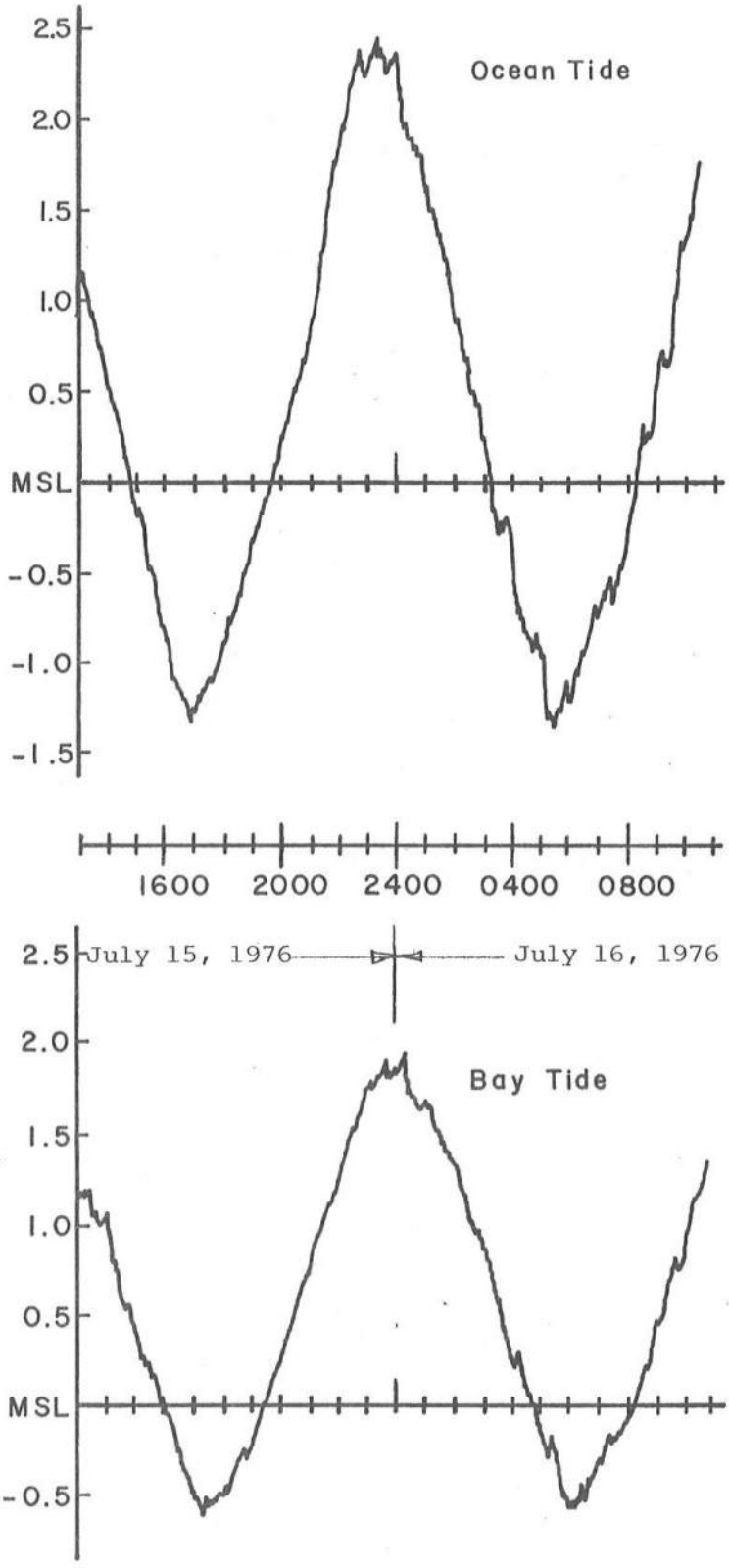

Figure 10. Sample Ocean and Bay Tide Records, July 15-16, 1976.

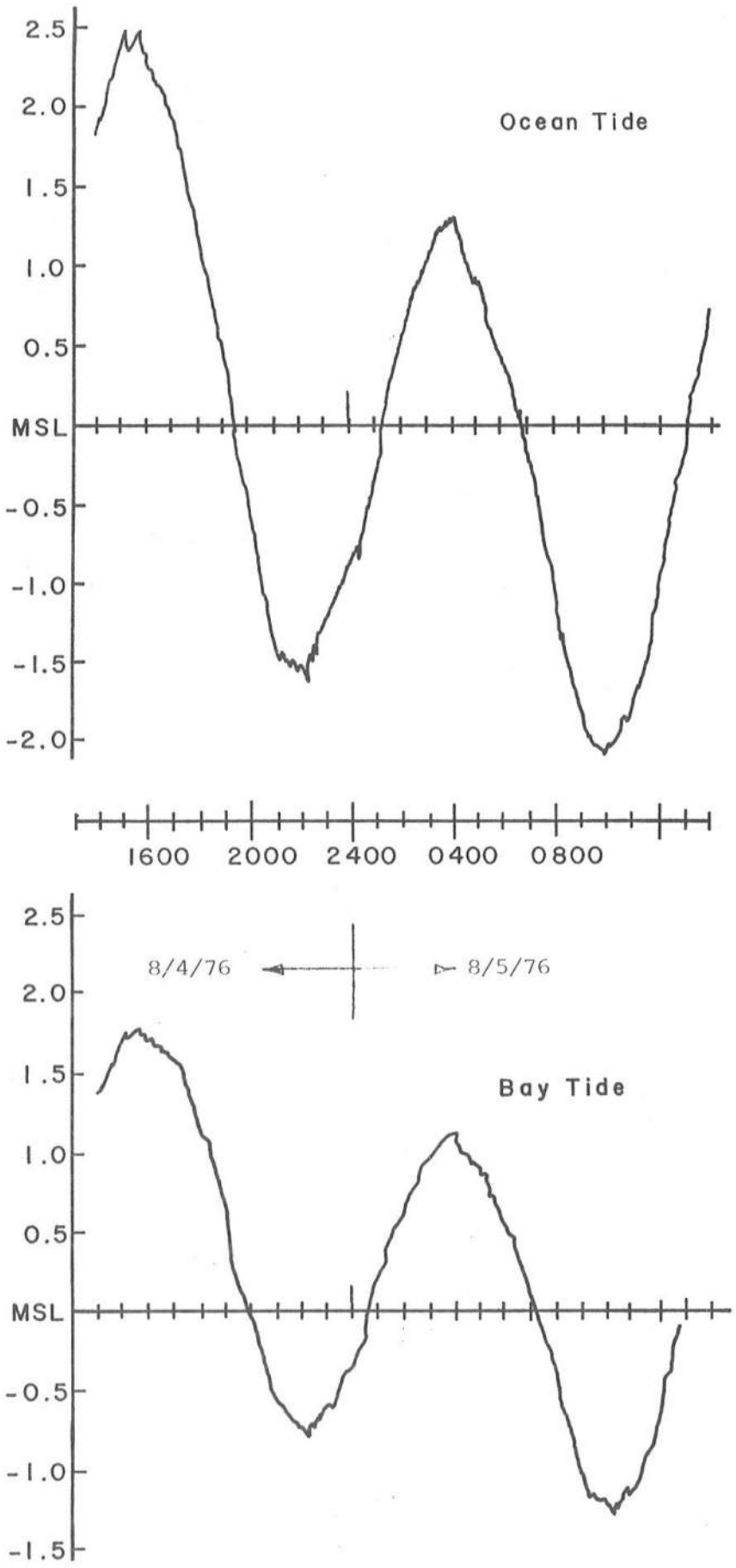

Figure 11. Sample Ocean and Bay Tide Records, August 4-5, 1976.

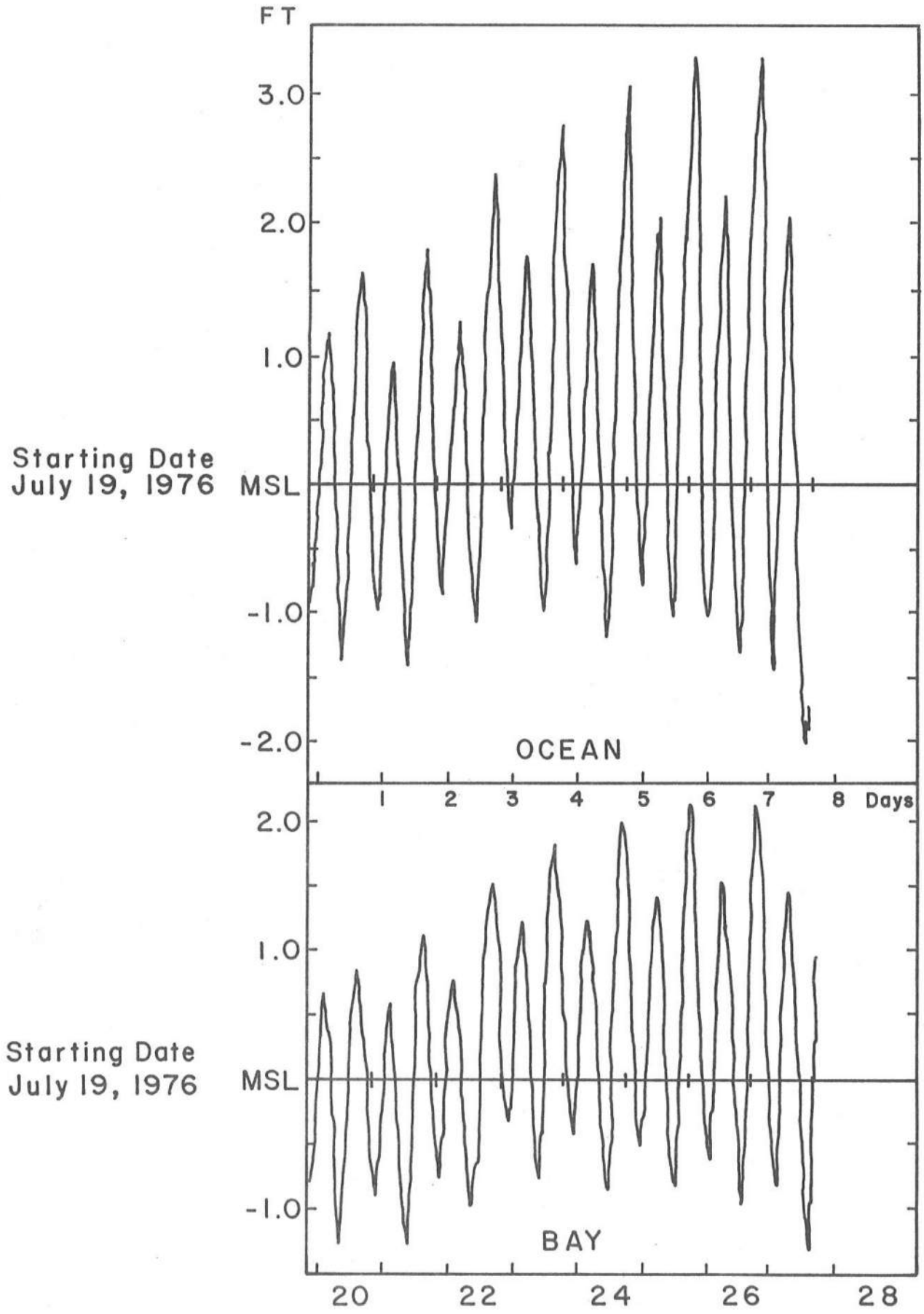

Figure 12. Sample Ocean and Bay Tide Records, July 19-26, 1976.

TABLE I. TABULATION OF TIDAL RANGE RATIOS

Date	Ocean Range, R_O (ft.)	Bay* Range, R_B (ft.)	Ratio: R_B/R_O
6/25/76	4.20	2.80	0.67
7/8/76	5.02	3.45	0.69
7/13/76	4.60	3.15	0.68
7/14/76	3.73	2.54	0.68
	4.26	2.83	0.66
	4.14	2.67	0.64
7/15/76	3.80	2.24	0.59 ← min.
	3.27	2.57	0.79
	3.30	2.54	0.77
8/4/76	4.04	2.54	0.63
to	3.95	3.19	0.81 ← max.
8/5/76	3.35	2.37	0.71

*Measured at Coast Guard Station, see Figure 9.

to construct a reasonably accurate depth chart. The boat personnel included one boat operator and an individual tending the fathometer. At frequent intervals, the boat operator communicated by radio to two transit operators who took horizontal angle measurements at the same time that a mark was placed on the fathometer chart. Thus, by knowing the locations of the transits, it was possible to determine the horizontal position of the boat for each reading. Several different transit base locations were needed to cover the entire area which was sounded. These locations are presented in Figure 13. The total area covered was approximately 1.2 square miles with soundings off Assateague extending 1 mile offshore and off the Ocean City Beach varying between 0.5 and 0.75 miles. Inside the inlet, the survey extended 1800 ft. southward into Sinepuxent Bay and 2000 ft. northward into Isle of Wight Bay*. The measured depths were transferred to a chart and contoured; the contoured version of the survey results is contained in the jacket of the rear cover of this report.

Beach Profiles and Leveling

Concurrent with the soundings another field crew measured beach profiles. Profiles were measured at 18th, 16th, 15th, 14th, between 13th and 12th, 11th, 10th, 9th, 6th, 4th and 2nd Sts., along with Surf Avenue, Division Street, Talbot Street, Somerset Street, and two profiles extending out from the Municipal Parking Lot just north of the north jetty. Each profile line was backsighted to a permanent reference. Elevations were then taken at regular intervals along the beach and at any marked change in beach slope. After completing the profiling, the survey crew, starting with the

*The areas in each of the bays and extending slightly into the inlet were not sounded on this initial field trip, but were sounded on July 19, 1976. The positions of the transit locations for this latter date are also shown on Fig. 13.

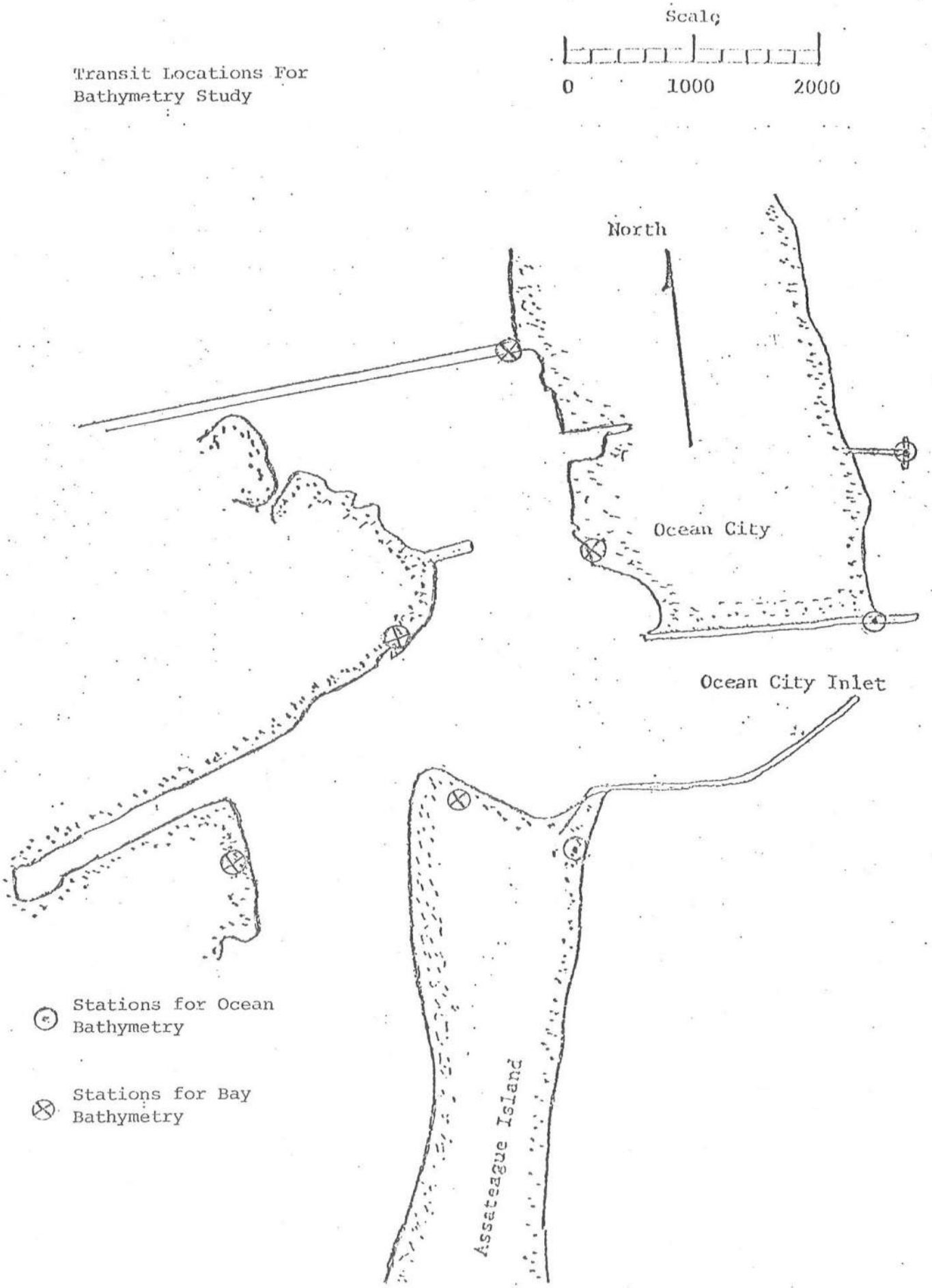

Figure 13. Locations for Shore Transit Stations Used in Bathymetric Survey.

U.S.C.G.S. elevation marker on the north jetty, proceeded to tie-in the elevations of the backsights for each of the profile lines. Once this had been accomplished, they leveled between the tide gages and the bench mark.

After this first major field trip, numerous shorter trips were undertaken and many different types of data were collected. Portions of each kind of data were collected on separate trips so that rather than reporting chronologically, the remainder of the field study will be reported according to relevant data obtained.

Aerial Photography

On 27 June 1976, aerial color photographs were taken of the area. The area included approximately 3500 ft. seaward and 6000 ft. landward of the jetty tips and 2.5 miles to the north and 3 miles to the south of the inlet making the total 10.4 square miles. These photos show areas of recent erosion or accretion and when compared to earlier photos show trends in the various shoreline changes that have taken place.

Current Data

Inlet currents were measured on June 25 and again on July 14, 1976. On the first occasion, measurements of both speed and direction were attempted. The current velocities were measured by timing a drogue attached to a line of known length. The direction which the drogue was displaced by the currents was to be determined by triangulation; however, due to the visual obstructions caused by boat traffic, etc., this method did not prove feasible for determining direction. Therefore, on the second field trip to measure currents, no attempt was made to obtain accurate current directions.

The data were taken at Stations A, B and C as depicted in Figure 14. The drogue was simply an orange float attached to a substructure of two "L"-shaped aluminum sheet metal pieces attached corner-to-corner to form an object which moved easily along with the current. The current data obtained at each station on both occasions are presented in Table II and Figure 15.

In addition to the current data in the immediate vicinity of the inlet, a program was carried out to define the general tidal characteristics of the bays comprising the inland water system. Tide staff readings were taken during tidal cycles on July 14, 1976 and later on August 6, 1976 in the Isle of Wight, Sinepuxent, and Assawoman Bays. The locations of the stations for August 6, 1976 are shown in Figure 16. In the first tide study the locations were such that they could be reached by automobile in order to cover the almost 14 mile traverse with short enough intervals between readings to obtain useful data. However, the second study was carried out with one boat taking readings in the Isle of Wight and Assawoman Bays, while a second boat conducted readings in Sinepuxent Bay. Working in this fashion, tide and current readings were taken over the complete tidal cycle enabling sufficient data to be obtained. These data were also used to calibrate a numerical model and establish its validity and will be discussed more completely in Appendix II. With the validity of the numerical model established, the complete hydraulics of the bay system up to the mouth of the inlet were better understood. The tide and current data have been graphed and are presented in Figures 17 and 18.

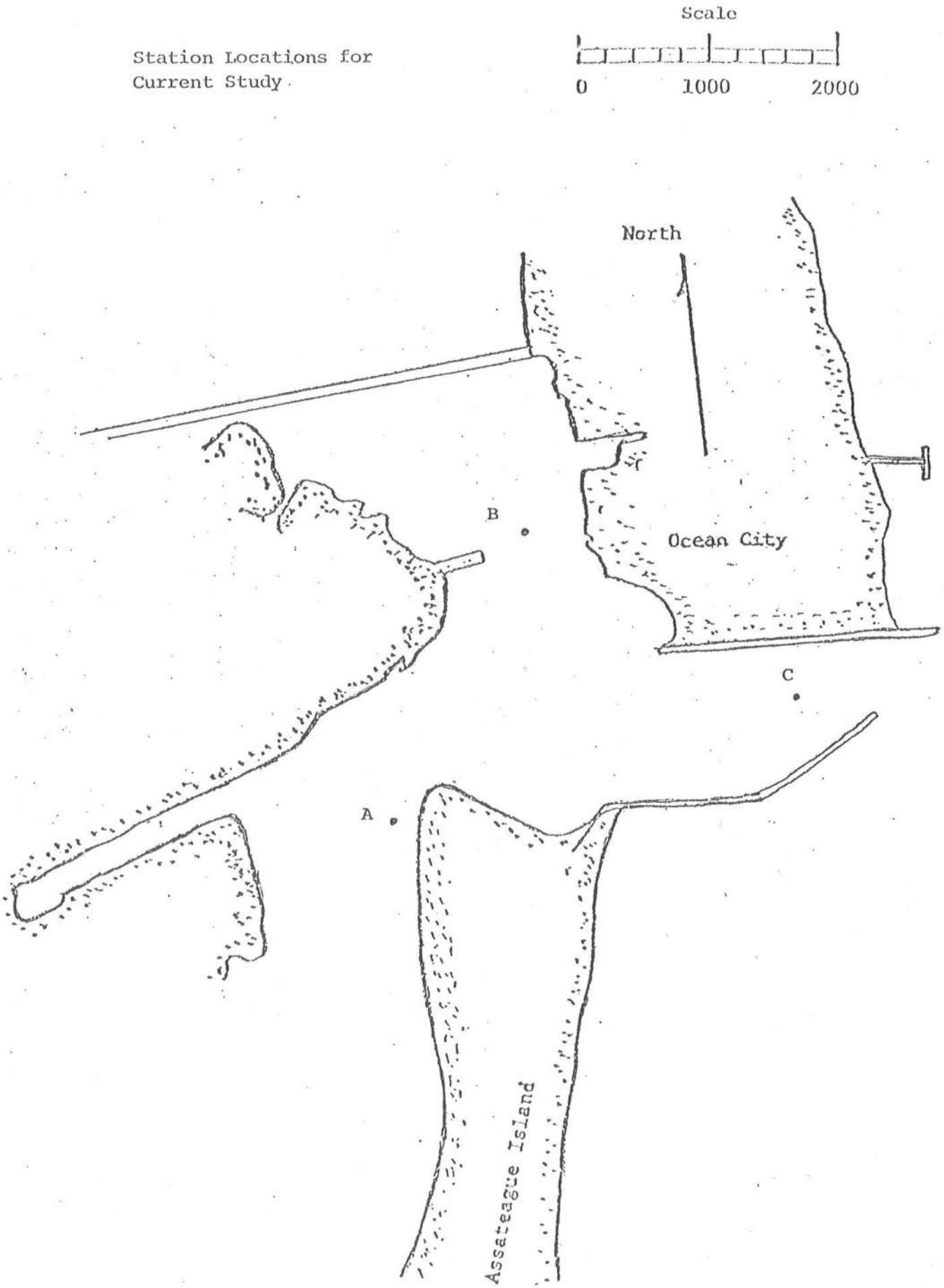

Figure 14. Locations of Current Measurements.

TABLE II. CURRENT STUDY IN THE IMMEDIATE VICINITY OF THE INLET

(July 14, 1976)

Station	Time	Velocity* (Ft./Sec.)
A	1045	1.29
B	1016	3.12
C	1028	3.00
A	1204	0.83
B	1133	1.72
C	1147	2.11
A	1305	0.00 (slack)
B	1239	0.68
C	1250	0.60
A	1420	-1.32
B	1340	-2.00
C	1405	-2.68
A	1517	-1.88
B	1440	-3.40
C	1505	-3.26
A	1648	-2.24
B	1611	-3.12
C	1636	-3.41
A	1741	-1.56
B	1711	-2.20
C	1731	-2.83
A	1845	-1.06
B	1827	-1.78
C	1835	-1.56
A	1952	0.00 (slack)
B	1918	0.00 (slack)
C	1942	1.00
A	2058	1.02
B	2025	1.85
C	2040	3.41

*A positive velocity represents flood tide, while a negative velocity is for the ebb tide.

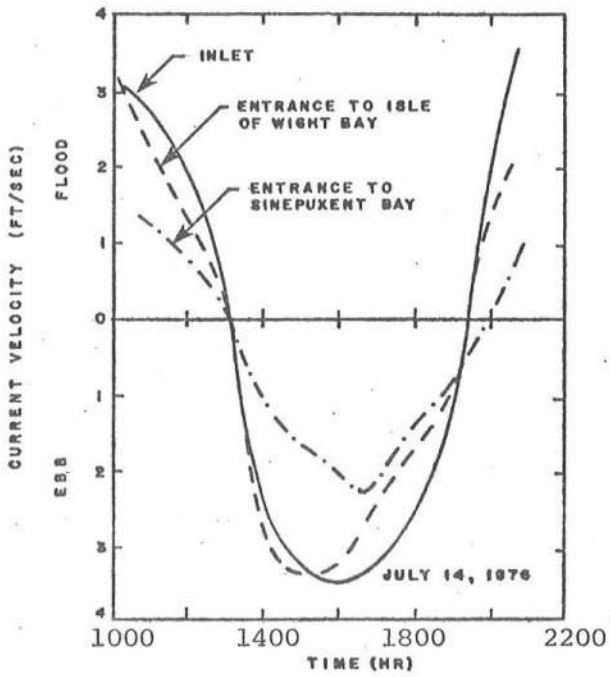

Figure 15. Currents in Immediate Vicinity of Ocean City Inlet.

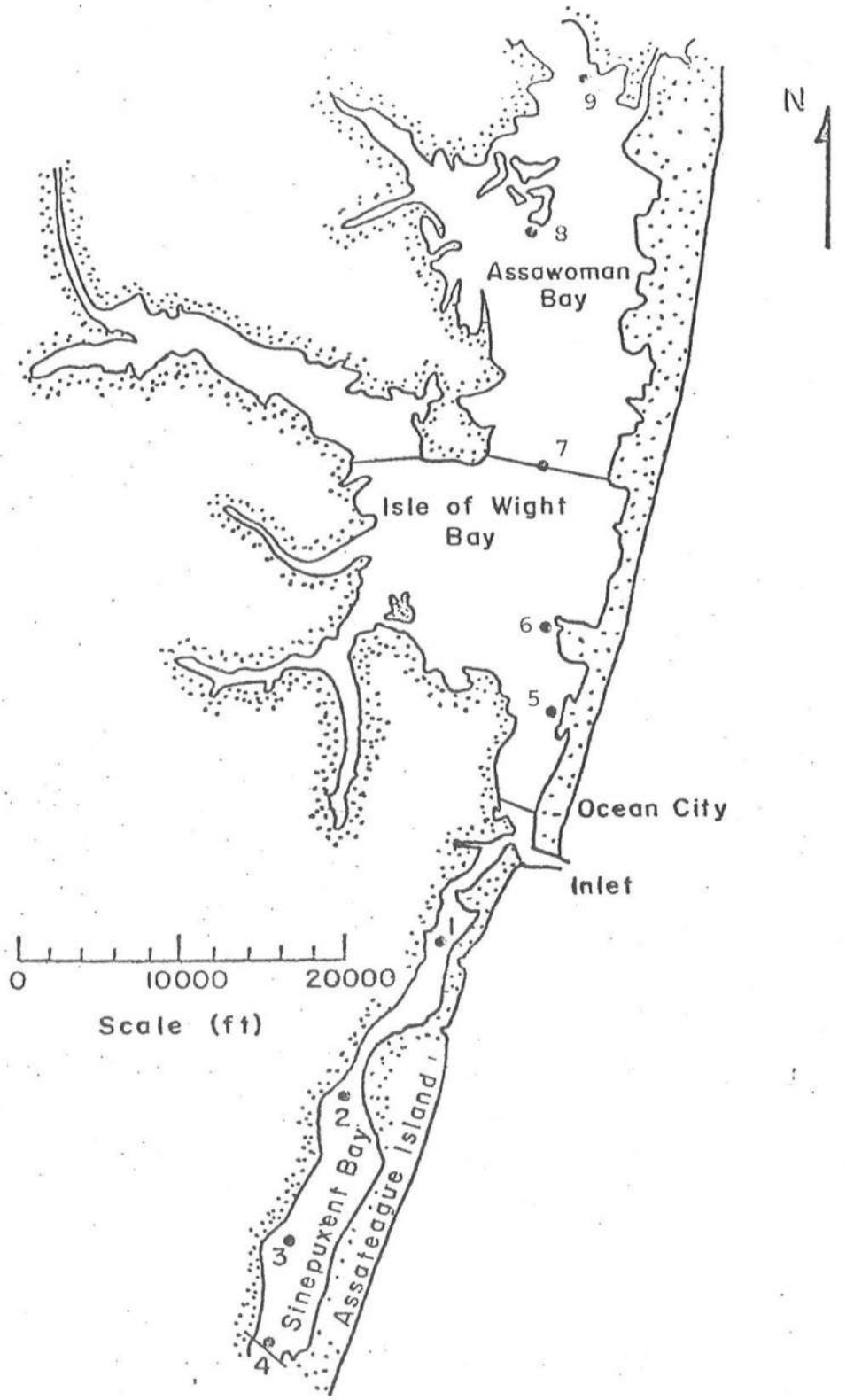

Figure 16. Locations of Tide and Current Measurements Conducted on August 6, 1976.

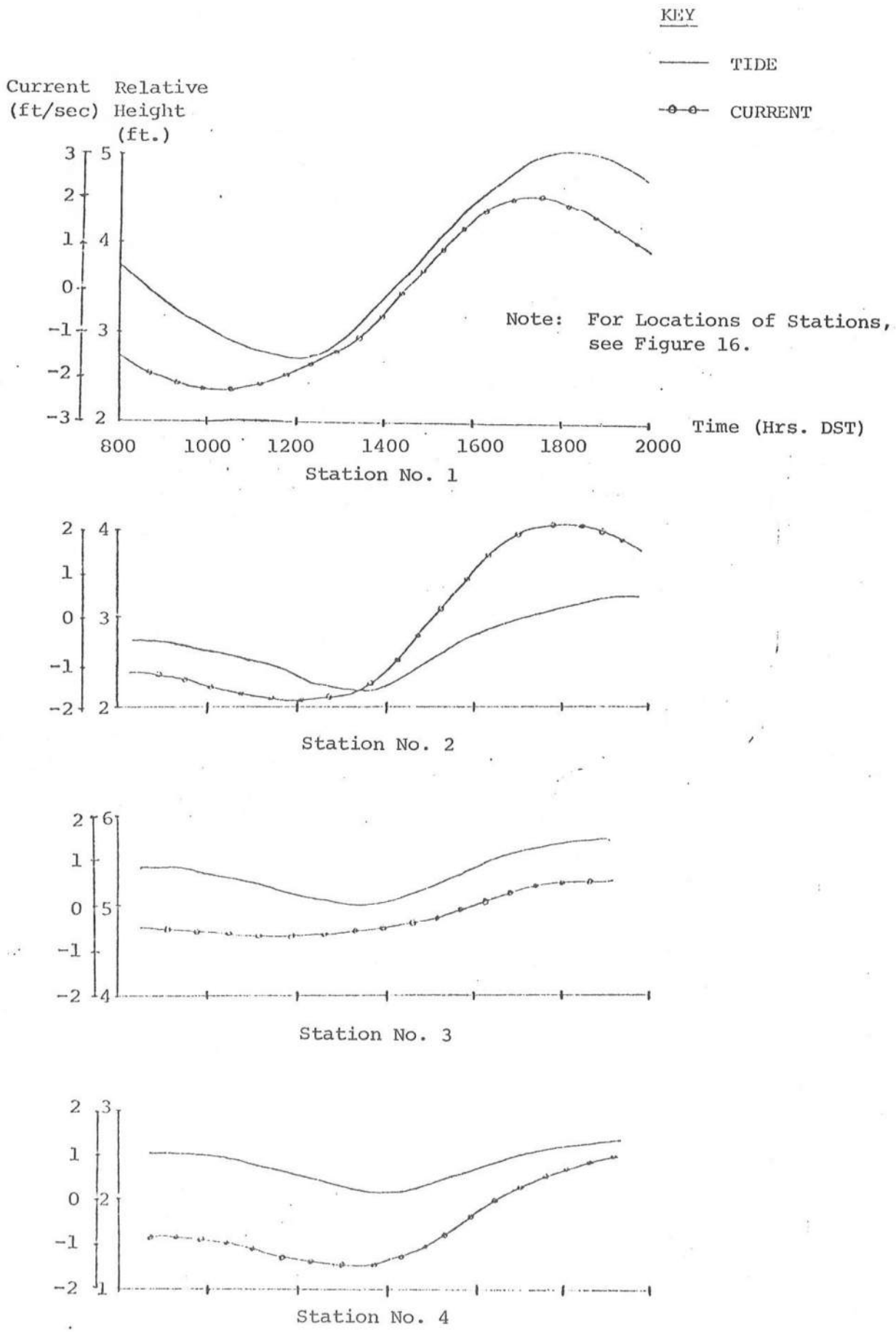

Figure 17. Tides and Currents in Sinepuxent Bay, Measured on August 6, 1976.

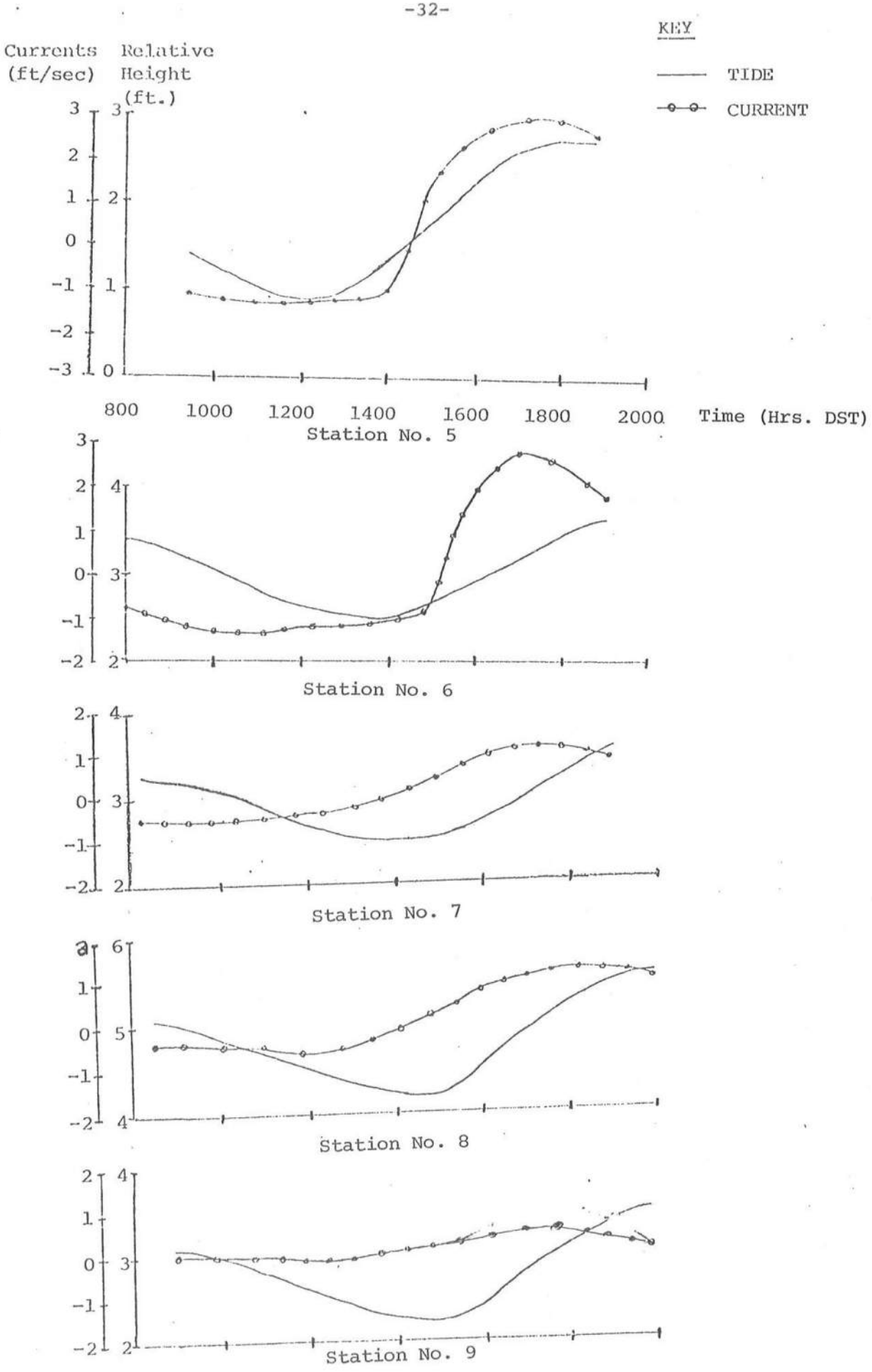

Figure 18. Tides and Currents in Isle of Wight and Assawoman Bays, Measured on August 6, 1976.

Beach Profiles - Assateague Island

To reference repeated beach profiles on Assateague Island, two baselines were established. The original stations were surveyed on June 22, 1976 with additional stations being added as they were needed. The baselines will be presented in later sections where the profiles are discussed. Once the baselines were established, beach profiles were taken at locations of special interest along the northern end of Assateague Island and along the inshore portion of the jetty. Initially, all of the elevations were taken using a bench mark (elevation taken as 0.00) on the extreme inshore section of the south jetty. Later the elevations were referenced to Mean Sea Level (MSL). Berm elevations on the ocean side of Assateague Island were measured on July 7, 1976. At this time only the immediate beach adjacent to the south jetty was surveyed. However, on September 1-3, 1976, beach profiles extending well out into the water and approximately 2700 ft. south were taken.

Sand Tracer Tests

Sand tracer tests on Assateague Island were performed on July 8 and September 7, 1976. These tests were carried out to provide a qualitative determination of whether or not sand was being carried over and through the low lying and permeable south jetty, into the inlet, and continuing to eventually reside in the proximity of the shoal on the northwest corner of Assateague Island. Placement of the tracer sand was on the ocean side of Assateague, just south of the jetty. Figure 19 shows the sampling stations and the times the samples were taken. One hundred and fifty pounds of red fluorescent tracer sand was placed on the beach surface and then fifty pounds of green fluorescent tracer sand was placed at each of three locations. Surface samples were then taken from the stations

SAND TRACING RESULTS

Tuesday, September 7, 1976

#100 Gram Samples

Location	Description	Time	Results Green	Red
1A	Shoreline, Lee of Jetty	1820	3	6
1B	Shoreline, Lee of Jetty	1825	2	7
2A	Near Shore, Lee of Jetty	2035	0	0
2B	Front of Shoal	2040	1	0
2C	Shoal Stake	2045	1	0
2D	Back of Shoal	2050	1	0
2E	Northwest Assateague Waterline, STA4-70	2055	0	0
2F	Northwest Assateague Waterline, STA4+00	2100	3	6

Note: Tracer Placed from 1330 to 1530, September 7, 1976.

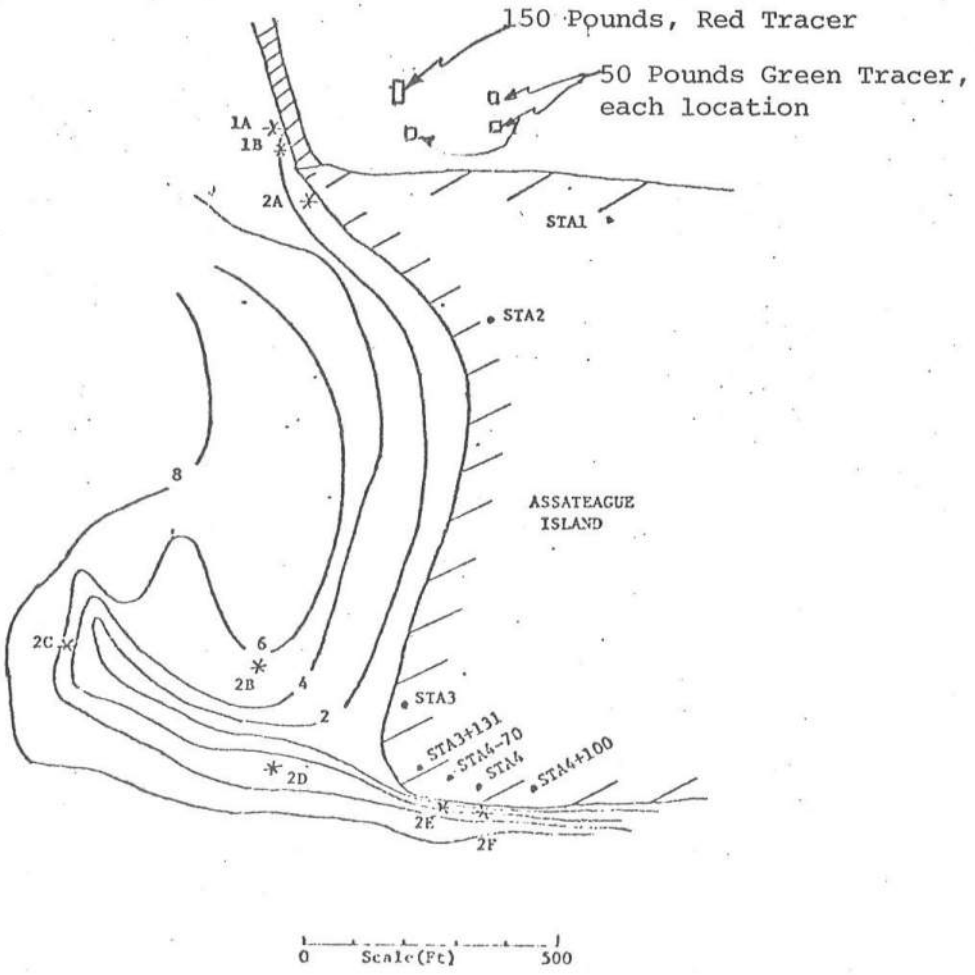

Figure 19. Sand Tracer Studies to Determine Transport Over South Jetty, Injection and Sampling Locations and Results.

and bagged and marked. These samples were dried in the laboratory and 100 gram quantities were taken at random from each bag and inspected under a "black" light in order to reveal the number of fluorescent colored sand grains it contained. These results are included in Figure 19 and demonstrate that sand is being carried from the ocean shore of Assateague Island around to the shoal of concern with a period of three to eight hours.

Swash Transport Measurements

On several occasions during the summer of 1976, sand and water were observed to be carried over the inshore portion of the south jetty during high tides. In an effort to develop a rough quantification of this effect a sediment trap was constructed of 3/8" reinforcing rod and nylon filter cloth. Figure 20 presents the trap dimensions and Figure 21 is a photograph showing the use of the trap. The method of using the trap was as follows. Two persons would carry the trap into an uprush area near to the jetty and would place the trap with the open face toward the uprush. The trap was left in place until a measurable amount of material was collected. The trap and material were then carried to a higher position of the beach where the volume collected was measured and recorded. In addition to volume trapped, the duration of trapping and the wave period and surge depth were recorded. Of course, the trap does cause a substantial interference with the flow and it is relevant to question whether the material trapped is largely due to the disturbance of the trap itself. The individuals involved in these measurements each considered this question independently and each arrived at the conclusion separately that the device "undertraps" rather than "overtraps" sediment. In many cases, it appeared that much of the suspended material did not deposit in the trap but rather a significant portion would be carried over the "sill" at the back of the trap.

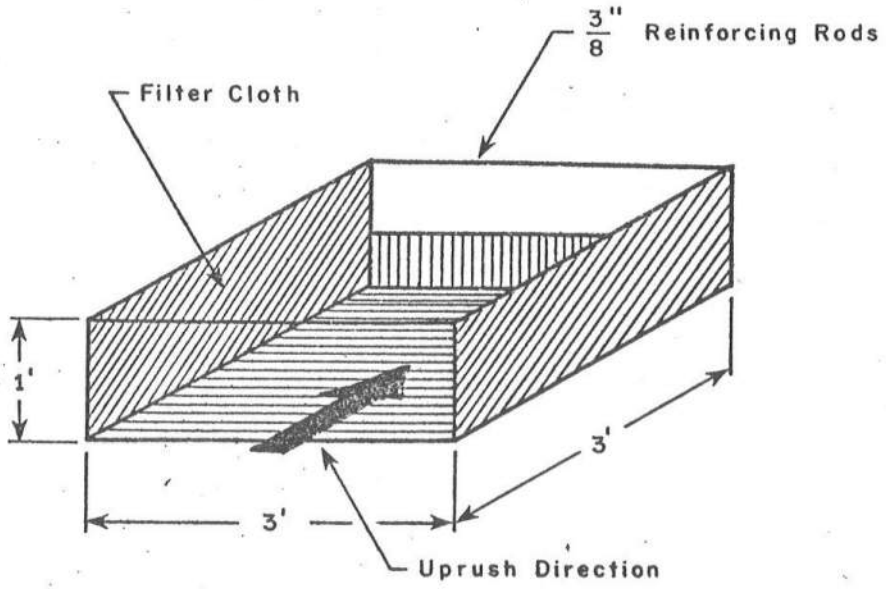

Figure 20. Sediment Trap Used in Measurements of Sand Transported by Wave Swash.

Figure 21. Photograph Showing Use of Sand Trap Looking East From South of South Jetty. Note Channel Transporting Water and Sand to and Through South Jetty.

There was a wide range of rates of sediment trapped with the maximum being a depth of 3/8" of sand on one uprush. One interesting visual observation was that the greatest amount of material appeared to be carried by the surges of intermediate depth. The surges of smaller depth did not appear to be dissipating enough energy to suspend large quantities of sediment. The energy dissipated by the large surges probably occurs predominantly near the water surface and does not penetrate sufficiently deep into the water column to cause a proportional mobilization of the bed particles.

The measurements described above were conducted at various positions on the beach profile ranging from positions where an occasional surge would occur to locations where the water depth was approximately one ft. It is clear though that the permeable conditions of the south jetty combined with the close proximity of the navigational channel to the south jetty results in considerable transport through the jetty in water depths greater than those included in the measurements. The results of two field measurements of swash transport and attempts to translate these measurements into annual quantities transported through the south jetty are presented below.

Swash Measurements, May 31, 1977. These tests were conducted over the peak of the tidal curve and comprised 25 measurements of swash transport. In addition, four measurements were conducted close to the jetty in water depths of approximately one ft. to determine sand transport along the portion of the jetty which is not in the uprush zone. The histograms of transport rates for these two zones are presented in Figure 22. It is of interest that the transport rates in the uprush zone are approximately

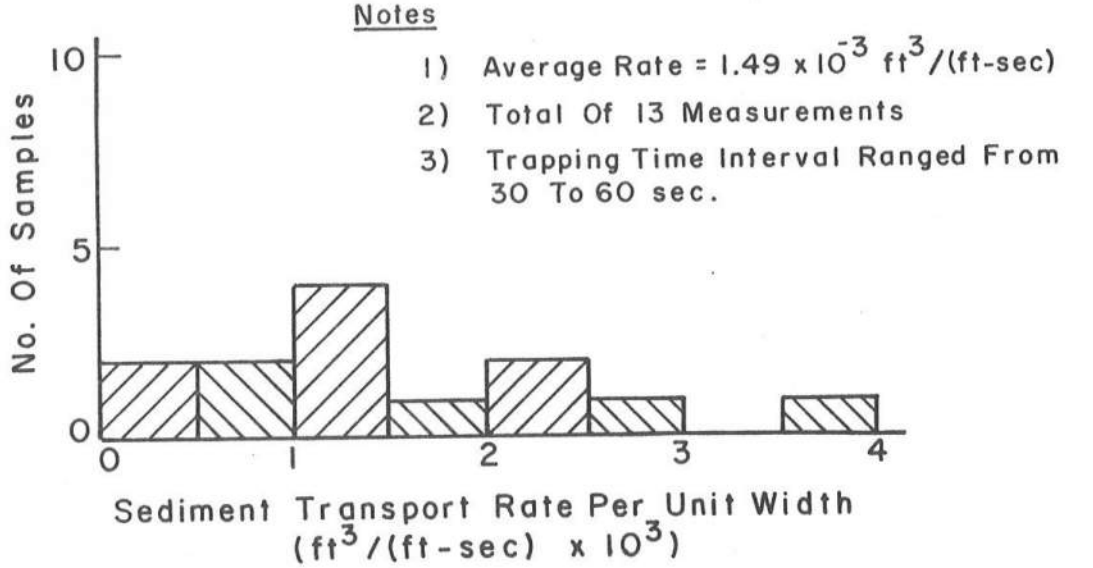

(a) Uprush Zone

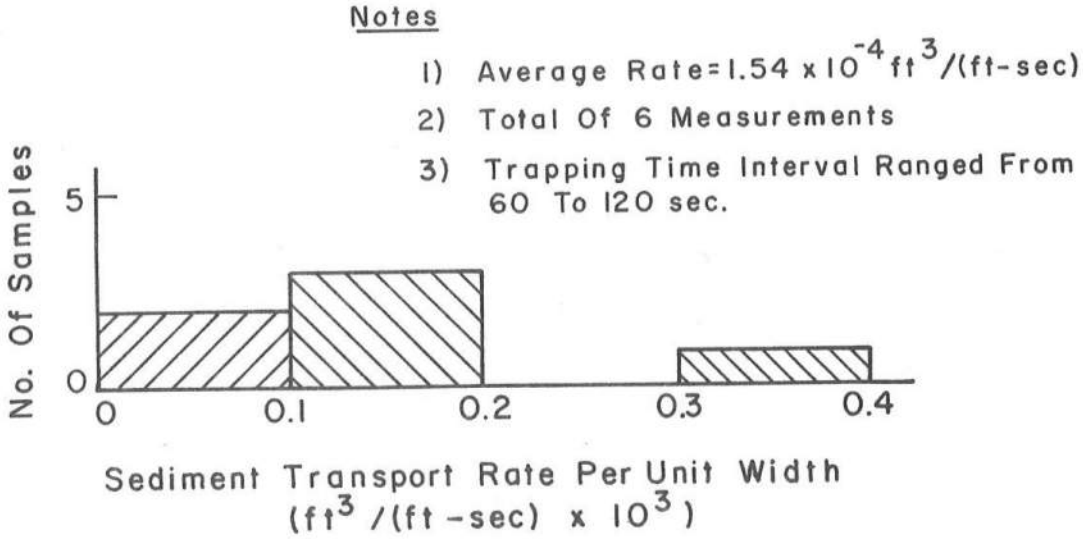

(b) Submerged Zone

Figure 22. Results of Measurements of Swash Zone Transport, May 31, 1977.

one order of magnitude greater than in the submerged zone. It is of relevance to note that the waves occurring during these measurements were considered to be low to moderate and that no overtopping of the south jetty was observed. However, water and sand did flow readily through the south jetty. Also of interest is the observation that a small channel around the landward end of the jetty indicated that minor flanking of the jetty had occurred within several days preceding this field trip.

The data were translated into approximate quantities of sand transported through the south jetty as follows. For the uprush zone, it was considered that sand transport would occur on an average for two hours every tidal cycle and that the zone length was 100 ft. The submerged zone was assumed to be always active and the zone length was also taken as 100 ft. The rates were taken as the average of those obtained in the field tests. These yielded:

Uprush Zone

$$Q_s = \left(\frac{3.35\ ft^3}{3\ ft.\ 750\ sec.}\right) \cdot \left(\frac{2\ hr.}{12.4\ hr.}\right) \cdot \left(\frac{365\ days}{year}\ \frac{24\ hours}{day}\ \frac{3600\ sec.}{hr.}\right) (100\ ft.) \frac{1\ yd^3}{24\ hr.}$$

$$= 28{,}070\ yd^3/yr$$

Submerged Zone

$$Q_s = \left(\frac{0.25\ ft^3}{3\ ft.\ 540\ sec.}\right) \cdot \left(\frac{365\ days}{year}\ \frac{24\ hours}{day}\ \frac{3600\ sec.}{hr.}\right) (100\ ft.) \left(\frac{1\ yd^3}{24\ hr.}\right)$$

$$= 18{,}025\ yd^3/yr$$

for an estimated annual total of $(Q_s)_{TOTAL} \cong \underline{46{,}000}\ yd^3/yr$.

Swash Measurements, June 1, 1977. These tests included 25 measurements in the uprush zone and four measurements in the submerged zone. The histograms of transport rates in these two zones are presented in Figure 23. Estimated annual transport rates based on the average measured results determined as described above are

Uprush Zone:	$Q_s = 19{,}850\ yd^3/yr$
Submerged Zone:	$Q_s = 45{,}420\ yd^3/yr$
Total:	$Q_s \cong 65{,}270\ yd^3/yr$

In evaluating these estimated transport rates, it is very relevant to note that the wave activity was low to moderate on both days. Also where it was necessary to assume quantities, a deliberate attempt was made to select values such that the estimated transport rates would be less than actual. The dominant sand transport over, through and around the south jetty definitely occurs during storm wave activity and high astronomical tides augmented by onshore winds. Although it is difficult to define the confidence associated with estimates of sand transported past the south jetty, the values presented above are believed to be too low due to reasons noted and a more realistic range is probably 100,000 to 200,000 yd^3/yr.

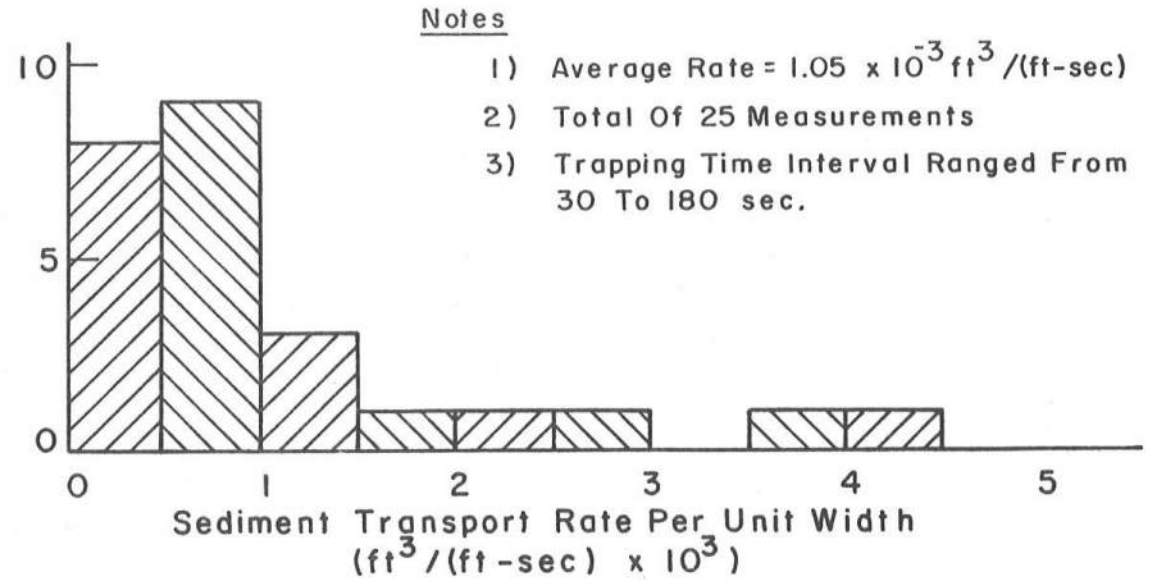

(a) Uprush Zone

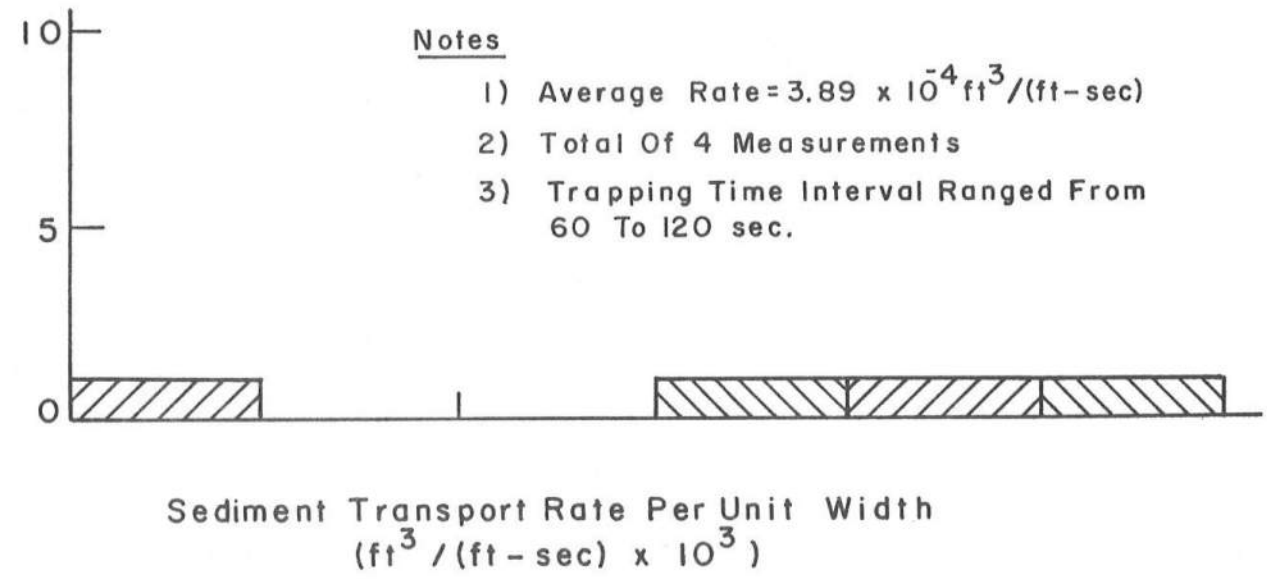

(b) Submerged Zone

Figure 23. Results of Measurements of Swash Zone Transport, June 1, 1977.

VII. OFFICE STUDIES

The two main elements of the office study are (1) an interpretation of shoreline changes and other relevant information as depicted by records and aerial photographs made available by the Baltimore District of the U. S. Army Corps of Engineers, and (2) the development of a numerical model to represent tides and currents in the bay system which is served by Ocean City Inlet.

Past Dredging Requirements

The past dredging requirements for the shoal area of concern will be presented first to aid in later interpretations of aerial photography. Very briefly, there have been ten dredging events since the inlet was formed in 1933 and the dredging requirements increased markedly from an average annual amount of 10,000-15,000 yd^3 to 50,000 yd^3 in the period of 1969 to 1973. Since 1973, the annual dredging requirements have been approximately 30,000 yd^3. Figure 2 presents both the average annual dredging requirements between events in bar graph form and the cumulative dredging. It is seen that approximately 0.6 million cubic yards have been removed from the shoal area since the inlet was formed. It is difficult to identify, with confidence, trends in the dredging requirements; however, it does appear that there has been a general increase on which is superposed a short-term increase in the period 1969 to 1973. One probable contributor to this short-term increase will be identified in the discussion of the aerial photographs.

Inspection of Aerial Photographs

Prior to inspecting individually the thirteen aerial photographs to be presented, a description will be given of the general features which

are observable from the photographs.

Shoreline Response

There has been an accumulation of material north of the north jetty and an erosion of material south of the south jetty. Figure 24 presents the changes between September 1933 and June 1976 as scaled from aerial photographs. The northern shoreline advancement immediately adjacent to the inlet amounts to approximately 700 ft. within 200 or so ft. from the jetty tip. It is likely that this structure (north jetty) is impounded to capacity and, as a result no further shoreline advancement can occur. The maximum southern shoreline recession immediately adjacent to the south jetty is on the order of 1700 ft. which amounts to approximately 40 ft. per year. It is interesting that the immediate shoreline response (following inlet formation) both north and south of the inlet was recession with the greatest effect occurring south of the inlet. With construction of the north jetty, the adjacent shoreline responded by accreting.

Minimum Flow Width Into Sinepuxent Bay

Field surveys demonstrated the effectiveness of ebb currents in eroding "excess" material from the northwest corner of Assateague Island and transporting and depositing this material in the shoal area of concern. Since any further westward or northwestward migration of Assateague Island would cause an additional constriction of the channel into Sinepuxent Bay enhancing currents and increasing their erosive and transporting capacity, it is of interest to examine this flow width with time. Figure 25 based on aerial photography documents the variations in the width of the channel between Assateague Island and the mainland. The initial width was on the order of 1400 ft. and initially decreased to approximately 300 to 400 ft.

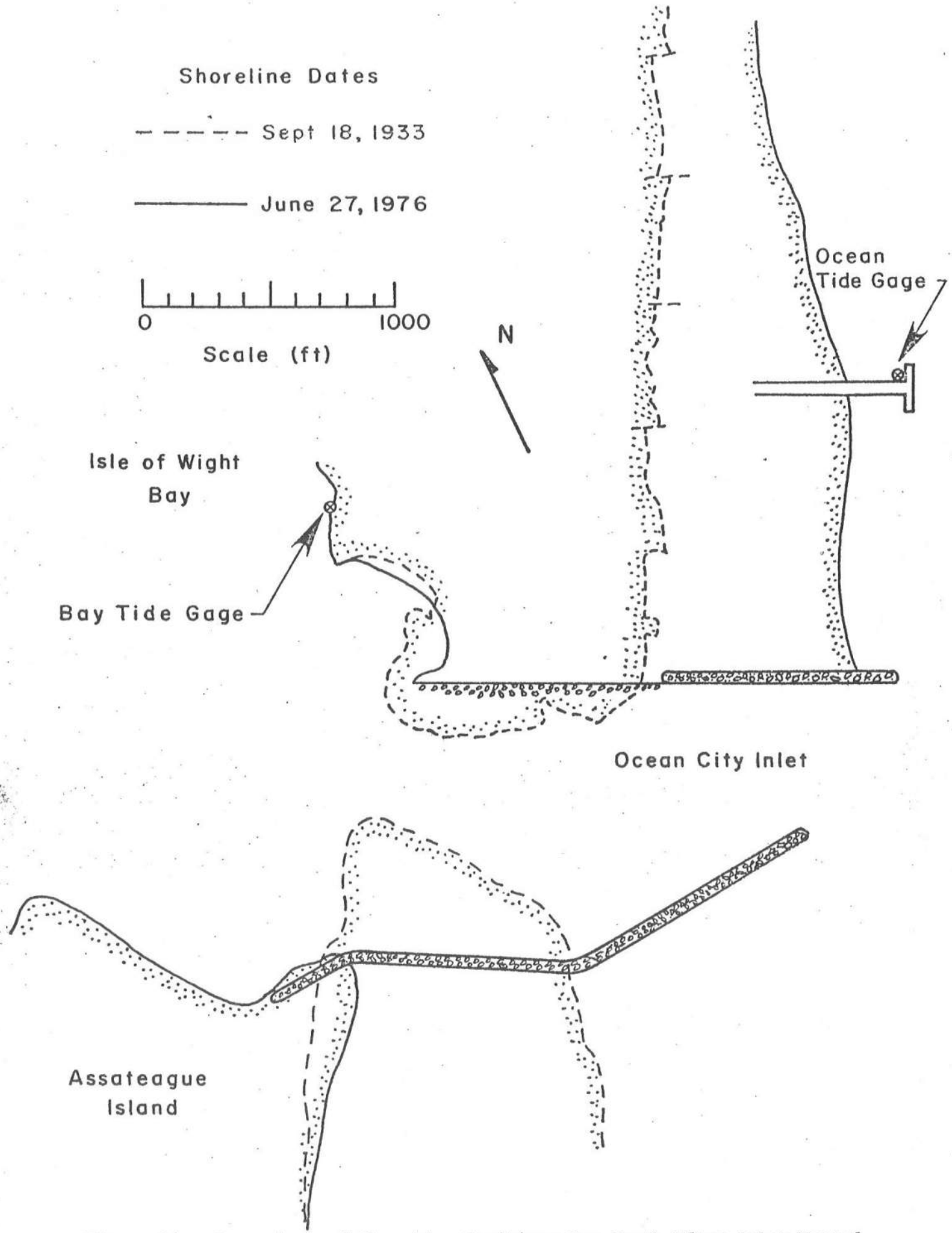

Figure 24. Comparison of Shoreline Positions One Month After Inlet Formed With That in 1976. Location of Tide Gages Also Shown.

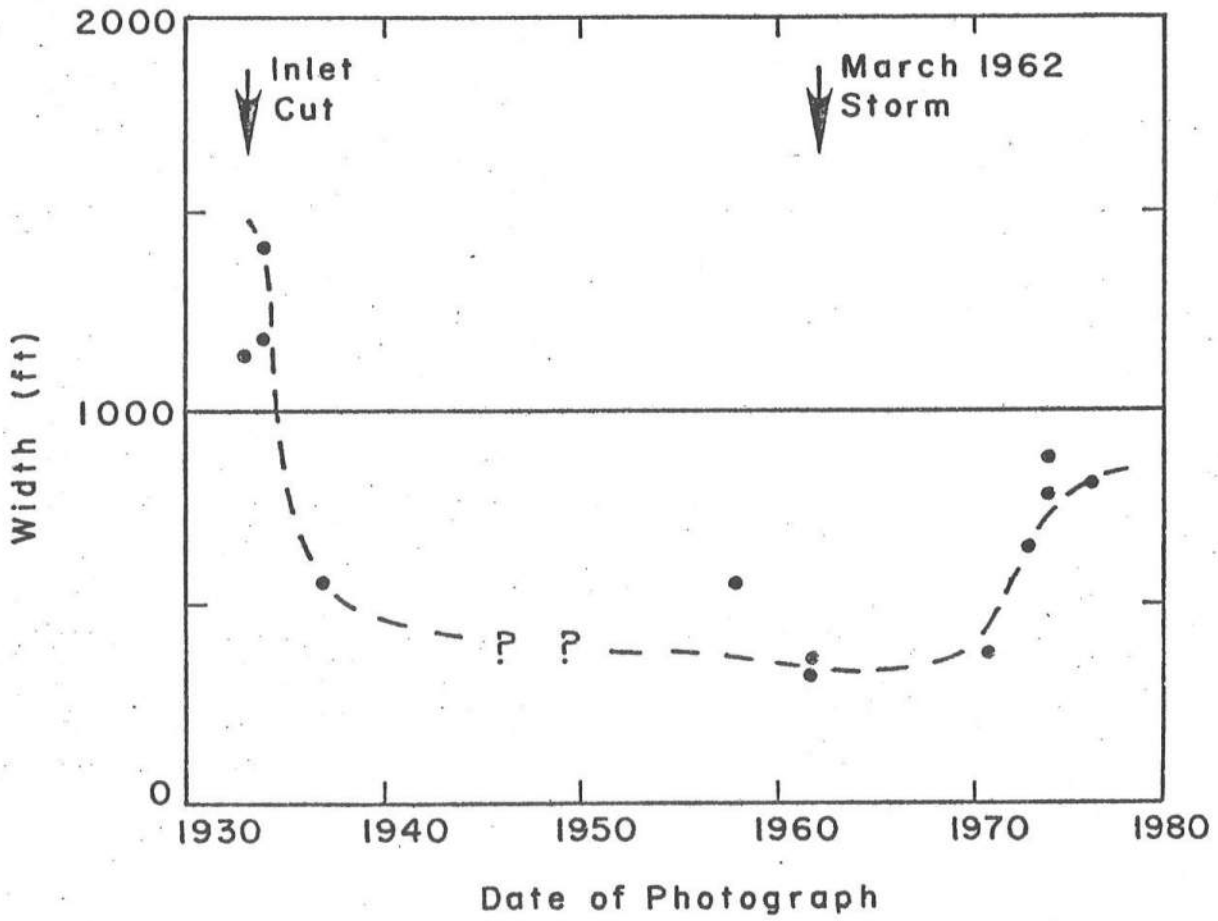

Figure 25. Minimum Width Between Mainland and Northwest Point of Assateague Island. Based on Aerial Photography.

with the minimum width apparently occurring as a result of the March 1962 storm. The width has since increased and is now approximately 900 ft. A complicating (and erosive) factor since the 1962 storm is believed to be the concentration of currents adjacent to the western shoreline of Assateague Island. This concentration may be due, in part, to the dredging of large quantities of material to repair the breach adjacent to the south jetty which was enlarged significantly by the March 1962 storm.

The following pages present and discuss thirteen photographs on an individual basis. For each case the photograph, interpretation and discussion are arranged so that they can be examined in one view.

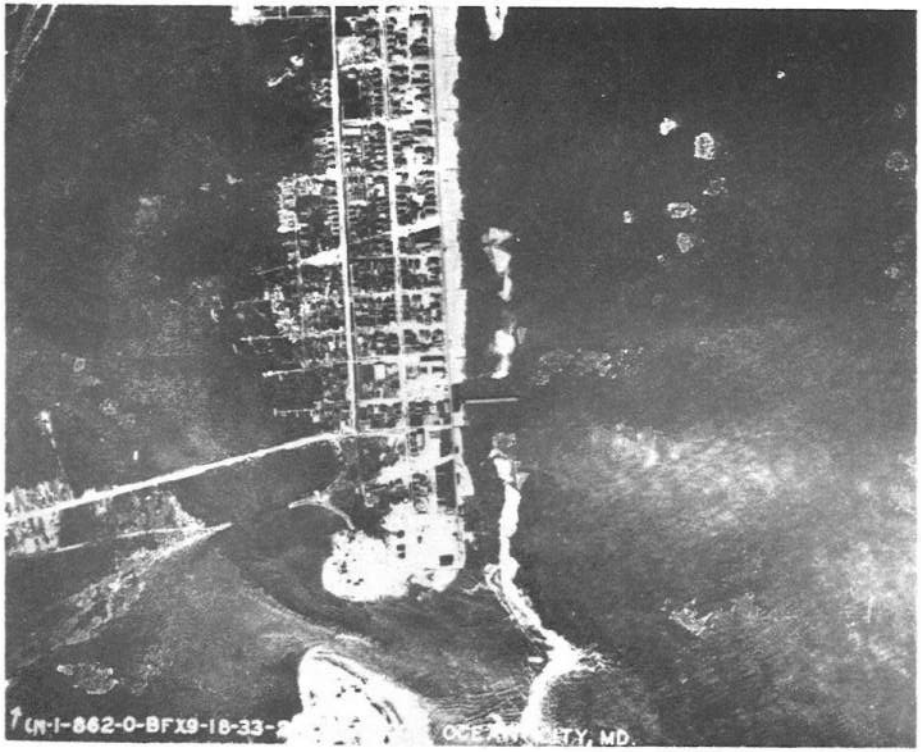

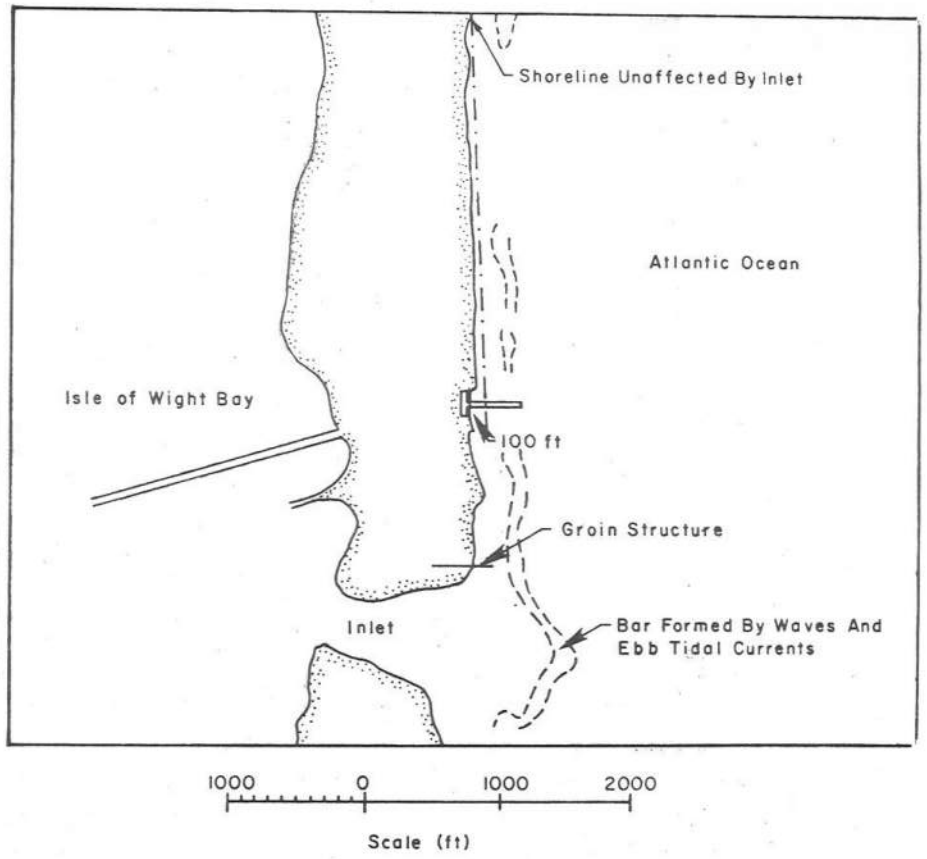

Figure 26. Aerial Photograph of Ocean City Inlet and Interpretation, September 18, 1933.

Aerial Photograph: September 18, 1933 - This photograph is presented as Figure 26 and shows the inlet and north shore 26 days after the inlet was formed during the Hurricane of August 23, 1933. Of interest is that a seaward bar has started to form as shown by the breaking waves seaward of the inlet. Also, for purposes of later comparison, it is noteworthy that, as expected, the shorelines north and south of the inlet lie more-or-less on the same line. Local interests have apparently constructed a groin structure just north of the inlet to stem the loss of sand into the inlet. The bar north of the inlet, as defined by the breaking waves, is some 360 ft. offshore and is undoubtedly the product of shore erosion and offshore transport resulting from the hurricane. Finally, also for purposes of comparison with later photographs, the shoreline position, unaffected by the inlet, is some 100 ft. seaward of the seaward side of the building at the base of the Ocean City Pier. By comparison, an attempt to establish the same result from a 1973 photograph yielded a beach position of some 700 ft. The 1933 photograph does not reveal significant sand deposits in the inlet, although if present, these may not be apparent due to the sunlight angle or water coloration.

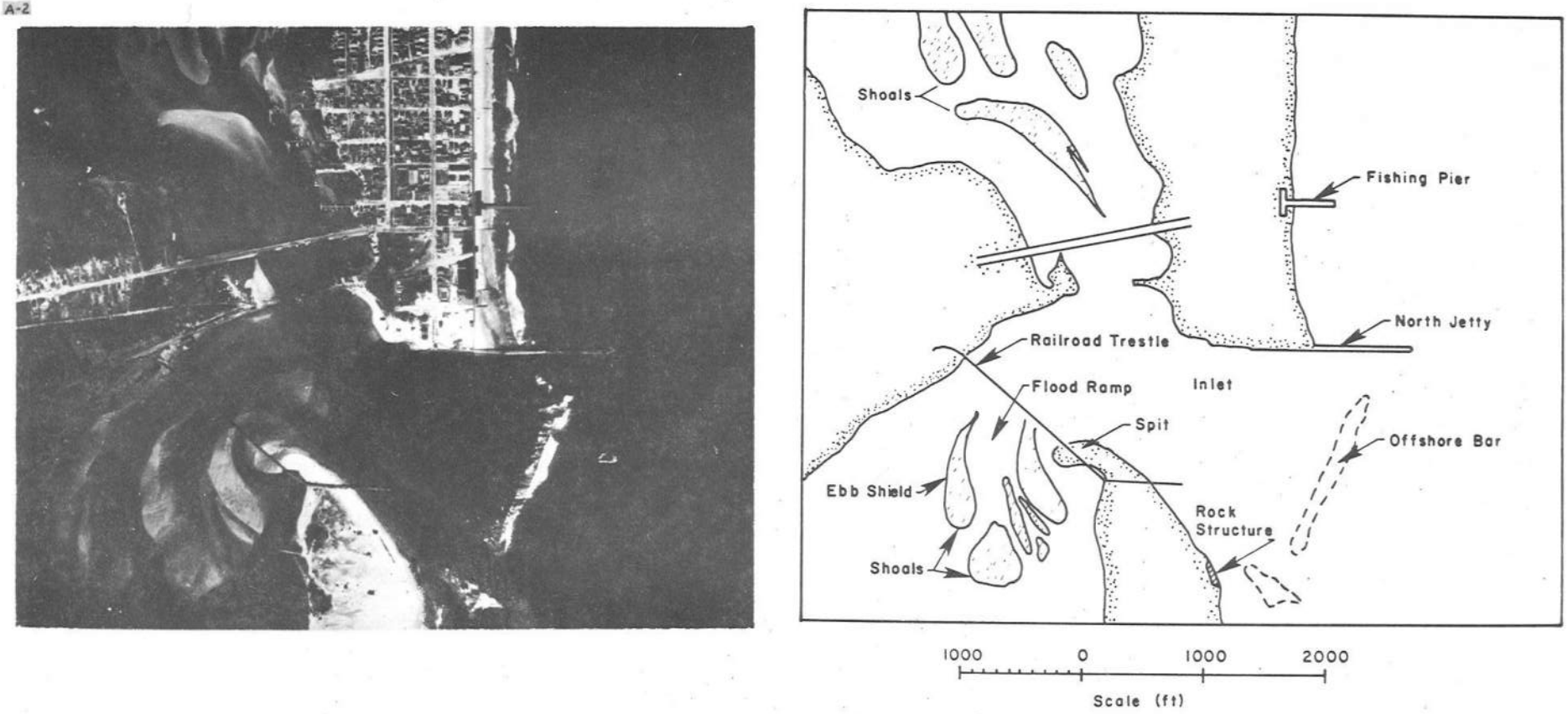

Figure 27. Aerial Photograph of Ocean City Inlet and Interpretation, October 9, 1934.

Aerial Photograph: October 9, 1934 - Figure 27 shows several interesting features. The north jetty construction has been completed and sand has started to be impounded especially just adjacent to that structure. The railroad trestle has been built for delivery of rock to Assateague Island for construction of the south jetty. It appears however from this photograph that the extension of this trestle seaward of Assateague Island is permeable as there is no evidence of a fillet forming against (on the south side) of the structure. Indeed there is a small spit indicating sand transport through the trestle. On the northern shore of Assateague Island, there appears to be either a rock structure or a peat outcrop. This may be rock placed by local residents to reduce sand losses into the inlet. This photograph taken some thirteen months subsequent to the formation of the inlet shows considerable sand deposition in the bay both north and south of the inlet. The classical flood current ramps and ebb current shields (Hayes, Reference 2) are evident on some of the deposits and aid in interpreting flood and ebb tidal current patterns. Finally, the aerial photograph shows that the offshore bar has realigned from the 1933 photograph and that breaks in the bar occur adjacent to the north jetty and to the south adjacent to Assateague Island.

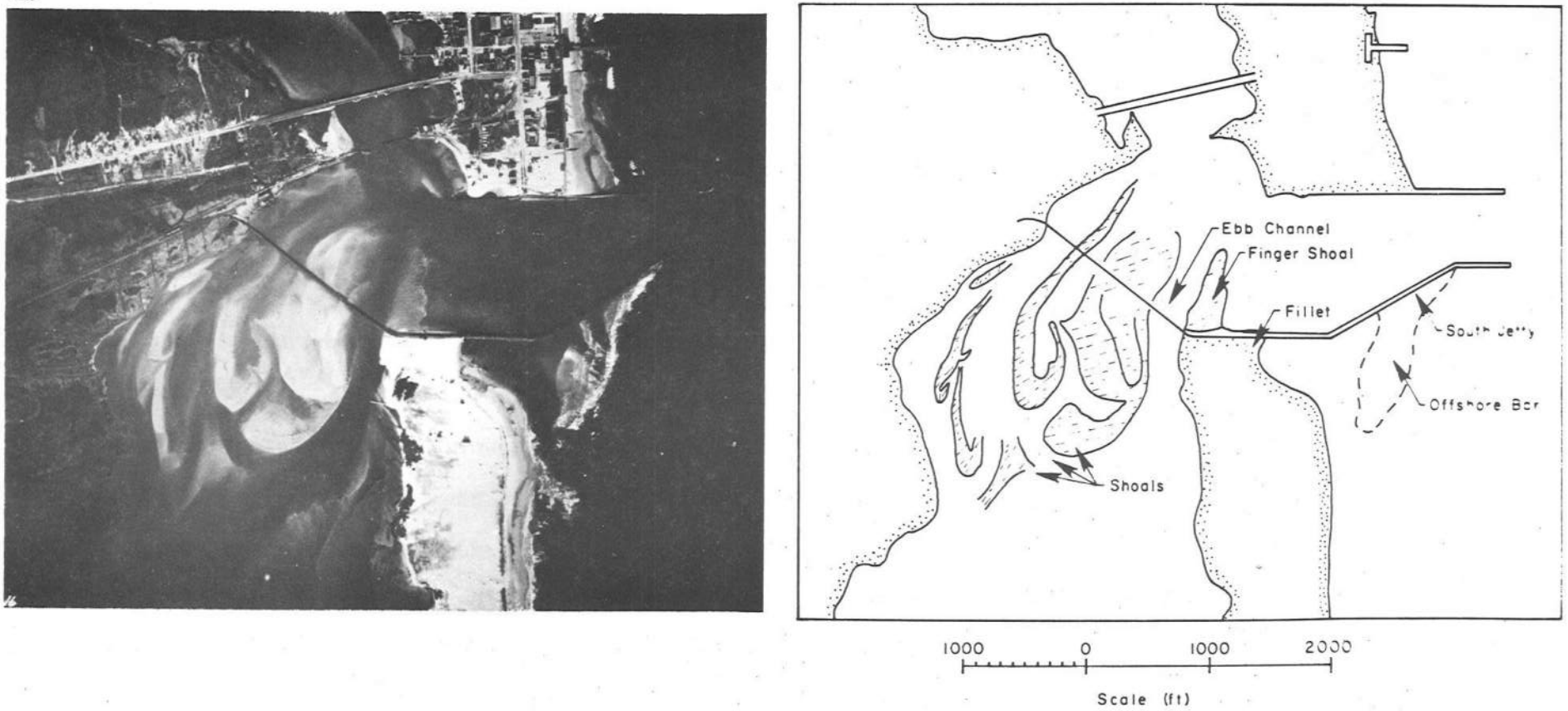

Figure 28. Aerial Photograph of Ocean City Inlet and Interpretation, December 6, 1934.

Aerial Photograph: December 6, 1934 - Although a period of only two months has elapsed since the previous photograph, significant changes appear to have occurred. First, considerable construction progress has been made on the south jetty. The jetty appears to be impermeable as indicated by the fillet on the south side and the bar on the south side of the south jetty appears to be moving landward due to wave action and the elimination of the balancing force of the ebb currents by construction of the south jetty. The sand transport into the bay from Assateague Island appears to have been reduced at the time of this photograph by the south jetty although comparison of this and the previous photograph leaves the impression that a considerable quantity of sand has been transported into the inlet in the intervening period. Also of interest is that an ebb channel has formed between the major shoal in Sinepuxent Bay and the northwest corner of Assateague Island. This ebb channel is transporting sand to the north and the resulting deposition represents the initial indication of the finger shoal which is responsible for the present shoaling problem. The northern shoreline of Assateague has migrated landward a distance of some 500 ft. since the inlet was established. This sand has been primarily carried into Sinepuxent Bay and deposited as the major shoals discussed earlier.

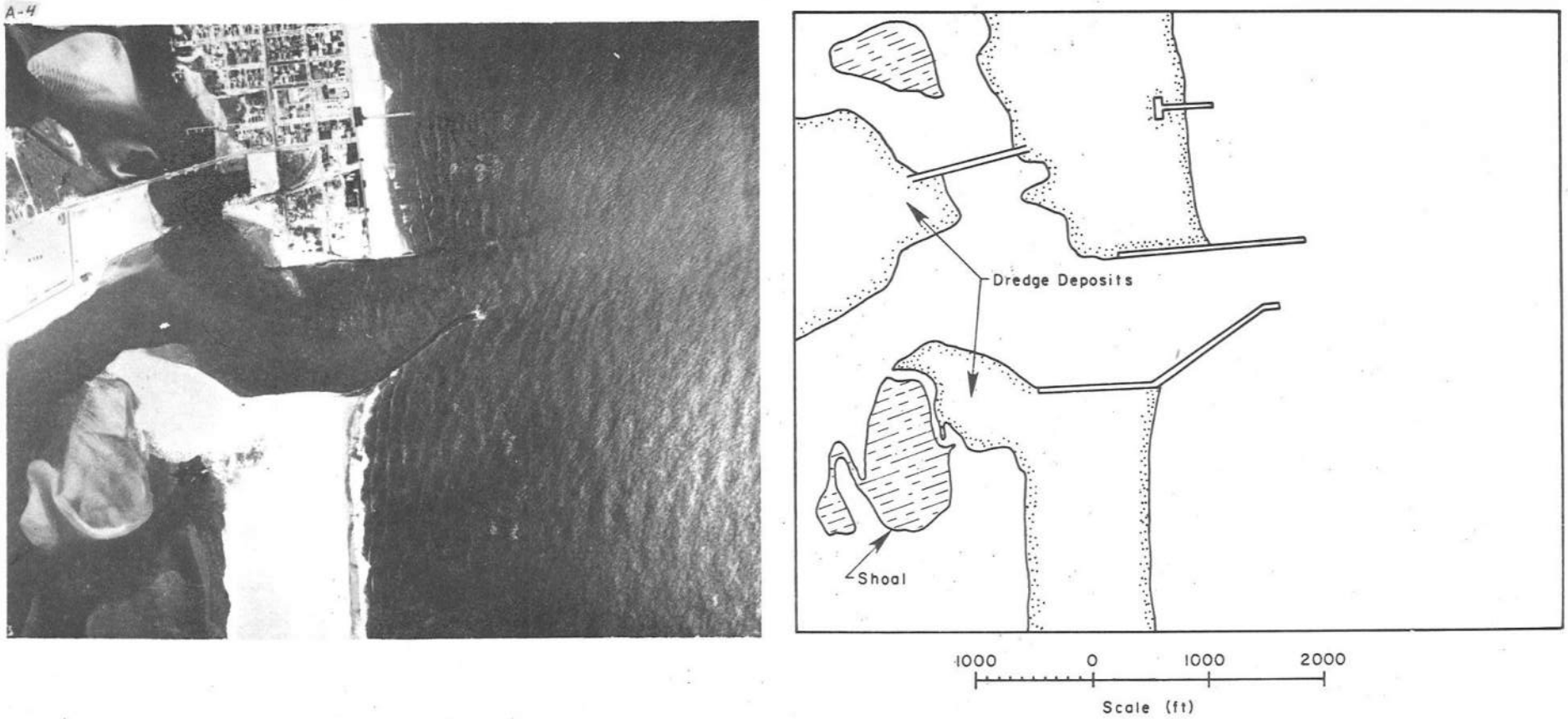

Figure 29. Aerial Photograph of Ocean City Inlet and Interpretation, August 17, 1937.

Aerial Photograph: August 17, 1937 - This photograph, presented as Figure 29, represents a time interval of 32 months since the previous photograph. There has been considerable dredging and filling in the area with substantial quantities of dredge material placed to the northwest of the present Commercial Fish Harbor and to the south of U. S. Route 50. Also the railroad trestle, constructed to transport rock to Assateague Island has been removed. The shoal at the northwest corner of Assateague Island has been consolidated (by nature or man) and the jetty appears to be relatively impermeable as noted by the shape of the fillet. Some sand transport may be occurring over the crest of the south jetty, however this does not appear to be substantial. There are no houses remaining in the portion of Assateague Island encompassed in this aerial photograph. Also there is almost no discernible vegetation and this may be due to the placement of some dredge spoil material on the north end of the Island. This aerial photograph indicates a shoreline recession of approximately 540 ft., i.e. there was a shoreline loss of only 40 ft. since the last aerial photograph in 1934. As noted, this reduced rate of erosion is due to the effect of the south jetty in reducing further sand losses into the inlet.

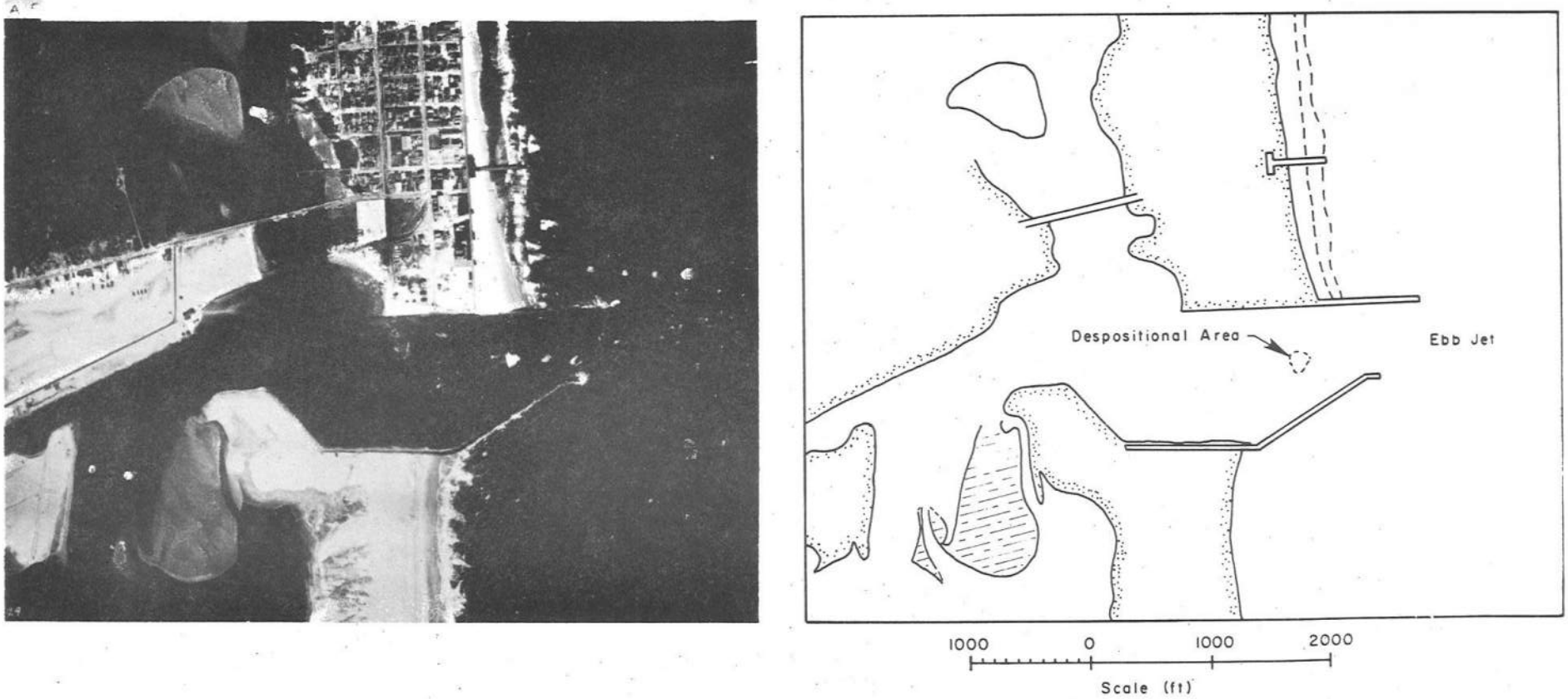

Figure 30. Aerial Photograph of Ocean City Inlet and Interpretation, October 18, 1937.

Aerial Photograph: October 18, 1937 - This photograph, shown as Figure 30, is taken only two months after the earlier photograph shown in Figure 29. The photograph shows a more stormy condition with the bar north of the inlet clearly outlined by breaking waves. There does not appear to be a bar present south of the inlet. The photograph was taken on an ebb tide as shown by the presence of breaking waves on the jet seaward of the jetties. The location of the breaking waves immediately inside the inlet suggests a shoal in a location where shoaling also currently occurs.

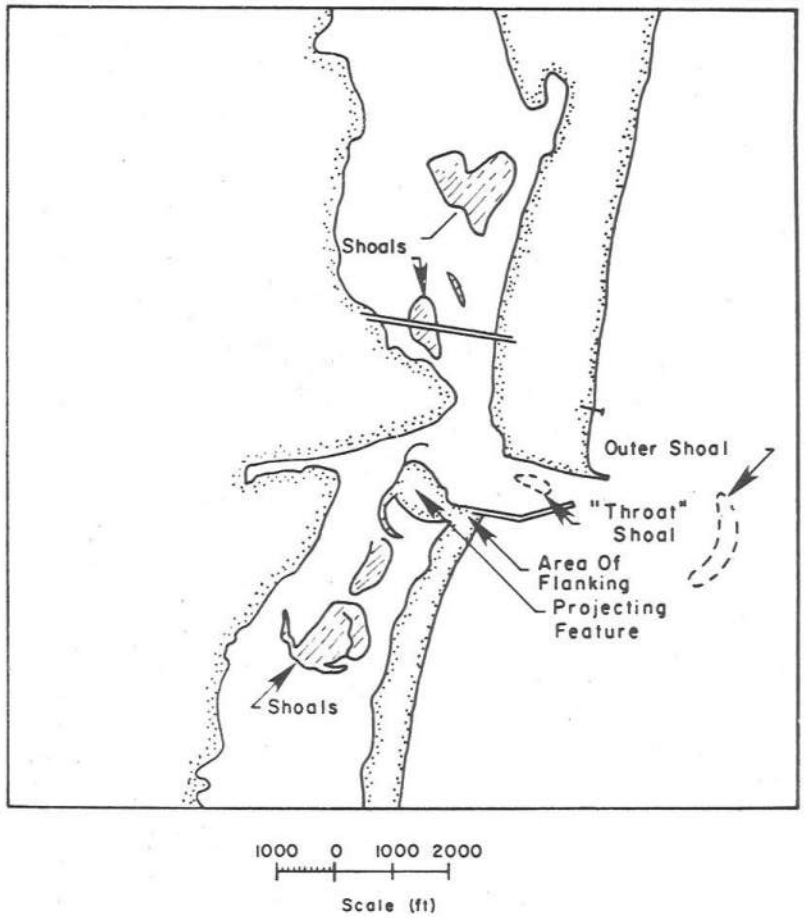

Figure 31. Aerial Photograph of Ocean City Inlet and Interpretation, May 29, 1958.

Aerial Photograph: May 29, 1958 - This photograph represents a time lapse of over 20 years from the previous photograph and is shown as Figure 31. There has been very substantial shoreline recession of Assateague Island and considerable accretion on the north side of the inlet. The north shores of Assateague Island have receded approximately 1200 ft. since the inlet was established in 1933 and there appears to be evidence of flanking of the south jetty, i.e. water (and sand) being transported into the inlet by flowing over and adjacent to the south jetty. The photograph also shows the presence of the large shoal areas inside the bays to the north and to the south. These shoals to the south show the influence of the projecting emergent feature just west of the south jetty in sheltering the easterly portions of these depositional fans to the south of the inlet and concentrating the currents such that the westerly portions have been eroded. Finally this photograph shows the presence of a shoal as noted previously in the throat of the inlet and a very large shoal located approximately 3300 ft. seaward of the original shoreline.

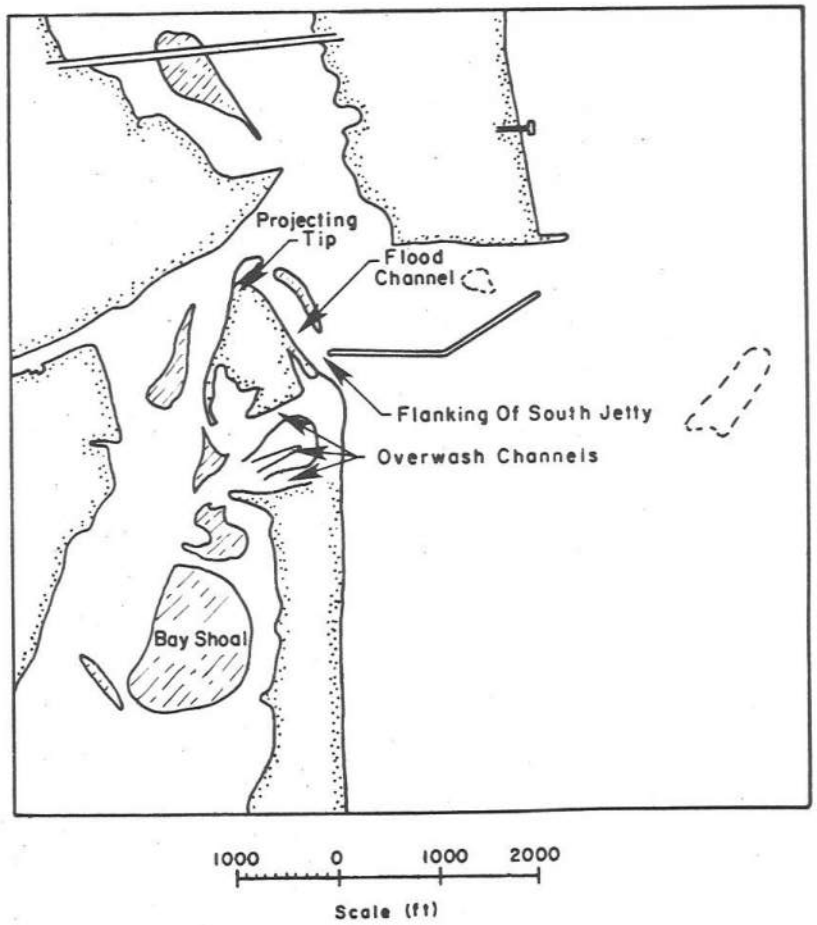

Figure 32. Aerial Photograph of Ocean City Inlet and Interpretation, January 17, 1962.

Aerial Photograph: January 17, 1962 - This photograph represents an elapsed time of four years from the previous photograph and is presented as Figure 32. Of greatest interest is that the flanking of the south jetty which appeared to have started in the 1958 photograph is now complete and the south jetty is completely detached from Assateague Island. This flanking is reported[9] to have occurred in a southern storm in October 1961. Much sand has been carried from the Assateague shoreline and deposited on the north tip projecting into and nearly closing the channel to the south into Sinepuxent Bay. This represents a source of material which is later reworked by waves and currents, with a portion ultimately being deposited (at least temporarily) in the shoal area of concern. At the time of this photograph, the minimum width of this channel was 175 ft. In this four years, the northern shoreline of Assateague Island has receded an additional 350 ft. In addition to this sand deposition occurring as a subaerial extension to the north, there is evidence of deposition on the bay shoal to the south of the inlet. The overwash and channels cut across Assateague Island just south of the inlet are significant. The vegetation-free expanse of sand and linear features across the Island suggest substantial overwash occurrences and washover deposits in the several thousand feet south of the inlet. The character of the depositional features associated with the channel just south of the inlet (along with other evidence and physical considerations) suggest that this small channel is dominantly a flood channel.

The shoal in the throat of the inlet is highlighted by the breaking waves and the offshore shoal presence is very evident by the breaking waves and diffracted wave patterns. It appears that the offshore shoal may be located south of the location shown in previous photographs.

It is noteworthy that this photograph was taken before the Ash Wednesday Storm of March, 1962.

MAY 6, 1962

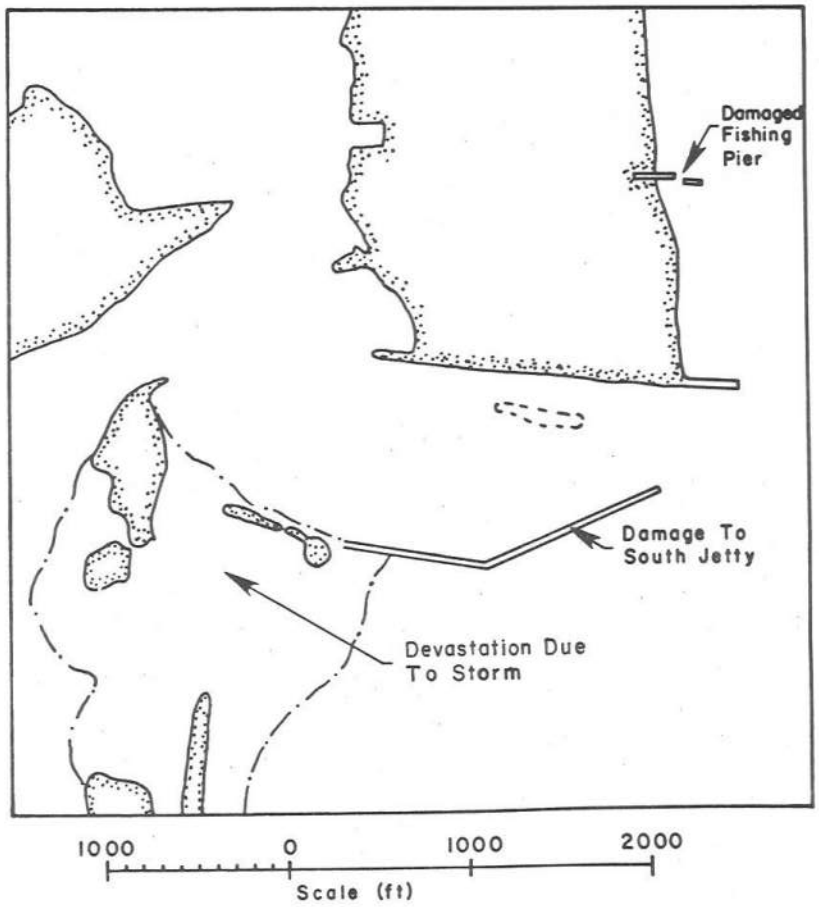

Figure 33. Aerial Photograph of Ocean City Inlet and Interpretation, May 6, 1962.

Aerial Photograph: May 6, 1962 - This photograph, shown as Figure 33, was taken approximately two months subsequent to the March 1962 Ash Wednesday northeastern. This photograph shows the devastation which occurred to the northern shores of Assateague Island. At the time of the photograph, dredging and placement of material is underway to close the breach between the south jetty and the north end of Assateague Island. There is evidence of modification of the shape of the shoal inside of the inlet and damage to the south jetty and to the fishing pier north of the jetty.

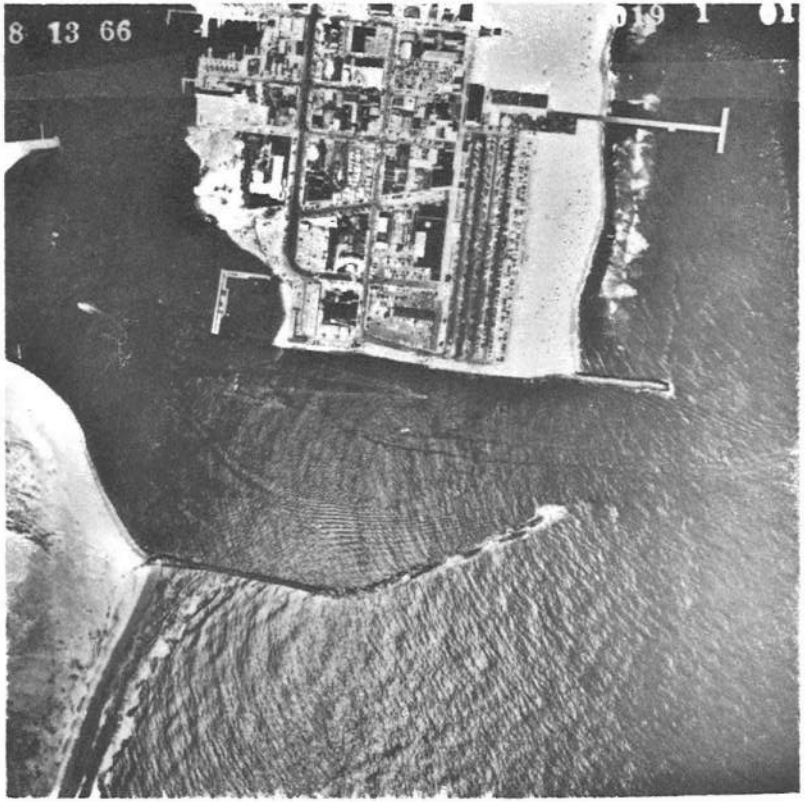

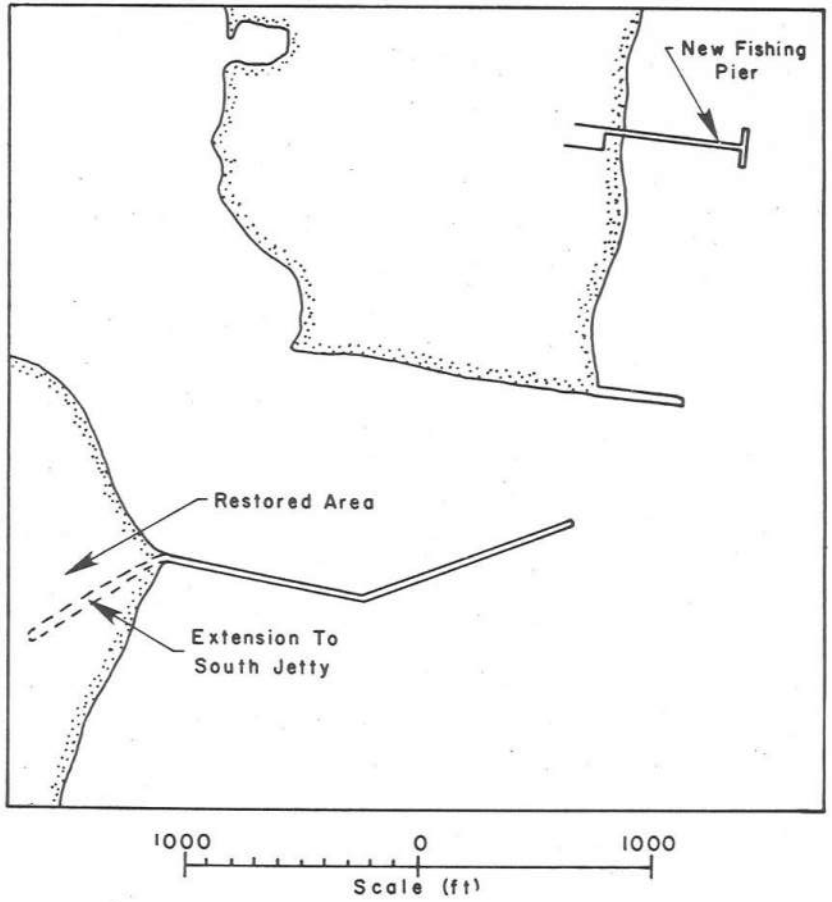

Figure 34. Aerial Photograph of Ocean City Inlet and Interpretation, August 13, 1966.

Aerial Photograph: August 13, 1966 - This photograph, presented as Figure 34 indicates that the repair of the north end of Assateague Island by placement of dredge material has been completed. In addition, a spur extension (680 ft. long) has been added in a southwesterly direction to the shore terminus of the south jetty. The purpose of this spur is to tie the south jetty into Assateague Island. It is noteworthy that the north shore of Assateague Island is now located west of the original landward terminus of the south jetty! This represents a shoreline recession of approximately 1300 ft. since the inlet was constructed. It is also interesting that the north shoreline at the north jetty has receded slightly, apparently due to waves from the south. An extension of approximately 230 ft. has been added to the fishing pier.

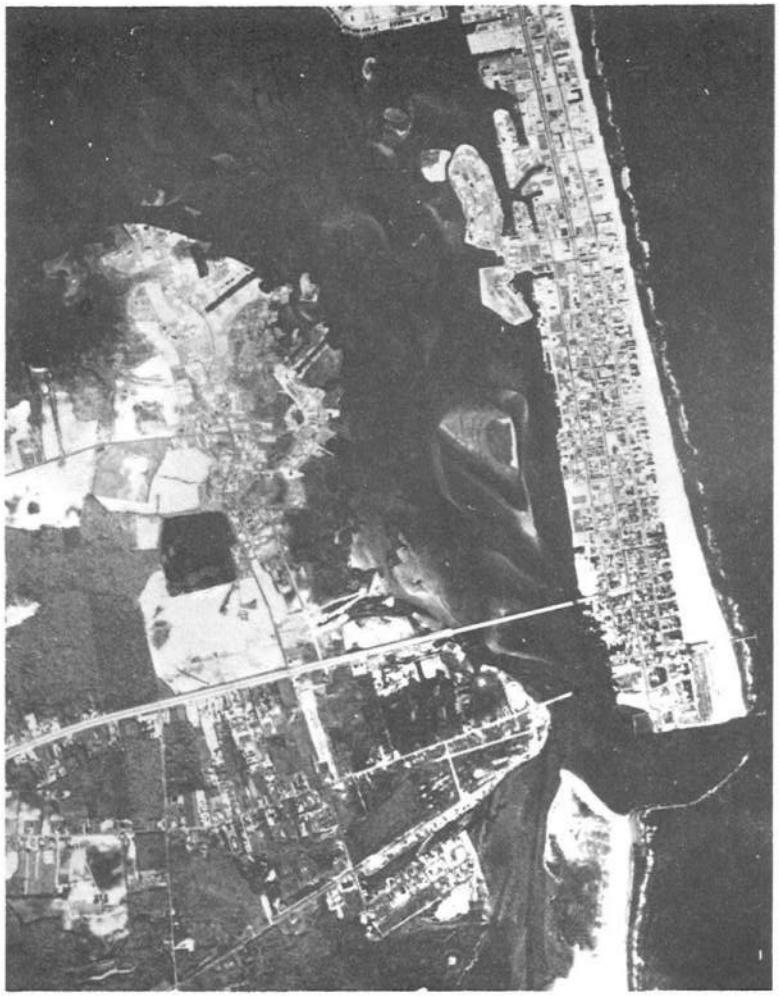

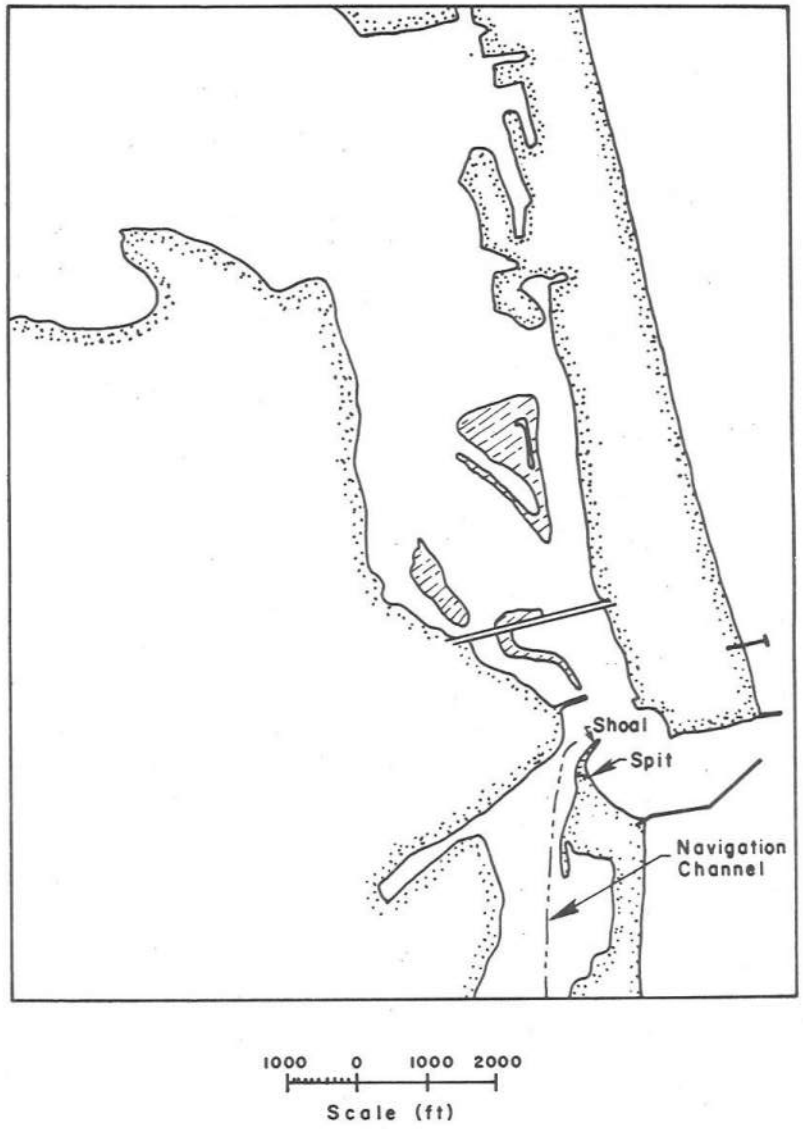

Figure 35. Aerial Photograph of Ocean City Inlet and Interpretation, June 8, 1971.

Aerial Photograph: June 8, 1971 - This photograph clearly shows the shoal areas in the bay system. Of particular interest are the almost uniformly shallow areas to the south with the navigational channel indicated as the darker area. The shoreline to the south has not receded significantly since the previous photograph, although there is evidence of sand being transported past (over or through) the south jetty, being transported around the north end of Assateague Island and deposited on the small spit on the northwest corner of Assateague Island. This photograph also suggests that the ebb flows from Sinepuxent Bay transport material from this spit (probably during Spring tide when these currents are strongest) and deposit the material in the channel leading to Commercial Fish Harbor. Large areas of the northern end of Assateague Island are now vegetated.

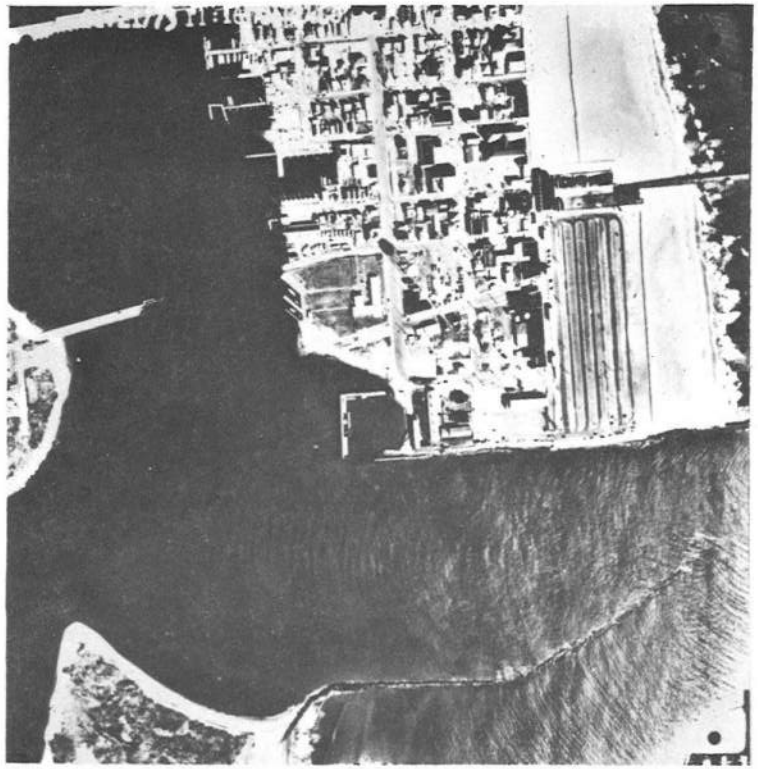

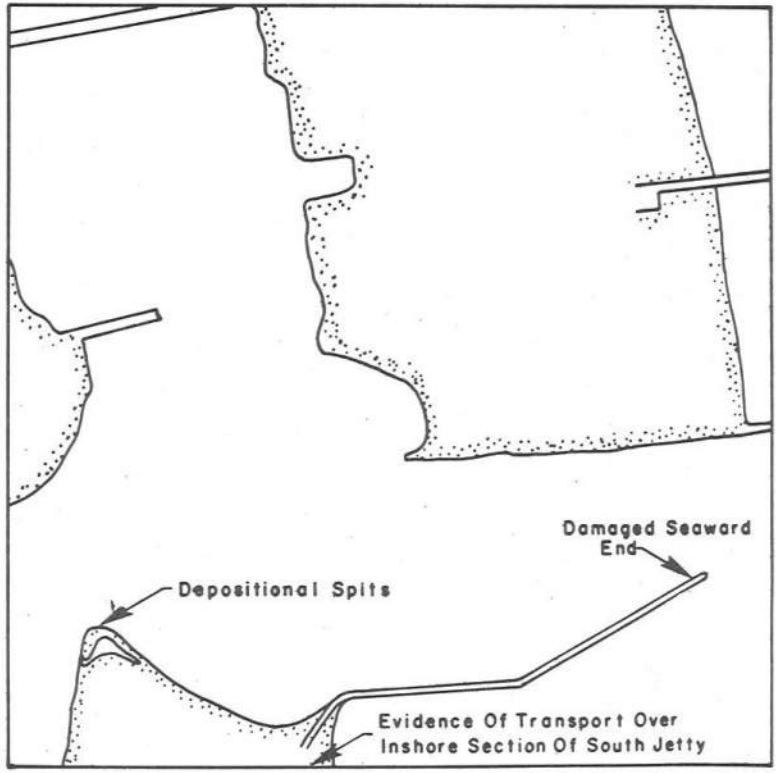

Figure 36. Aerial Photograph of Ocean City Inlet and Interpretation, January 21, 1973.

Aerial Photograph: January 21, 1973 - This photograph presented as Figure 36 shows the south jetty in good detail. The seaward terminus of the south jetty has suffered considerable damage and there is evidence of sand being carried over the inshore section of the south jetty. Note again the depositional feature on the northwest corner of Assateague Island.

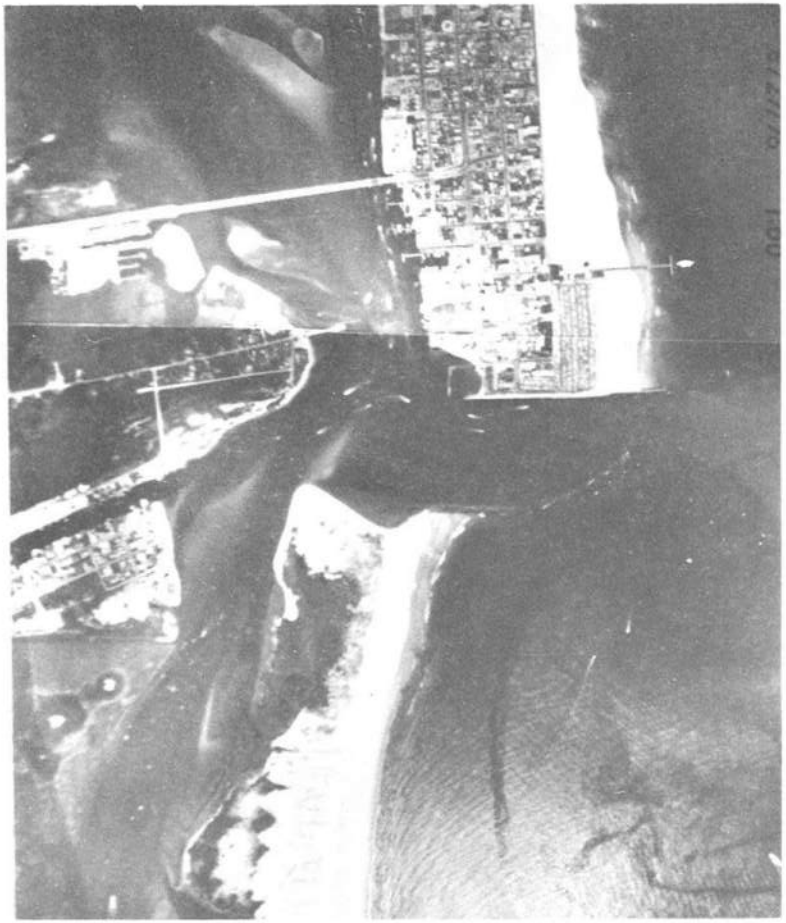

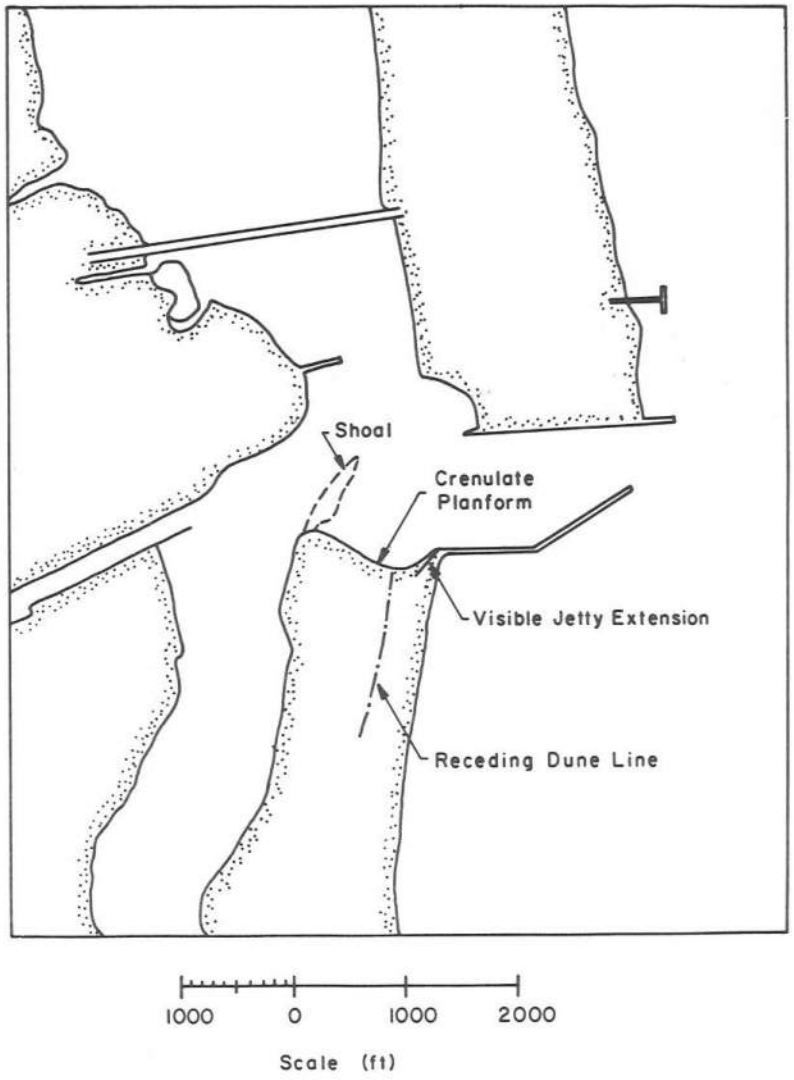

Figure 37. Aerial Photograph of Ocean City Inlet and Interpretation, June 27, 1976.

Aerial Photograph: June 27, 1976 - This photograph, which was taken in conjunction with this study, is presented as Figure 37. Of major interest in this photograph is the continued erosion of the Assateague Island shoreline as evidenced by the recession of the dune line (when compared to the earlier 1973 photograph) and the entire 680 ft. extension of the south jetty now being visible. This is due to the lowering of the beach through erosion to a level below the crest of this jetty extension. Due to water clarity and favorable sunlight angle, this photograph also clearly shows the shoal extending from the northwest corner of Assateague Island northerly toward the navigational channel. This is strong evidence as to the source of material causing the shoaling problem of concern. Also of interest are the changes evident along the north (inlet) shore of Assateague Island. In particular, the shoreline planform has become more "crenulate-shaped" which indicates that sediment transport capacity along this section of shoreline is beginning to exceed the supply. Stated differently, the processes are beginning to be affected by the south jetty limiting the sediment inflow.

Assateague Island Beach Profiles

As noted, during the initial stages of the study, it became apparent that an important sand transport pathway to the shoal of concern could be sand flowing over and through the south jetty then along the north end of Assateague Island, residing temporarily on the northwest tip of Assateague Island and eventually swept to and deposited at the shoal of concern by ebb tidal currents. In addition to the sand tracer tests and swash measurements described earlier to document sand transport over and through the jetty, beach profiles in two different areas were measured on Assateague Island to provide a qualitative indication of this transport pathway.

The profiles to be described first were located on the ocean side of Assateague Island and extended from the approximate location of the jetty to some 2700 ft. south of the jetty. Figure 38 presents the baseline for this set of profiles. Two complete sets and one partial set of beach profiles were measured and these are presented in Appendix I. Of special interest is the downward slope of the beach toward the south jetty. For example, Figures 39a and 39b present profiles at distances of 200 and 2700 ft. south of the jetty for two different surveys. Referring to the profiles in Figure 40b which are located some 2700 ft. south of the south jetty, it is seen that there are substantial differences between the two profiles taken at different times due to the action of waves and wind; however, of particular relevance is that the crest of the beach berms range from approximately 5.8 to 6.6 ft. above Mean Sea Level (MSL). The crest elevation of the inshore portion of the south jetty as determined from surveys is also shown on Figure 39b and it is seen that the crest

BEACH CONTOURS: OCEANSIDE ADJACENT TO SOUTH JETTY

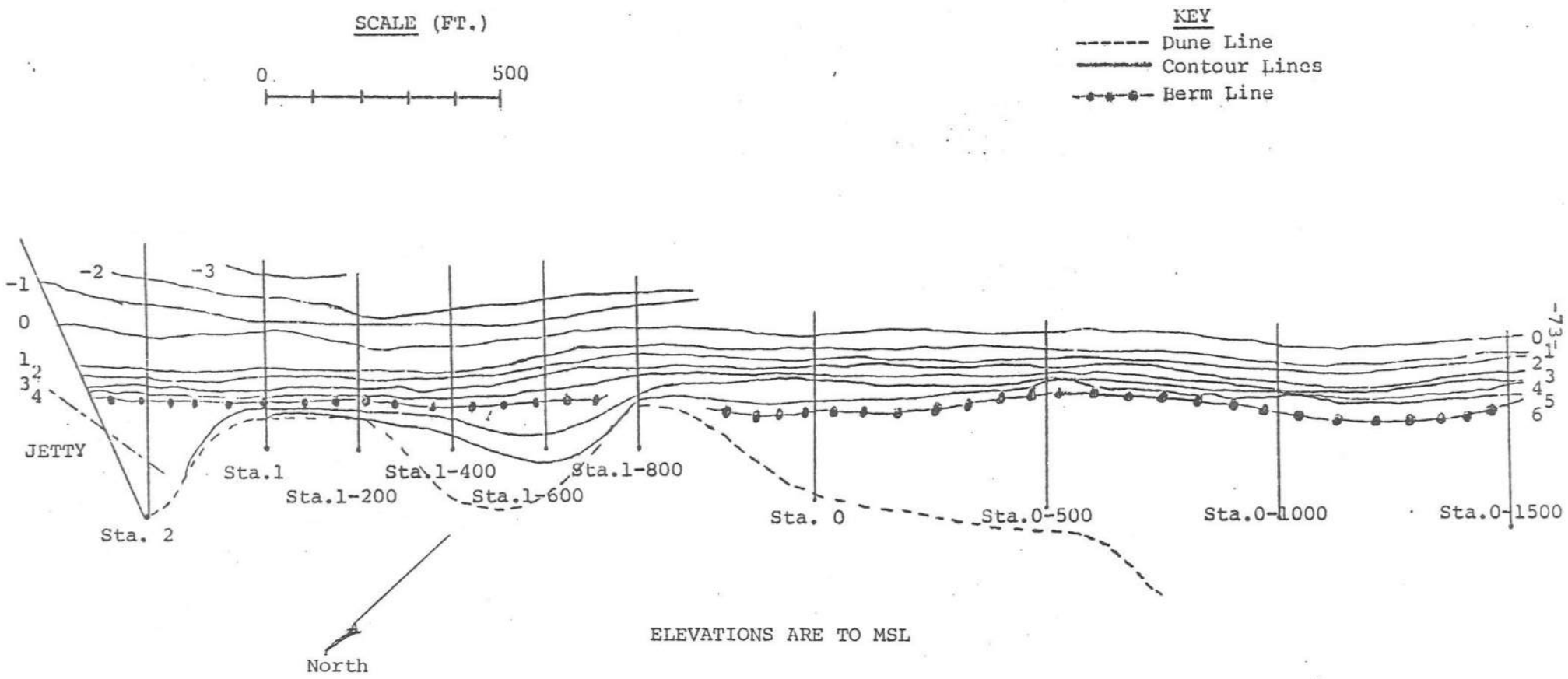

Figure 38. Contours of Assateague Island Beach South of Jetty, Baseline for Profiles is Also Shown.

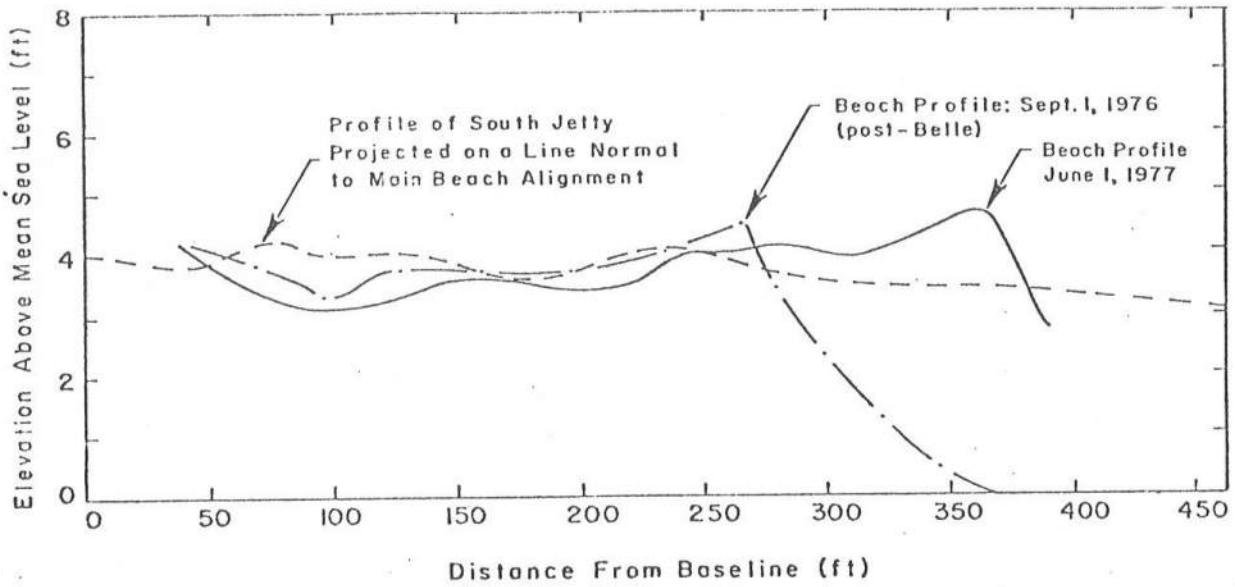

a) Beach Profiles Approximately 200 ft. South of South Jetty.

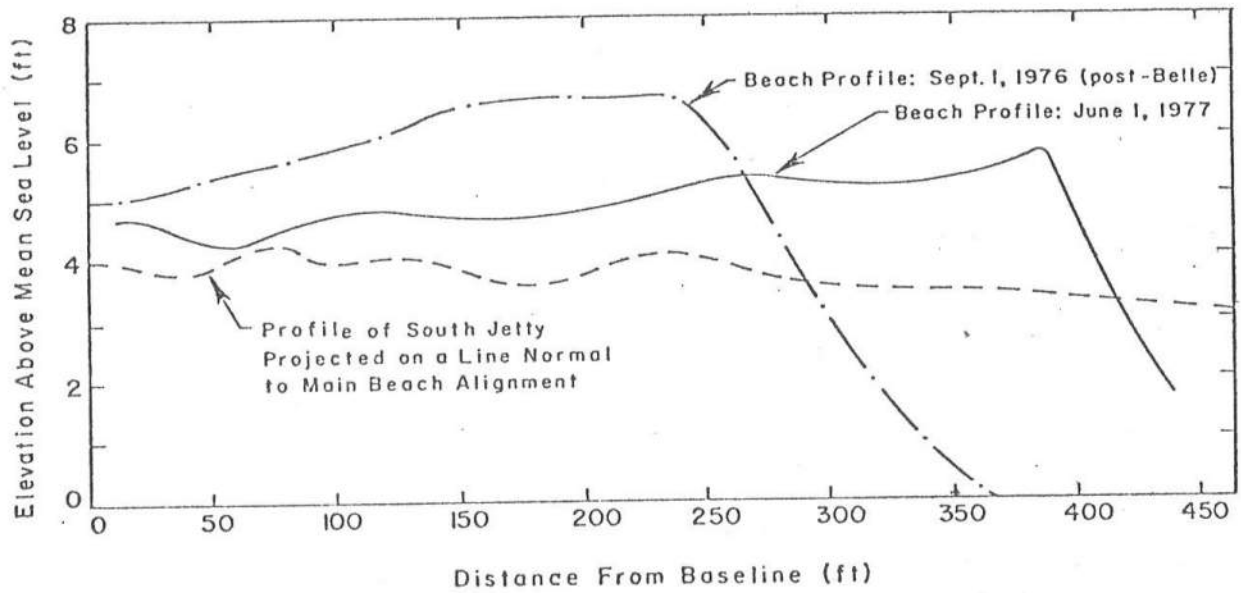

b) Beach Profiles Approximately 2700 ft. South of South Jetty.

Figure 39. Comparison of Elevations of South Jetty and Beach Profiles at Two Locations South of Jetty.

elevation is approximately 4 ft. MSL. Figure 39a presents beach profiles for the same times as in Figure 39b; however, this profile line is only 200 ft. south of the jetty. It is clear that the elevation of the south jetty serves to "control" or limit the adjacent beach elevation. In a sense, the jetty acts as a "template" or "weir" for the south beaches. The resulting downward slope of the beach in conjunction with the mobilizing action of the waves can cause a northward sand transport even if the waves are directed so as to cause southerly transport under normal conditions. Figure 40 presents the variation in beach berm elevation and demonstrates the downward slope toward the south jetty. The quantitative effect of this low jetty is not known; however, even under mild wave conditions, it appears that substantial quantities of sediment can be transported northward over the jetty into the inlet channel. Of course if the south jetty is flanked (as has occurred at least twice since the inlet was formed) the transport capacity into the inlet would be greatly enhanced.

The second set of beach profiles was located on the northwest corner of Assateague Island; the shore stations for each of the seven lines and some of the results obtained are presented in Figure 41. A total of five complete surveys was conducted. The purpose of these surveys was to document depositional/erosional activity associated with the aforementioned sediment transport pathway. A specially developed positioning procedure was developed to obtain good accuracy. To provide good horizontal control for each profile, a taut nylon line was attached to a temporary anchor and float set approximately 300 ft. bayward of a permanent shore reference stake. The nylon line was marked every three ft. At a near-slack tide, the boat was manually displaced along the stretched line and readings taken from a level located on shore. Figure 41c shows for Profiles 4-147.5 and 4 + 400,

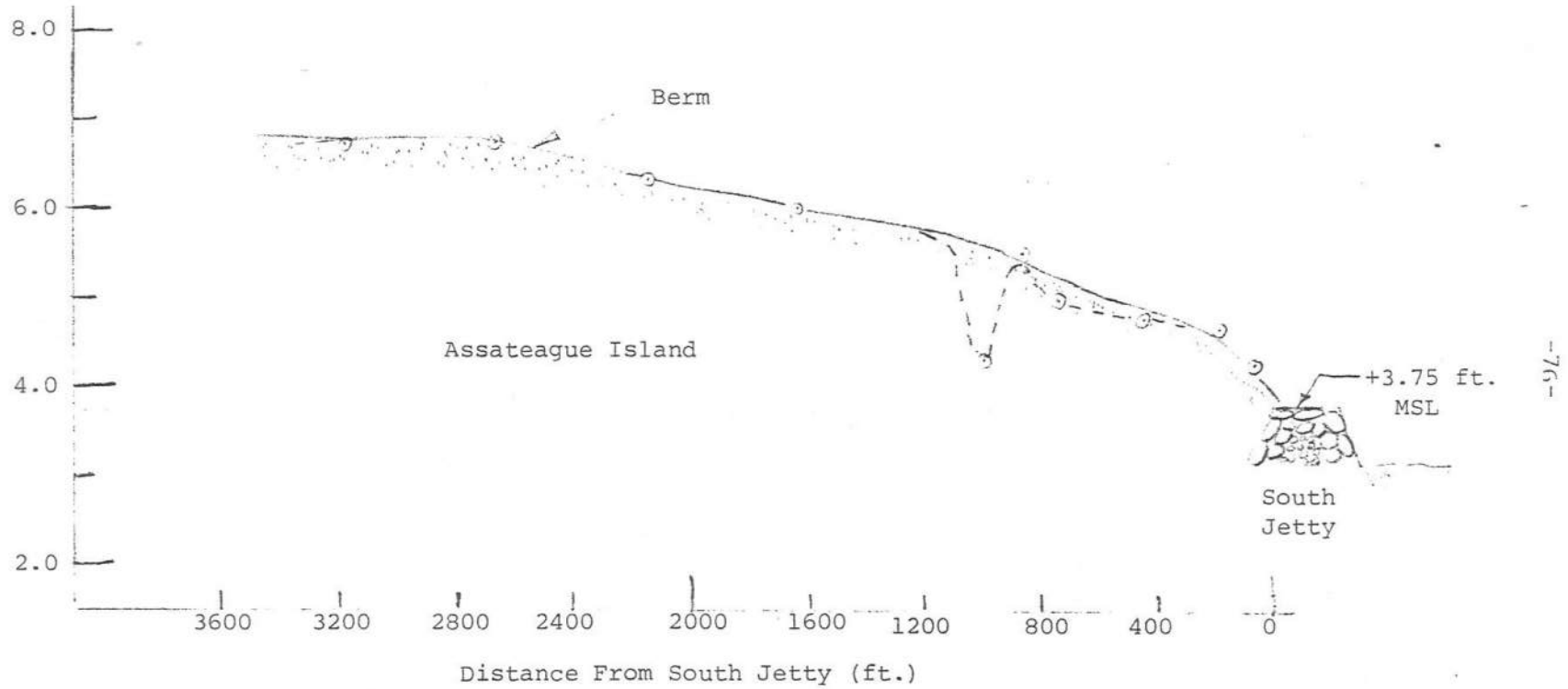

Figure 40. Effect of Low South Jetty in Reducing Berm Elevation on Assateague Island. View Looking West.

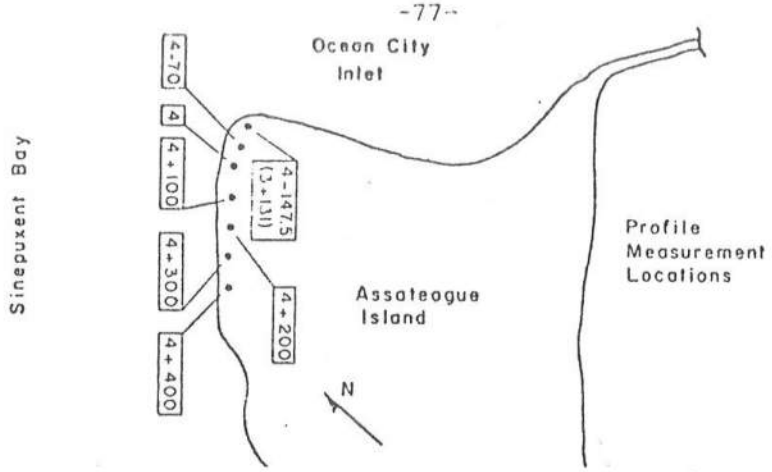

Figure 41a. Shore Stations for Profile Measurements.

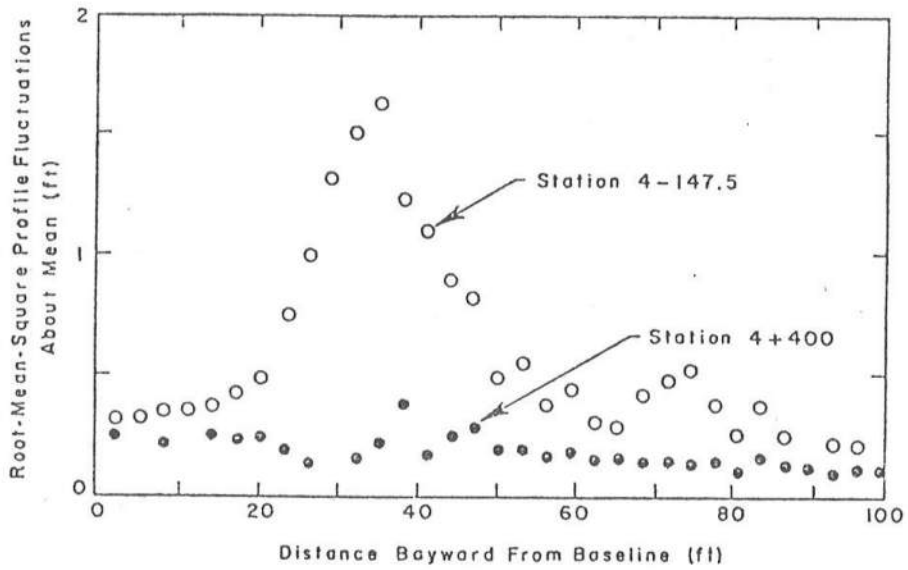

Figure 41b. Root-Mean-Square Profile Fluctuations For Stations 4-147.5 and 4 + 400.

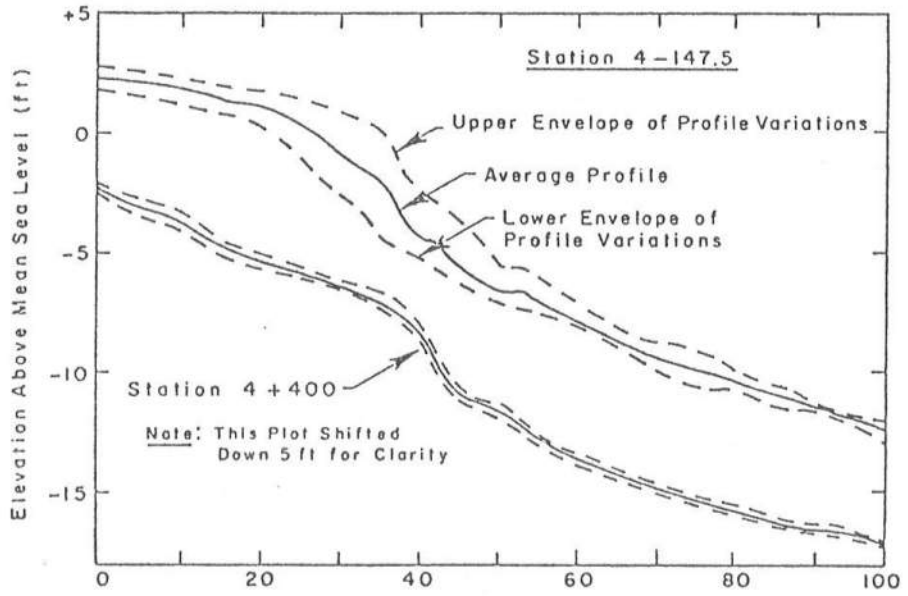

Figure 41c. Variability of Profiles 4-147.5 and 4 + 400.

Figure 41. Profile Measurements on Northwest Shoulder of Assateague Island.

the maximum, minimum and average profiles as functions of distance offshore. It is noted that the greatest fluctuations occur in the shallow water portions of the profiles. It is noteworthy that the most active profiles are those located near the northwest corner of Assateague Island, i.e. near the source of sand. Figure 42 shows the variation, with distance south, of the root-mean-square deviations of the profiles at each station about the mean of each profile. Additional information providing support to the active sediment deposition and erosion in this area include observations of up to 8 inches of soft sand (recent deposition) following a fairly severe storm and scarps up to 2 ft. high cut by spring ebb tidal currents. Figure 43 presents two photographs showing a scarp cut by ebb currents associated with a spring tide. Finally, the transport of sand by ebb currents from the west side of the northwest corner of Assateague Island to the shoal area of concern is strongly supported by visual indications at the site, including current patterns and shape of the shoal of concern.

Numerical Model

A fairly coarse one-dimensional finite difference numerical model was developed to represent the overall response characteristics of the Ocean City Inlet/Sinepuxent Bay/Isle of Wight Bay and Assawoman System. The various elements of the numerical model and their approximation to the bay and inlet geometry are shown in Figure 44. The basis of the numerical model including the representation of the governing differential equations by the finite difference equations is presented in Appendix II. The specified input to the model was the ocean tide at the entrance to Ocean City Inlet and the observed tide displacement inside Sinepuxent Bay approximately 6.4 miles south of the entrance to Ocean City Inlet. The

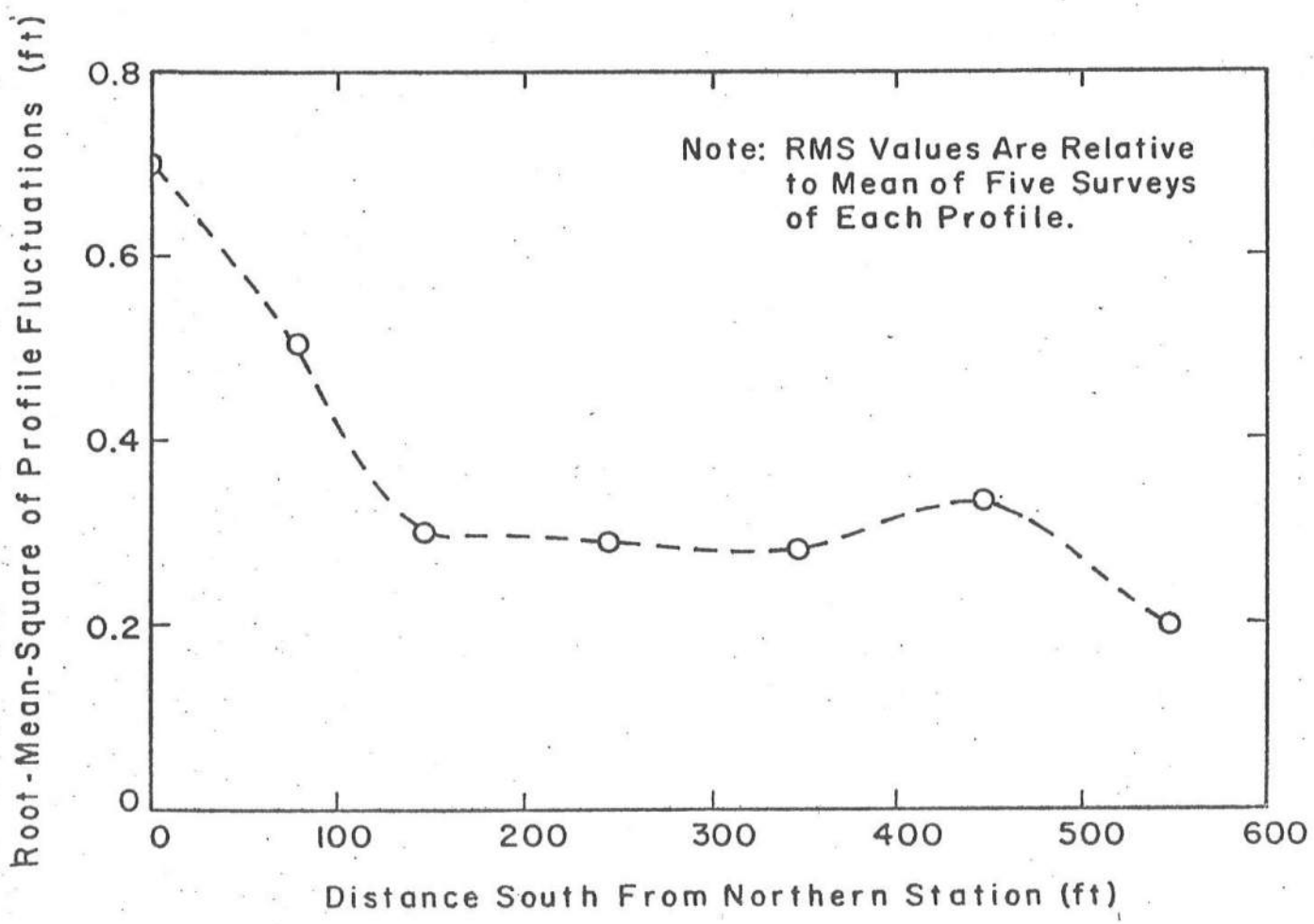

Figure 42. Variation of Root Mean Square Profile Fluctuations With Distance South Along Northwestern Shore of Assateague Island.

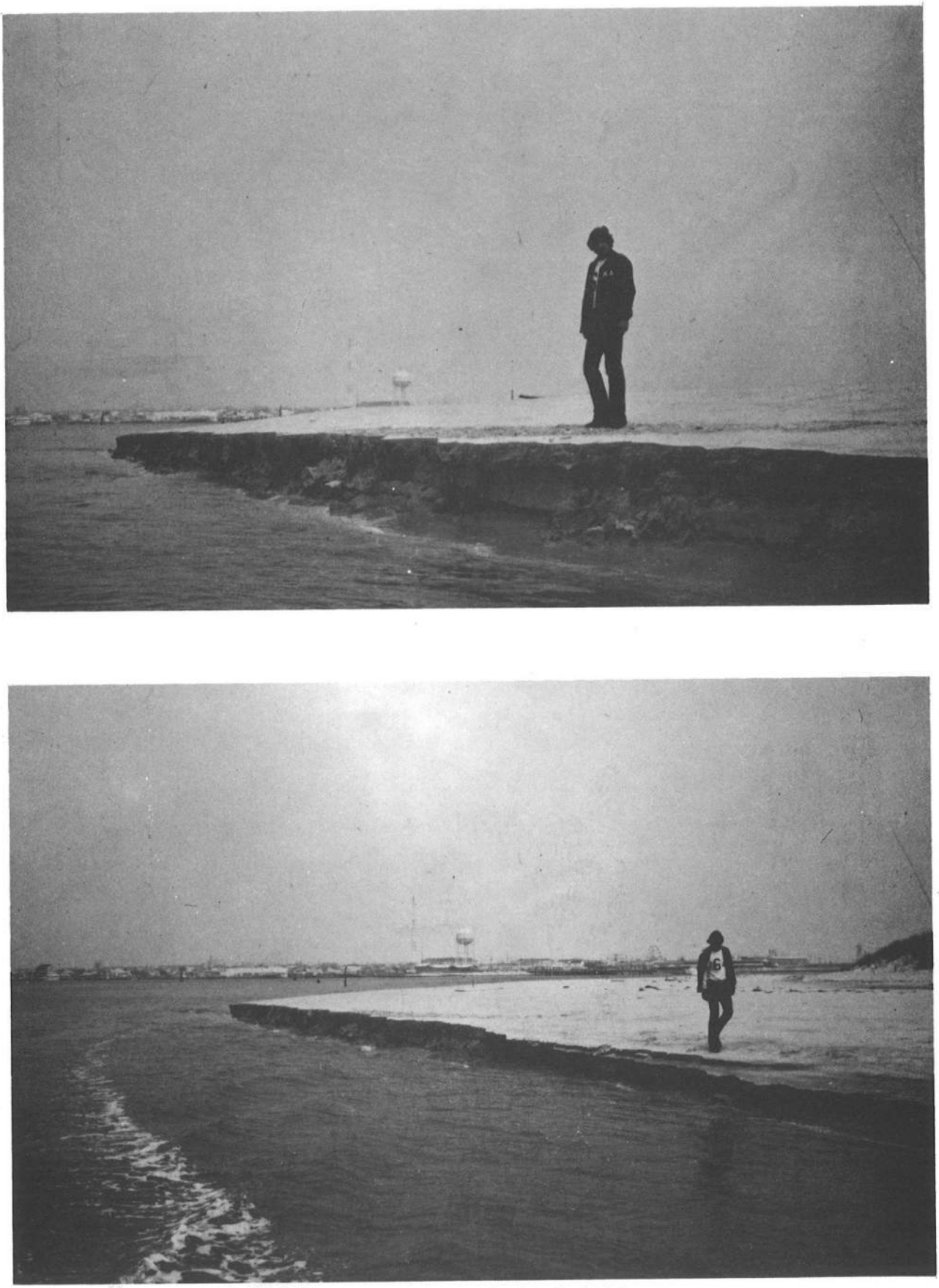

Figure 43. Photographs Looking Northeast Along Northwest Shoulder of Assateague Island Showing Scarp Cut by Spring Tidal Ebb Currents.

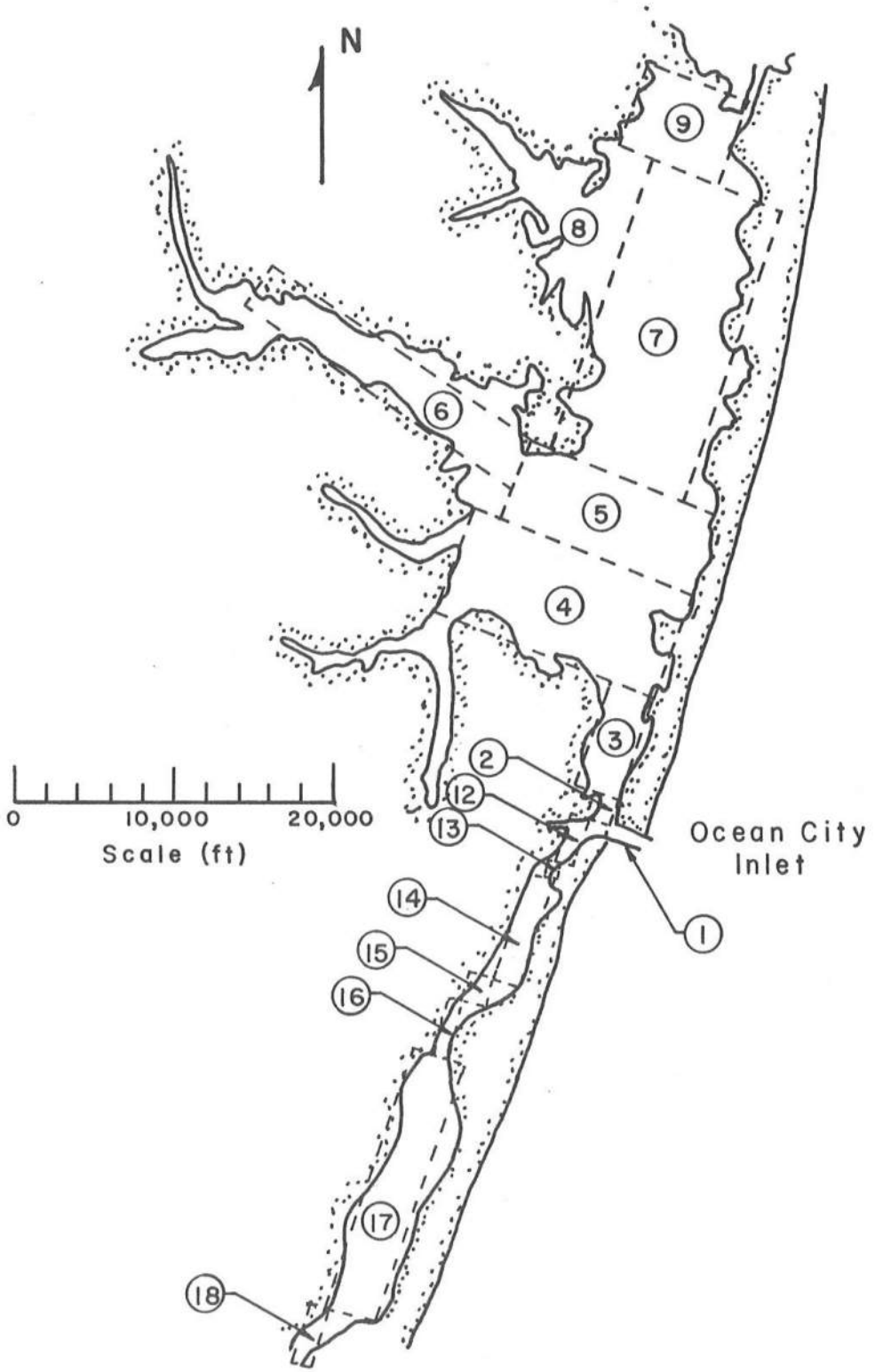

Figure 44. Numerical Model Representation of Inlet/Bay System.

boundary condition at the north end of Isle of Wight Bay was approximated by a "no flow" requirement. Various results obtained through application of the numerical model are presented in the following paragraphs.

Tidal Prism and Flow Distribution

The mean and spring ocean tidal ranges as given in the Tide Tables at Ocean City are 3.4 and 4.1 ft., respectively. The mean tide level is 1.7 ft. above mean low water.

The total tidal prism* occurring for a spring tide range of 4.1 ft. as calculated by the numerical model is 0.81×10^9 ft^3. This is approximately 10% larger than the value of 0.73×10^9 ft^3 obtained using M. P. O'Brien's[6] relationship between minimum cross-sectional area-tidal prism relationship, see Figure 45, and 23% higher than Jarrett's[3] more recent correlation. The minimum cross-sectional flow area through the inlet was determined to be 13,250 ft^2. This agreement is considered reasonable in view of the complexity of the flow patterns in the inlet vicinity and the fact that the empirical relationship for cross-sectional area-tidal prism is accompanied by a scatter of at least this amount[3]. In addition to total tidal prism, the distribution of this prism is of interest. According to the numerical model, the predominant flow (85%) is toward the north into Isle of Wight Bay with only 15% of the total flow toward the south into Sinepuxent Bay. Figure 46 presents the variation in tidal prism at the junctions of the numerical model segments.

*Volume of water flowing in (or out) of inlet on a flood (or ebb) tide.

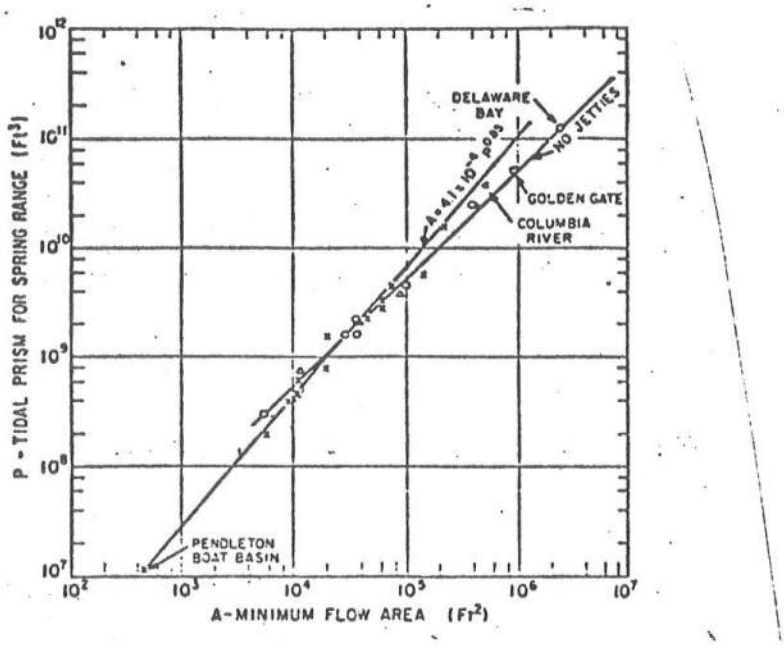

Figure 45. Tidal Prism Versus Minimum Cross-Sectional Flow Area. Empirical Relationship Determined by O'Brien[6].

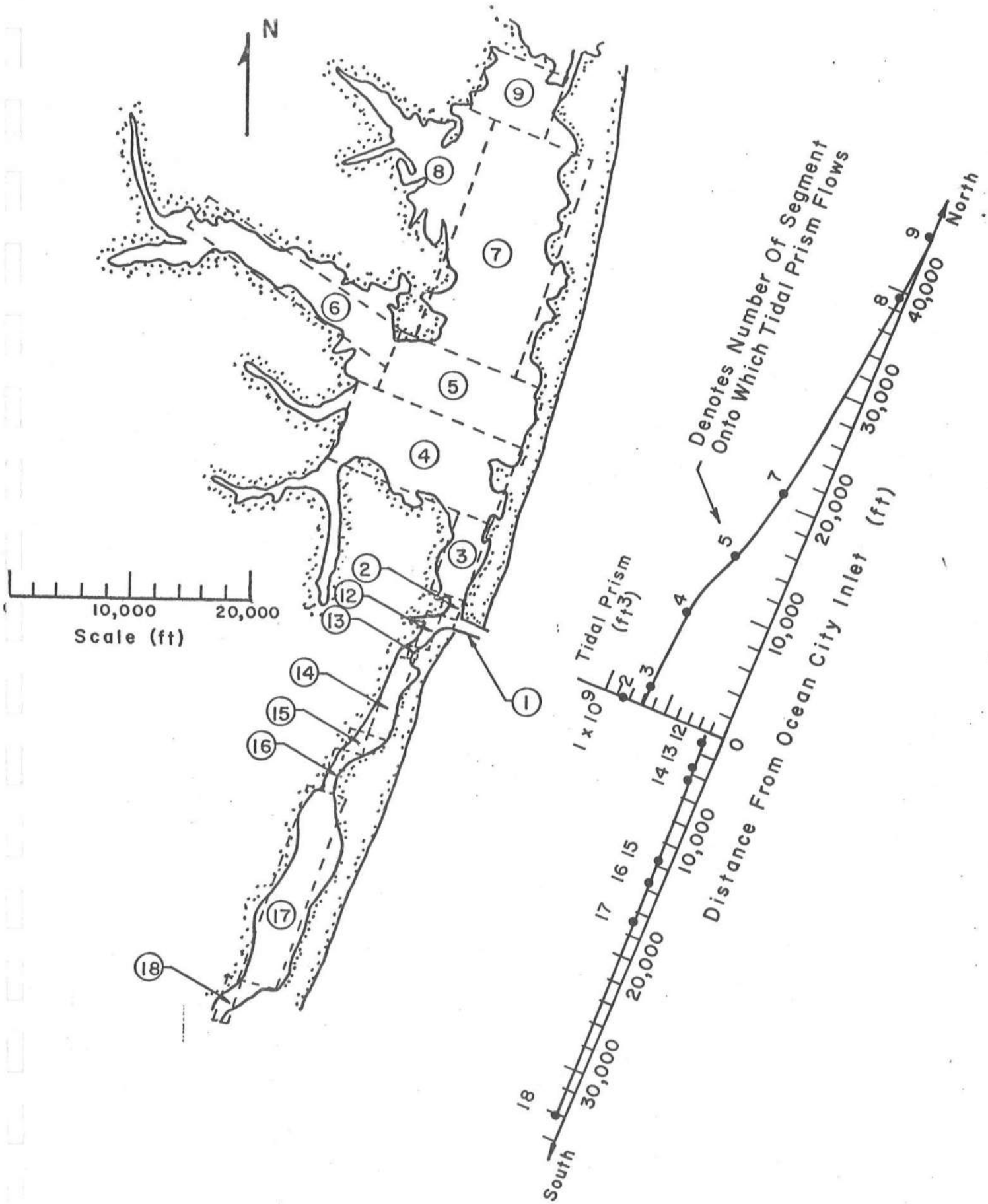

Figure 46. Variation of Calculated Tidal Prism at Various Segment Junctions of Numerical Model.

Tidal Ranges and Lags

Comparisons of measured and calculated ratios of tidal ranges in the Bays to the north and south are presented in Figures 47 and 48 respectively. The corresponding information for tidal lags is presented in Figures 49 and 50 respectively. The agreement is considered reasonable.

A more complete discussion of the numerical model formulation, calibration and results will be deferred to Appendix II.

Interpretation of Water and Sand Flow Patterns Within the Inlet Entrance

Water Flow Patterns

The predominance of water flow (85%) to the north into Isle of Wight Bay as determined from the numerical model has been presented previously. Because the numerical model is only a one-dimensional representation, it does not provide any information relating to the distribution across a cross-section; however, some characteristics can be inferred from knowledge of hydraulics, the inlet bathymetry and experience with other inlets.

Flood Flow. The flood flow into the inlet would occur in a reasonably symmetrical pattern because the north and south jetties extend approximately the same distance seaward. There should be a minor asymmetry with a slight predominance of flow from the south, since the north jetty extends somewhat further seaward than the south jetty.

Ebb Flow. The asymmetry of flows into and from Isle of Wight and Sinepuxent Bays causes a significant effect on the ebb tidal flows at

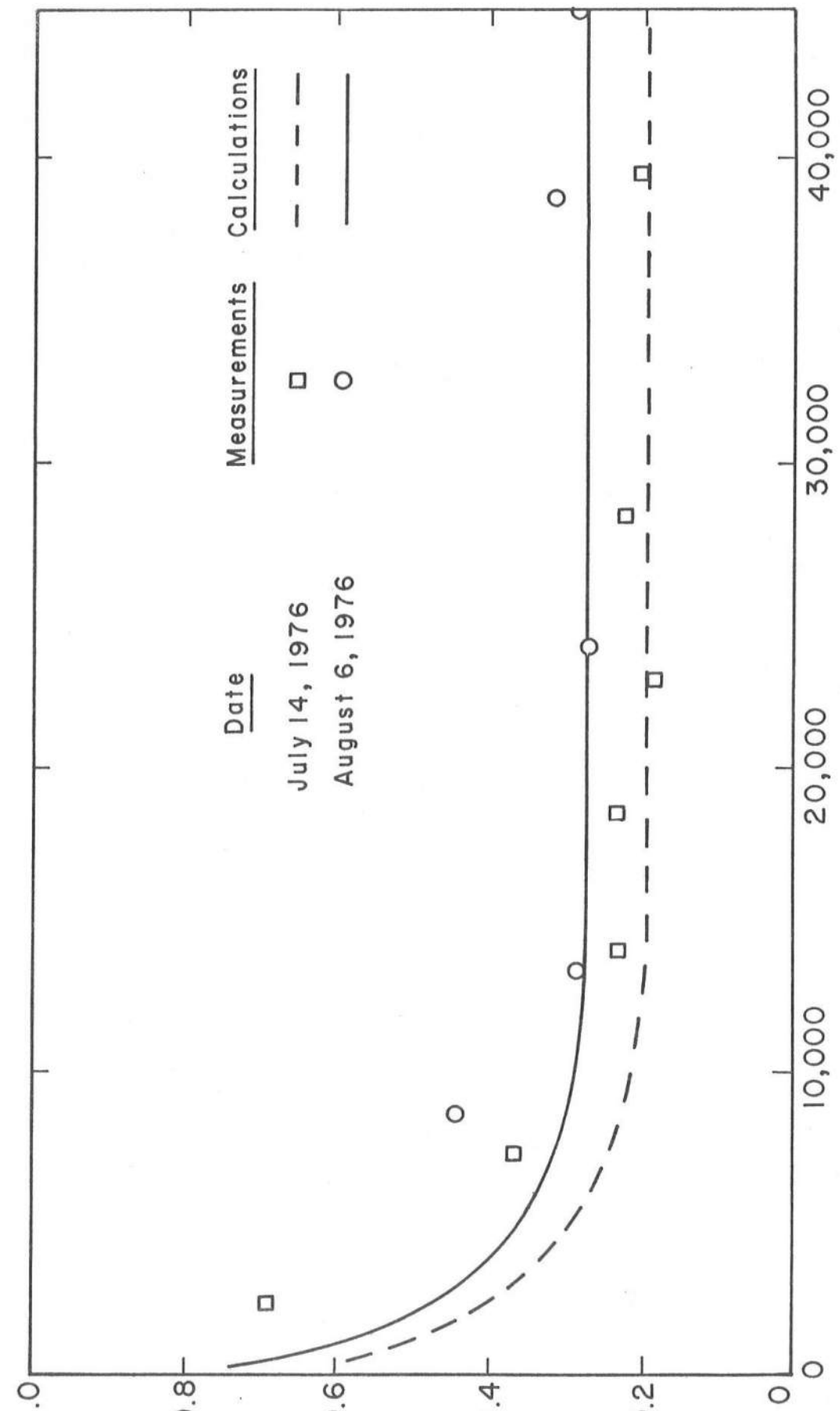

Figure 47. Comparison of Ratios of Measured and Calculated Tidal Ranges in Isle of Wight and Assawoman Bays.

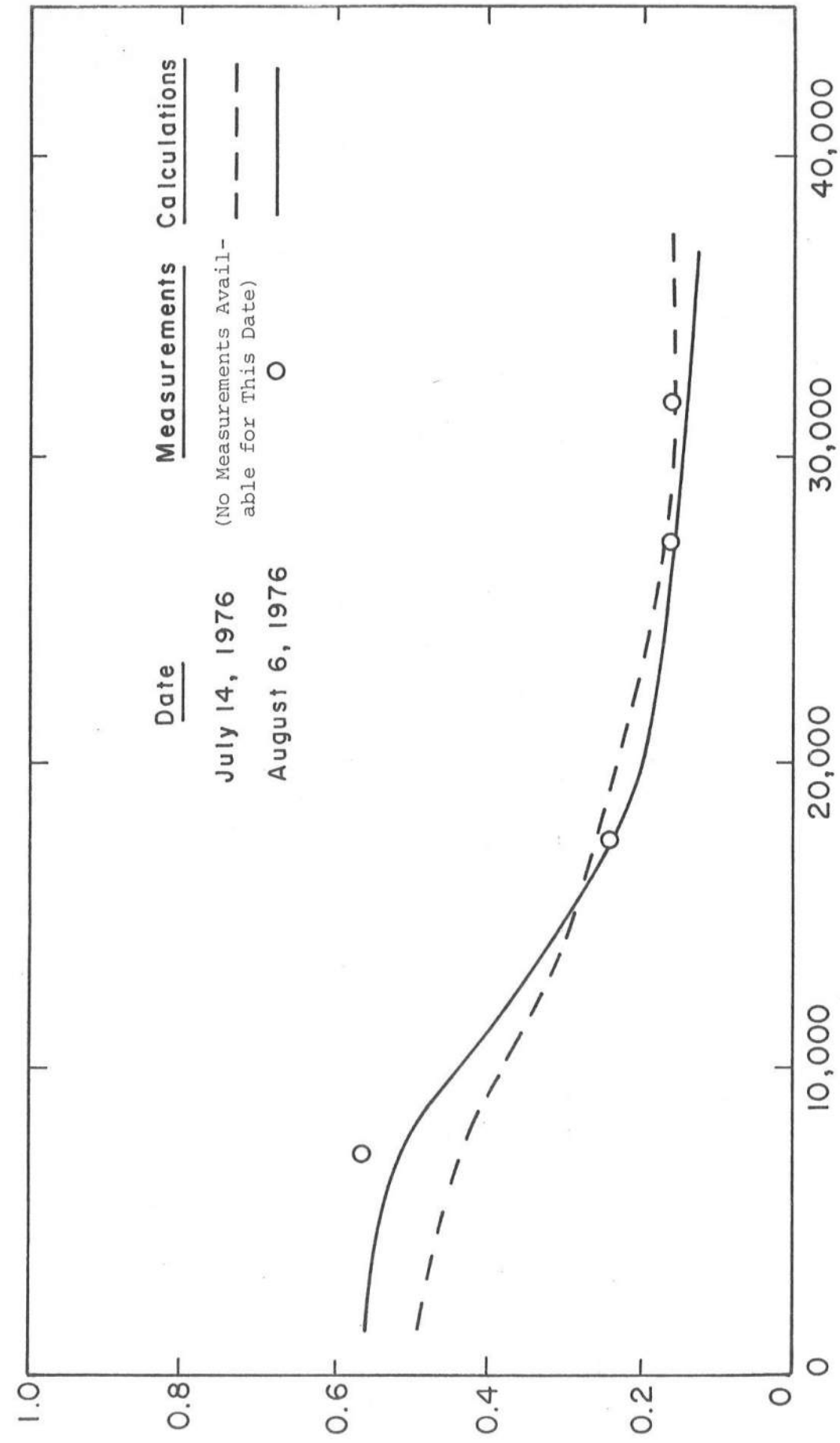

Figure 48. Comparison of Ratios of Measured and Calculated Tidal Ranges in Sinepuxent Bay.

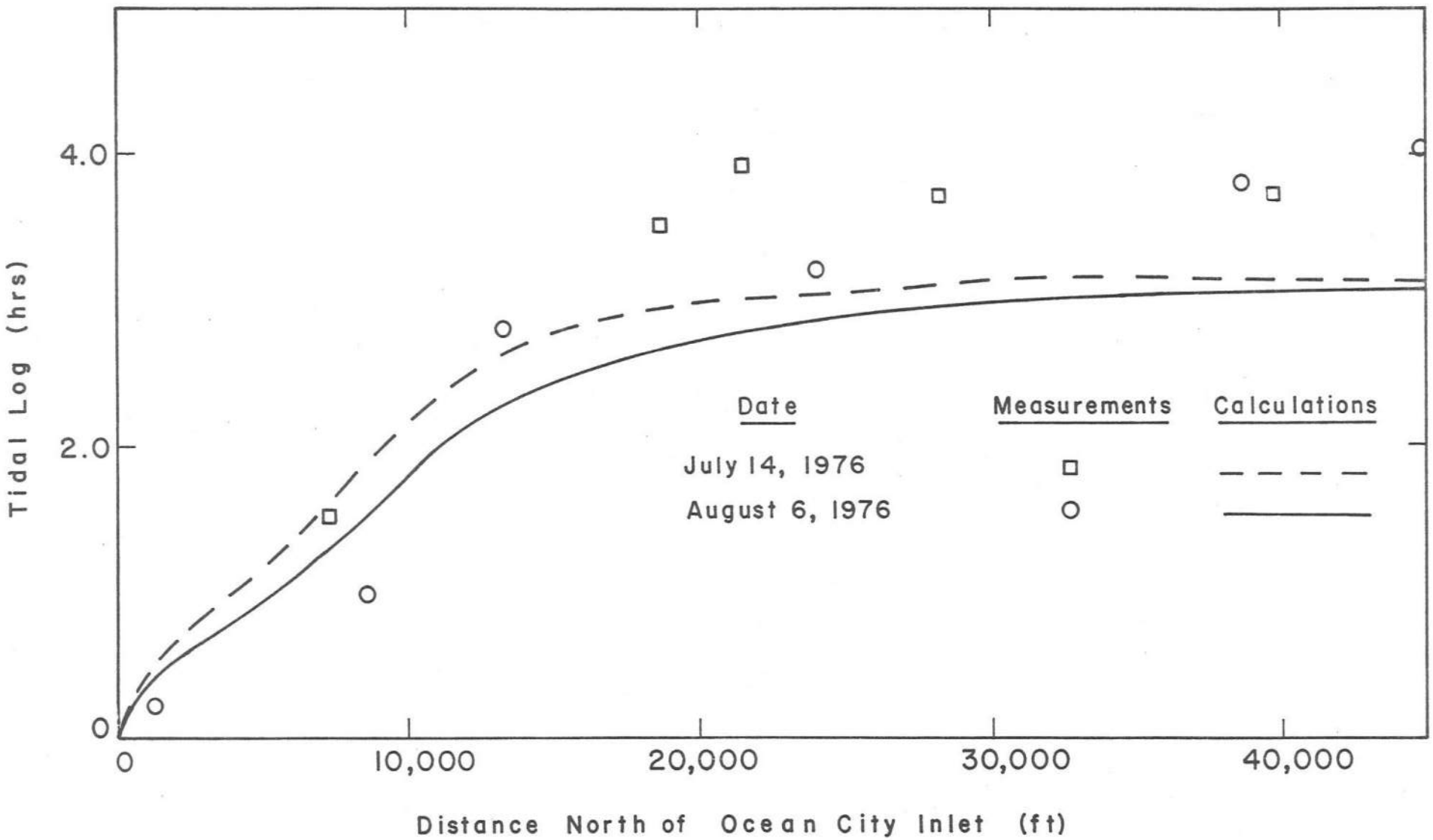

Figure 49. Comparison of Measured and Calculated Tidal Lags in Isle of Wight and Assawoman Bays.

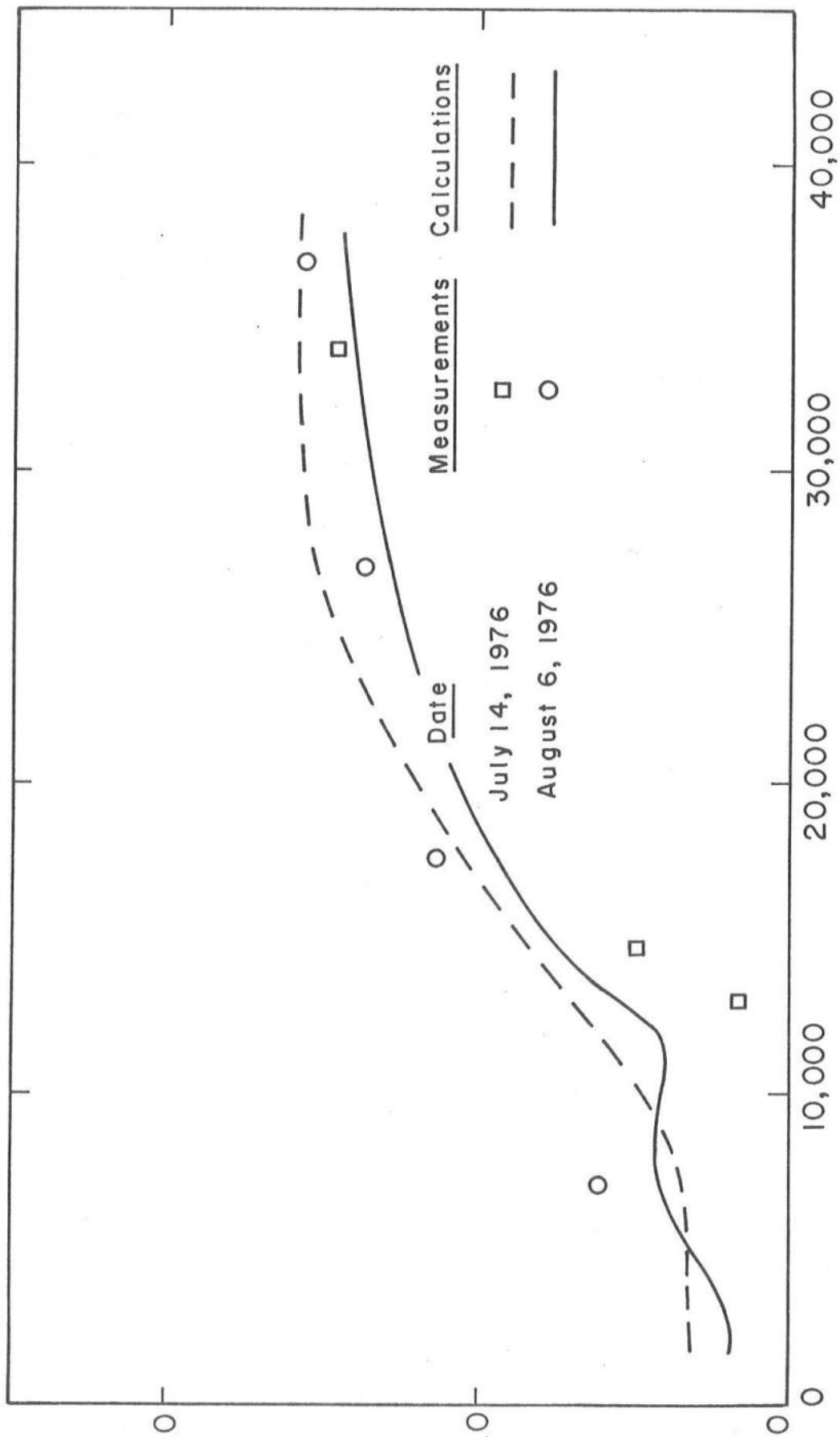

Figure 50. Comparison of Measured and Calculated Tidal Lags in Sinepuxent Bay.

the juncture between the inlet and these two bays. If the ebb flows from the two bays were symmetrical, one would expect that the ebb discharge through the inlet would be centered on the centerline of the inlet. The flow (and momentum) dominance from the north causes the axis of the ebb flow to sweep south of the geometric axis of the inlet. In a sense, the ebb discharge is "trained" by the south jetty and the channel is therefore very close to the south jetty, see Figure 51 which shows the bathymetry in the vicinity of the inlet. In Figure 52, which presents an idealized interpretation of the main ebb and flood tidal currents, the areas deeper than 20 ft. and less than 10 ft. have been shaded and the axis of the ebb channel should lie along the general alignment of the deeper water and, near the inlet entrance, along the south jetty.

Sand Flow Patterns

In the following discussion, it is accepted that along the Ocean City beaches, there is a net southward longshore transport of sand. Although the magnitude is still in question, reasonable estimates are in the range of 50,000 to 150,000 yd^3/year. The north jetty is completely impounded with sand to its full capacity and it is therefore clear that the net alongshore transport is being transported around the north jetty and carried into the inlet by the flood tidal flows.

Flood Flow Sand Transport. Because the source of this sand is at or near the seaward tip of the north jetty, the sand tends to be carried landward along the north portion of the inlet, see Figure 52. This supply (source) of sediment is manifested by the shoal region marked "A" in Figure 52.

Figure 51. Bathymetry in Vicinity of Inlet as Established in this Study.

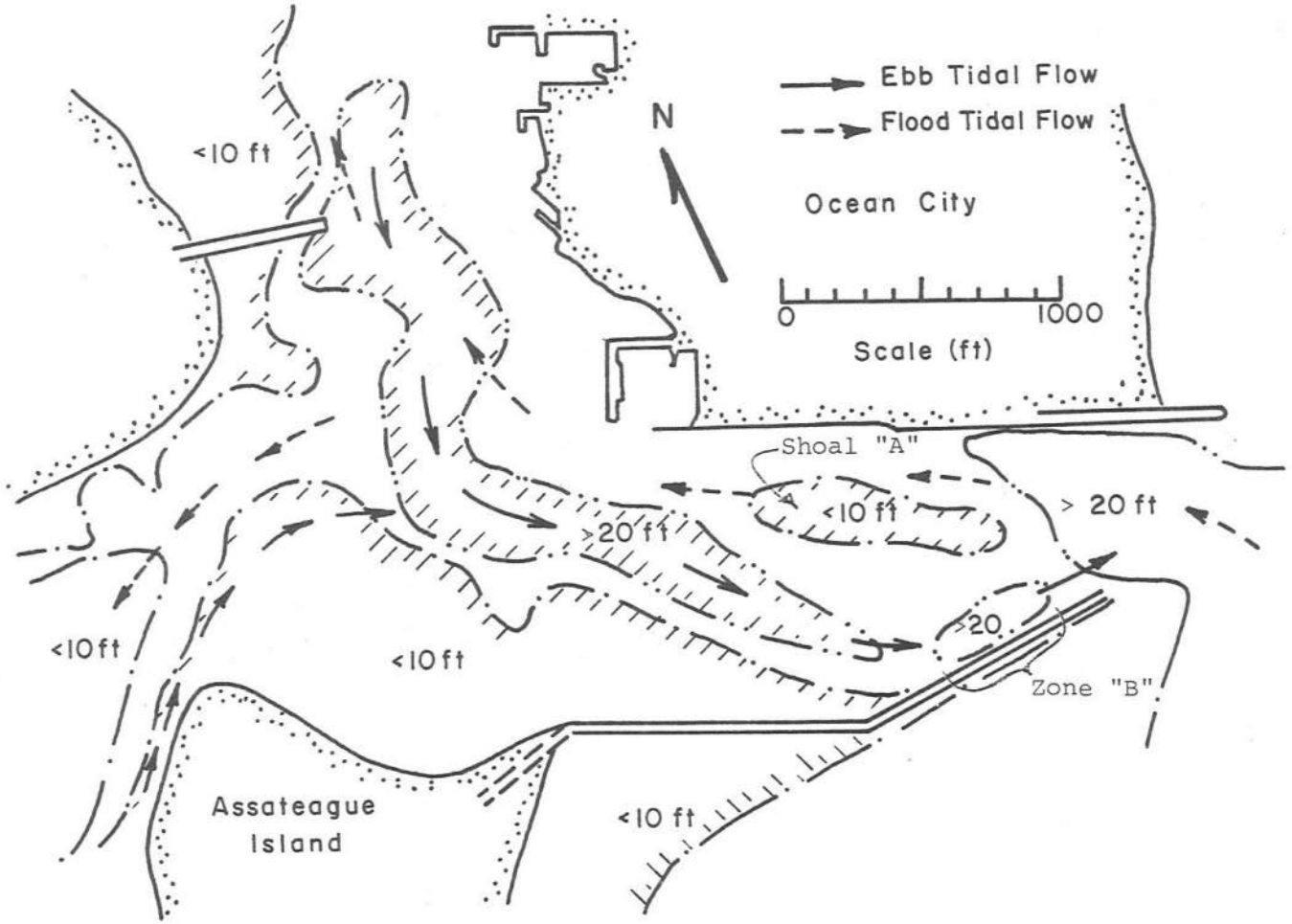

Figure 52. Ocean City Inlet Channels and Shoals and Inferred Ebb and Flood Tidal Flows.

Ebb Flow Sand Transport. It was noted previously that the main ebb flow axis is from Isle of Wight Bay along a sweeping curve aligned adjacent to the south jetty and then more or less directly seaward. The primary flushing of sand from the inlet occurs during ebb flow and reference to the bathymetry indicates that the ebb flow "trims" the base of the deposition occurring from sand entering around the north jetty (labeled "A" on Figure 52). This flow transports the sediment seaward and jets it to the ocean shoal located some 3,000 ft. from the original (pre-inlet) shoreline and some 2,000 ft. from the seaward limits of the jetties. A by-product of this concentration of flow along the south jetty is the deep scour hole and associated degradation of the south jetty at the zone indicated "B" in Figure 52.

It is also of interest to examine the sand transport to the shoal of concern in the navigational channel. Reference to Figure 53 strongly supports the interpretation that the shallow waters immediately adjacent to the north shore of Assateague Island are the combined result of (1) erosion by waves and currents causing the shoreline to recede by longshore transport to the west, and (2) the formation of the shoal formed by the erosion of sand from the northwestern shore of Assateague Island and transported northward by ebb tidal currents. The water currents at this point are directed initially north and then east when they encounter the dominant southeastern directed currents from Isle of Wight Bay. Figure 53 illustrates this transport pattern in this area and Figure 54 is a cross-section looking south along the line A-A shown in Figure 53. Note that the channel is located very close to Assateague Island and that the slope of the profile is fairly close to the angle of repose for sand.

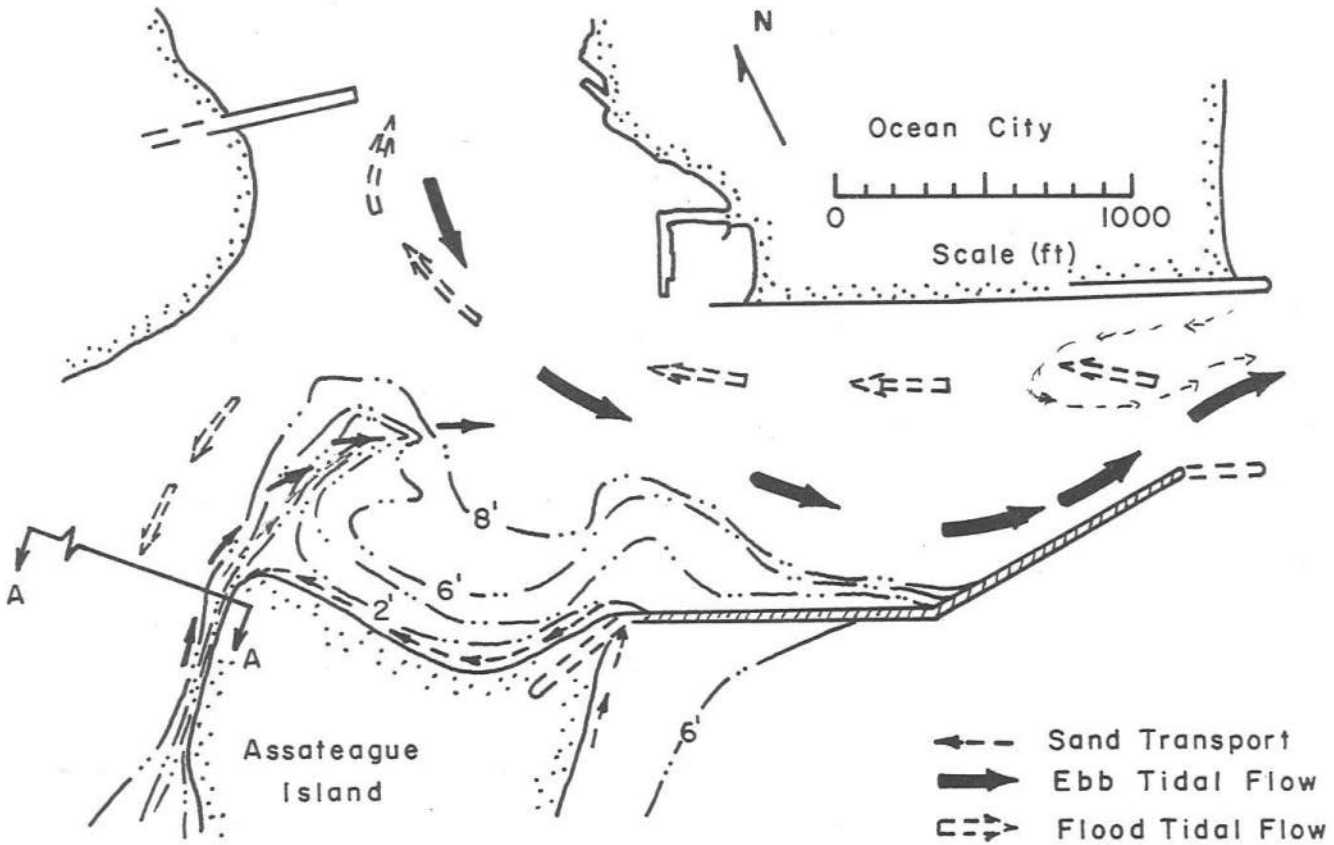

Figure 53. Water and Sand Transport Patterns Near the Shoal of Concern.

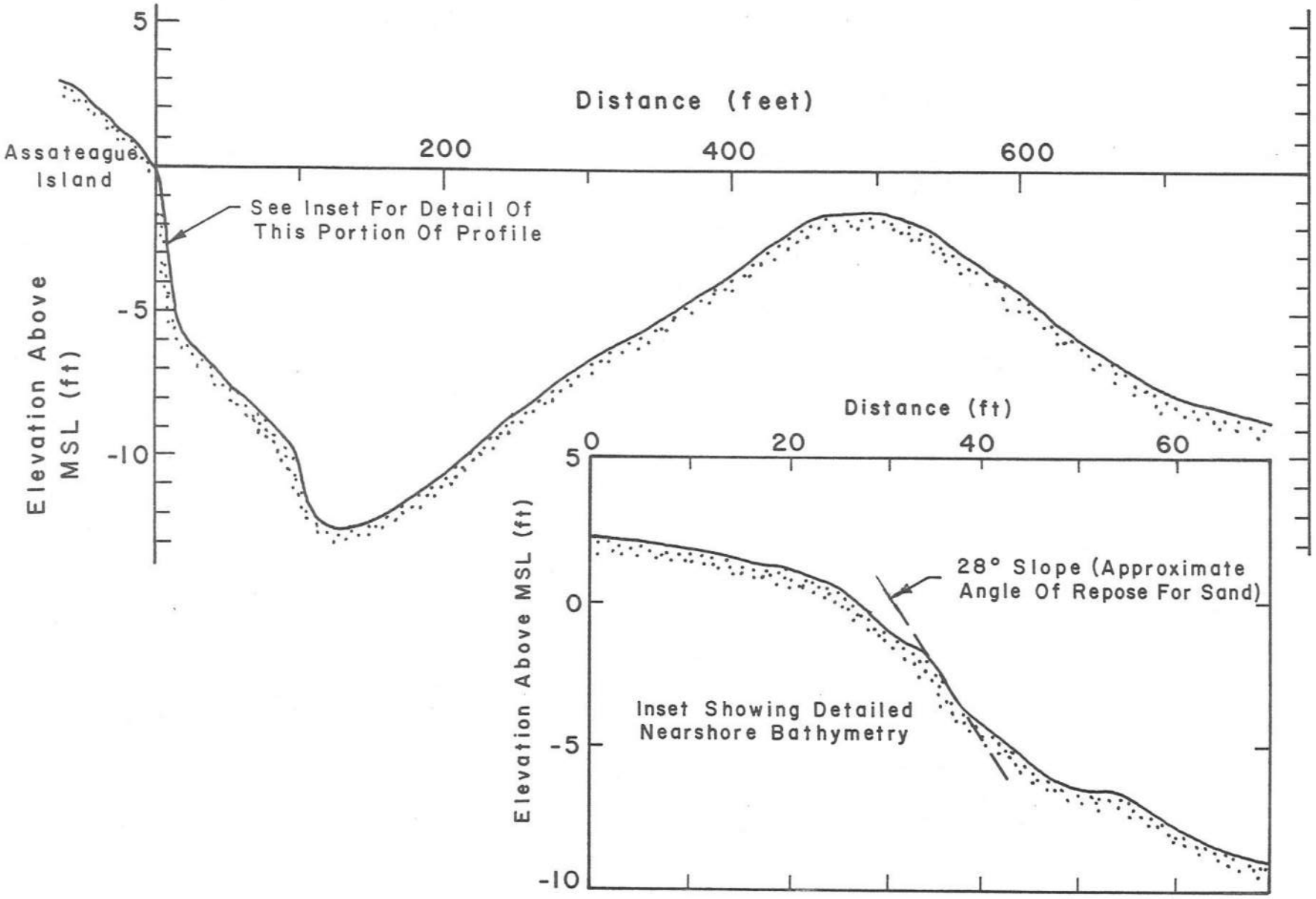

Figure 54. Profile Looking South Adjacent to Northwest Shoulder of Assateague Island (Line A-A in Figure 49).

VIII. SUMMARY OF SALIENT FACTORS RELATED TO SHOALING PROBLEM IN OCEAN CITY INLET

Preceding sections of this report have discussed in detail the results developed during this study which pertain to the shoaling problem in Ocean City Inlet. In this section, in preparation for the recommendations to be made in the following section, an attempt will be made to view, in perspective, those results of greatest importance.

Longshore Sediment Transport Along the Open Coast

Unfortunately, but not atypically in coastal engineering problems, the magnitudes of the average annual net and gross longshore transports in the vicinity of Ocean City must be regarded as poorly known. Estimates of the net longshore transport of approximately 150,000 yd^3/year (southward) have been made based on the early filling rates adjacent to the north jetty. These estimates may be biased to the high side as jetty construction will usually cause accretion due to bar material moving ashore even if the net transport is zero. Calculations of net longshore transport based on LEO observations made approximately 8 miles south of the inlet are approximately 80% higher than the estimate presented above.

The best assessment that can be made regarding the longshore transport is that on an average basis, the net annual transport is to the south, and should be in the range 50,000 to 150,000 yd^3/year, although there may be years when the net transport is to the north. This estimate pertains to the situation unaffected by the inlet. As noted previously, the low south jetty causes a considerable modification of the transport, particularly along the northern shore of Assateague Island.

Tidal Flow Patterns in Inlet

Approximately 85% of the inflow tidal prism is into Isle of Wight Bay (north) and the remainder into Sinepuxent Bay. The asymmetries of the seaward ends of the jetties and the distribution of flows to Isle of Wight and Sinepuxent Bays are such that the flood flow occurs predominantly along the northern portion of the inlet and, due to momentum, sweeps north and south into the two bays along their western sides. The dominant ebb currents from Isle of Wight Bay sweep south and along the south jetty causing a deep scour at the point where the jetty changes alignment. The northward ebb flow from Sinepuxent Bay is deflected eastward by and flows seaward with the flow from Isle of Wight Bay. Figures 52 and 53 depict the water flow patterns.

Sand Transport Patterns in Inlet

Sand is presently entering the inlet from both the north (Ocean City) and south (Assateague Island) beaches. The sand from the north beaches is due to the net longshore transport and the fact that the north jetty is impounded to capacity. The sand enters primarily under the action of the flood currents and is carried westward and results in a large shoal (Figure 52) located adjacent to the north jetty where there is a balance between the flood and ebb currents. The ebb currents "trim" the south base of this shoal and carry the sand seaward. The shoal appears in a rough equilibrium in which the volume of sand carried past the north jetty is balanced by that transported seaward from the shoal by the ebb currents. A portion of the sand carried seaward is deposited in the large shoal (estimated volume = 8,000,000 cubic yards) which is approximately 2,000 ft. east of the seaward

ends of the jetties. As noted, the sand which enters the inlet from Assateague Island is due to waves mobilizing the sand which then passes over and through the south jetty, is transported by waves westward around and temporarily deposited on the northwest corner of Assateague Island. This sand is then transported northward and deposited in a shoal which extends into the navigational channel.

From considerations of remedial measures, it is noteworthy that: (1) the inlet appears to have considerable flushing capacity and if the source(s) of sand could be reduced, the need for dredging should be correspondingly reduced; (2) from the standpoint of shoaling in the area of concern, it is clear that sand entering from Assateague Island is much more of a problem than that from Ocean City beaches; and (3) if sand could be prevented from entering the inlet from the Ocean City beaches, there would be a possibility of improving the alignment of the channel (due to reduction or elimination of the shoal marked "A" in Figure 52).

Causes of Shoaling

There are clearly two dominant modes of sand transport from Assateague Island to inside the inlet where further transport to the shoal is possible. The first and most dramatic has occurred during relatively short periods when the south jetty is flanked and flood tidal currents and waves transport large volumes of sand into the inlet. An example is the October 1961-May 1962 period when it is estimated from aerial photography that approximately 250,000 yd^3 was transported into the inlet. The second is a more continuous mode and is the transport of sand over and through the low and permeable south jetty.

Effect of Reduction of Sand Supply to North Shore of Assateague Island

The sand transport pathway along the north (inlet) shore of Assateague Island has been discussed. If the supply of sand to this shore is reduced, further erosion will occur. It is therefore clear that if the requirement for dredging is to be lessened by reducing the sand supply through the south jetty, it will be necessary to stabilize the north shore of Assateague Island if continuing recession is to be prevented.

IX. RECOMMENDATIONS

This study has established the following primary sand transport pathway leading to the shoaling in the Ocean City Inlet navigational channel: Sand is transported from Assateague Island northward over and through the south jetty, around the north shore of Assateague Island, temporarily residing on the northwest shoulder on Assateague Island and finally swept by ebb currents to the problem shoaling area. Figure 55 portrays this sand transport pathway. The feature of the inlet/jetty system that leads to this sand transport and shoaling is the low and permeable inshore portion of the south jetty. This crest of the inshore section of the south jetty is at an approximate elevation of 4.5 ft. (MSL) whereas the natural berm elevation is approximately 7 to 8 ft. above MSL. This difference in elevation, combined with the mobilizing action of breaking waves, results in a northward transport of sand, even though the waves are propagating normal to shore or at some angle toward the south such that under normal conditions southward sand transport would occur. During extreme storms, the south jetty has been flanked, a condition which is extremely conducive for substantial sand transport quantities northward from Assateague Island.

To remedy the situation noted above, it is recommended that the south jetty be modified to reduce significantly (ideally eliminate) the northward sand transport over and through the south jetty. This will require: (1) increasing the crest elevation of the south jetty, and (2) rendering the jetty sand-tight. This modification will result in a reduction in sand losses from the ocean shoreline of Assateague Island and also a reduction in the shoaling rate in the entrance channel. It is important to recognize that the present sand flow over the south jetty

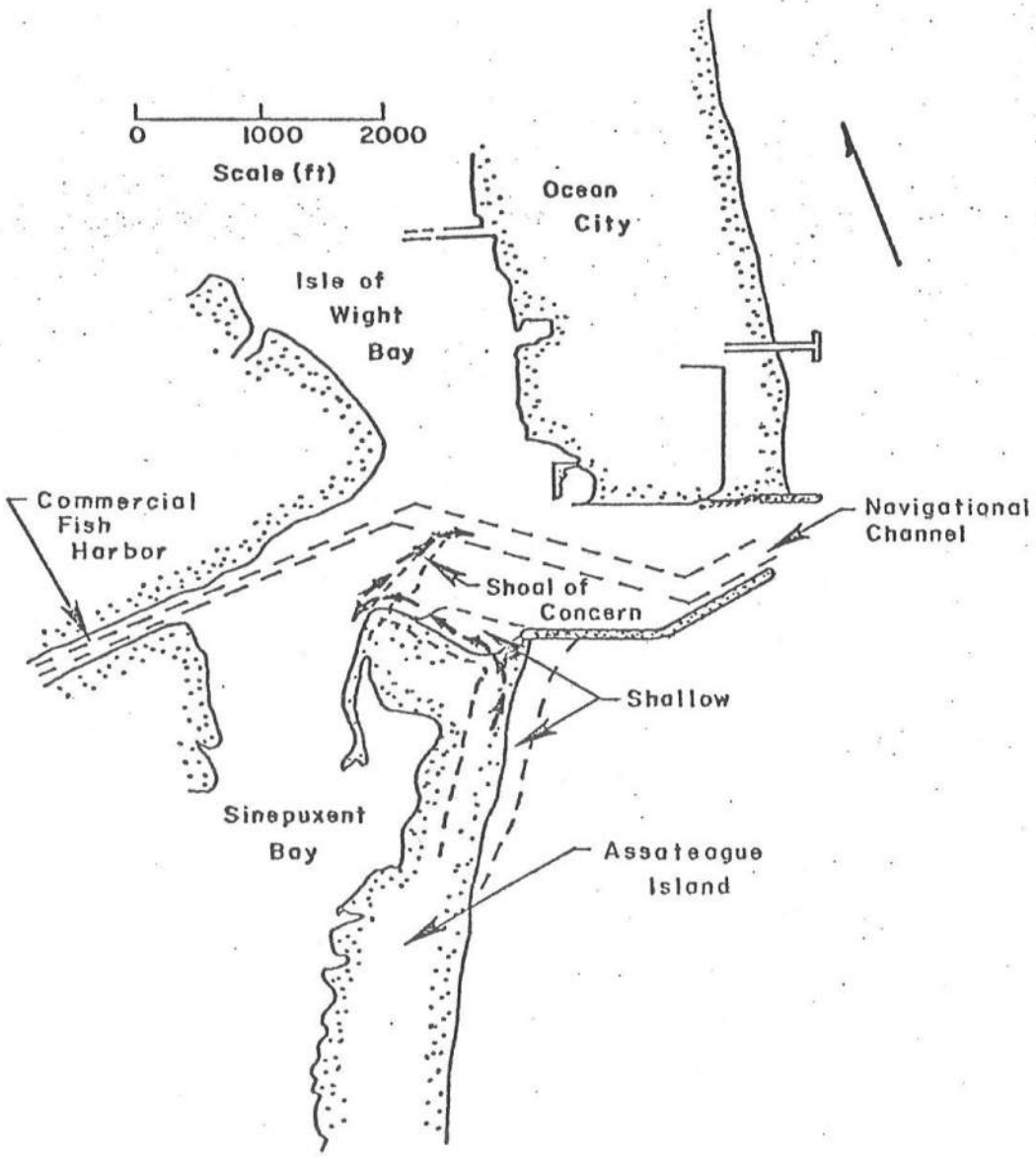

Figure 55. Sand Transport Pathways From North Ocean Shore of Assateague Island to Shoal of Concern.

and around the north tip of Assateague Island provides a stabilizing effect on the north (inlet) shore of Assateague Island. Therefore, any measures which reduce this sand supply should be accompanied by stabilization of the north shore of Assateague Island. If this stabilization is not carried out, sand will continue to be derived (by erosion) from and transported along the north shore of Assateague Island. This will eventually stabilize; however, as will be discussed later in this section, there are strong considerations indicating the desirability of stabilizing the north shore.

The following paragraphs describe, in conceptual terms, recommended design features of the south jetty and stabilization of the north shore of Assateague Island.

Modification of South Jetty

It is recommended that modifications be made to the south jetty to result in a significant reduction in the present and future transport of sand over and through this structure. Specifically, the following are recommended:

(1) Increase the crest elevation of the south jetty to at least 7.5 ft. MSL (preferably 9.0 ft. MSL) over a jetty length of 800 ft.

(2) Render a major portion of the south jetty sand tight. Of primary concern is the region lying within the zone of normal and storm breaking waves. Considering a 6 ft. breaking wave, this indicates a depth of approximately 8 ft. Based

on the bathymetric survey conducted in conjunction with this project, this modification would extend an approximate distance seaward of 800 ft.

(3) Provide an extension at the shoreward end of the south jetty to protect against flanking and overtopping during storms.

These recommendations, including specifics and alternatives, where relevant, are discussed in the following paragraphs.

Increased Crest Elevation and Sand-Tightening of South Jetty

As shown in Figure 56, there are two alternative approaches to increasing the crest elevation and reducing the sand transport through the south jetty. The first approach is shown in Figure 56a, and comprises an addition, on the south face of the jetty, of a blanket of quarry run and filter stone capped by armor rock.

The alternate approach to sand-tightening and raising the south jetty would not require the additional quantities of large stone as in the first method outlined. The large stone presently on the south jetty would be removed and later reused for armor stone after construction of the core and intermediate layer. A typical cross-section is shown in Figure 56b. The most appropriate approach will depend on the costs and availability of large rock and the construction methods selected.

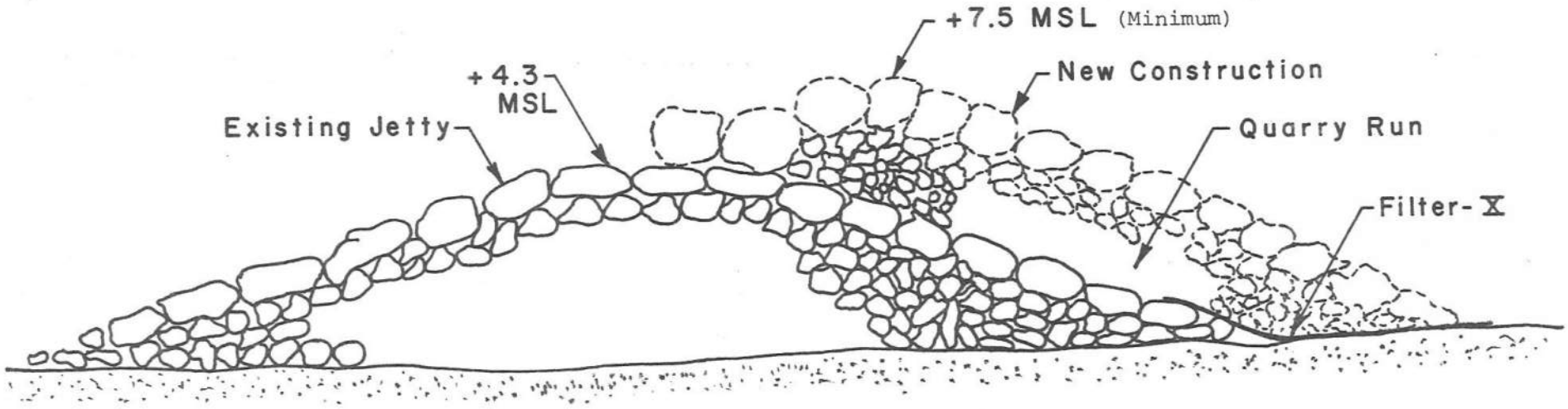

Figure 56a. Rehabilitation of South Jetty by Addition of Graded Rock on South Side of Jetty (Shoreward 800 ft. of Jetty).

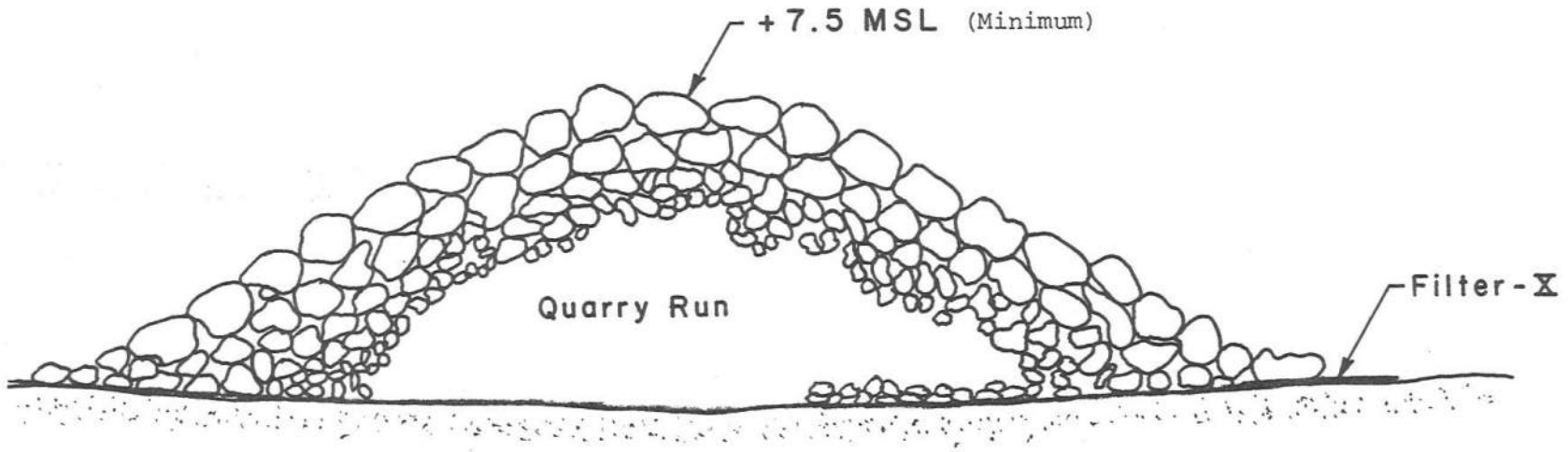

Figure 56b. Reconstruction of Shoreward 800 ft. of South Jetty by Relocating Large Stone.

Figure 56. Two Options for Increasing Crest of South Jetty and Rendering Jetty Sand-Tight.

Extension of Landward Section of South Jetty

Due to the recession of the north shore of Assateague Island the present south jetty is very vulnerable to flanking by a severe storm. If this should occur, significant quantities of sand would be transported into the inlet with a major fraction eventually residing in the navigational channel. Therefore it is strongly recommended that the south jetty be extended to provide an effective "tie" to high ground.

The design features of this tie-in depend on whether or not the north shore of Assateague Island is stabilized. Therefore two conceptual designs will be presented. The recommended design, which will require stabilization of the north shore of Assateague Island, is presented in Figure 57a. Basically the jetty is extended at full height landward a distance of approximately 250 ft. and forms a tie to high ground.

The second design alternative would be required in the event that the north shore of Assateague Island is not stabilized. Because of the expected erosion along the north shore of Assateague Island, this method would be more costly and less reliable. See Figure 57b for a possible layout of this extension.

Stabilization of North Shore of Assateague Island

As discussed, stabilization is recommended for the north shore of Assateague Island due to the anticipated reduction in sand supply. Three alternatives were considered and will be discussed below in their order of preference.

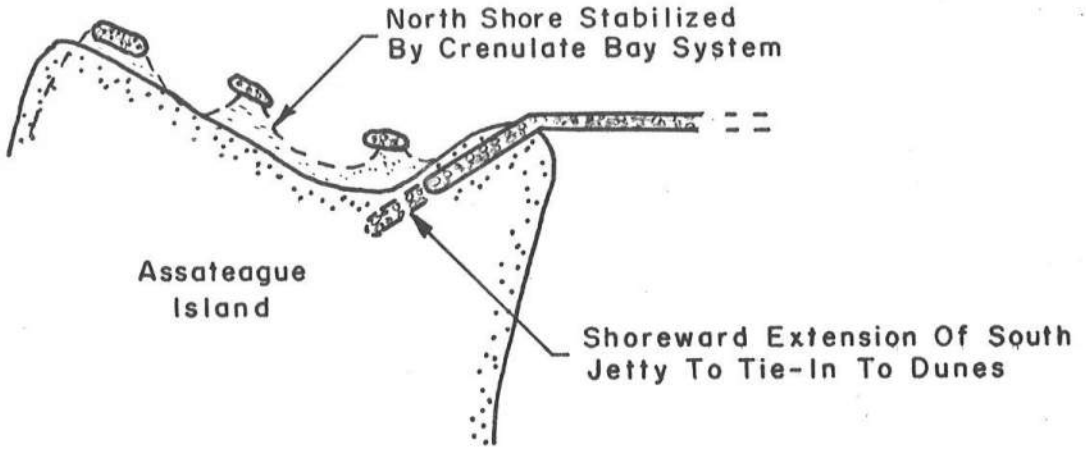

Figure 57a. Shoreward Jetty Extension With Stabilization of North Shore.

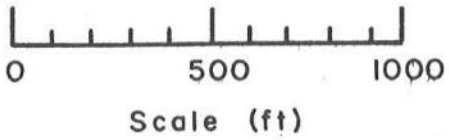

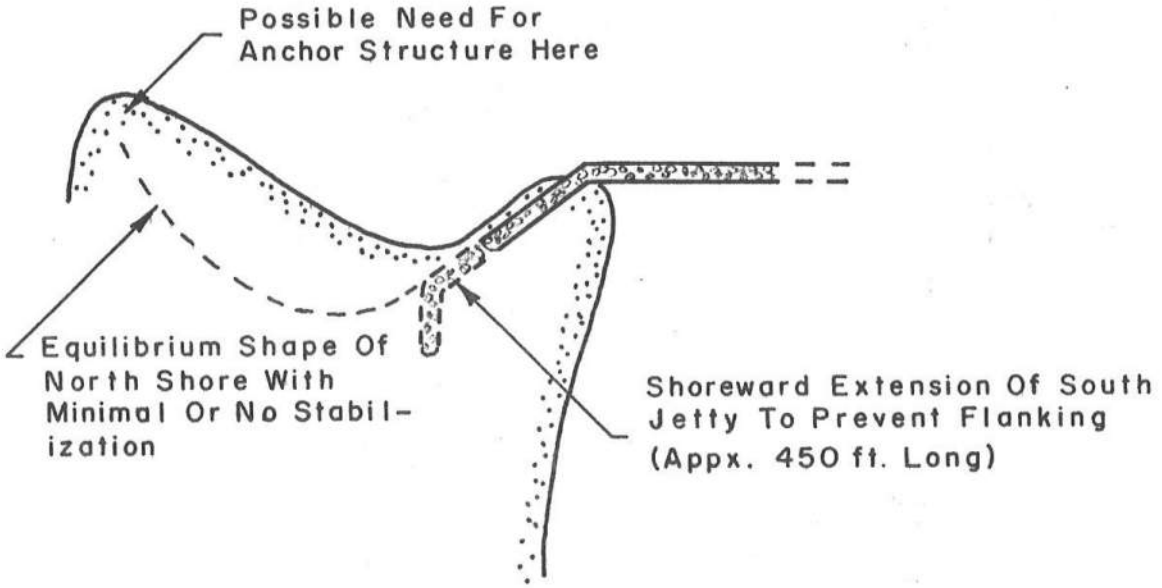

Figure 57b. Shoreward Jetty Extension with Minimal or No Stabilization of North Shore.

Figure 57. Two Options for Shoreward Extension of South Jetty.

Formation of a Series of Crenulate Bays

An innovative approach to shoreline stabilization is that of compartmenting the shoreline into a series of littoral cells through the construction of a series of shore-parallel structures. The resulting shoreline configurations are referred to in a variety of terms: crenulate bays, hooked bays, spiral beaches, etc. The attractive feature of crenulate bays is that primarily through diffraction, they cause a local reorientation of the waves such that the angle of the wave crest to the beach is everywhere such that the amount of sand available is transported. There can thus be a shoreline in equilibrium even without any sand transport. Figure 58a presents a conceptual layout of the stabilization of the north shore of Assateague Island by crenulate bays. As shown in Figure 59 and noted previously, if there is sand transport to the cell, the shoreline orientation will be modified to pass the amount transported to the cell. Additional advantages of the concept of shoreline stabilization by crenulate bays are their comparatively low cost and recreational attractiveness due to a variation of wave energy along the shoreline.

Terminal Structure on Northwest Shoulder of Assateague Island

One possibility of preventing further losses of sand from the north shore of Assateague Island and reducing sand transport into the navigational channel would be to construct a terminal structure on the north shore of Assateague Island as shown conceptually in Figure 58b. A somewhat more elaborate and effective method would utilize one or more intermediate shore-perpendicular structures (groins) thereby compartmenting the shoreline. This method has a number of features similar to the crenulate bay approach.

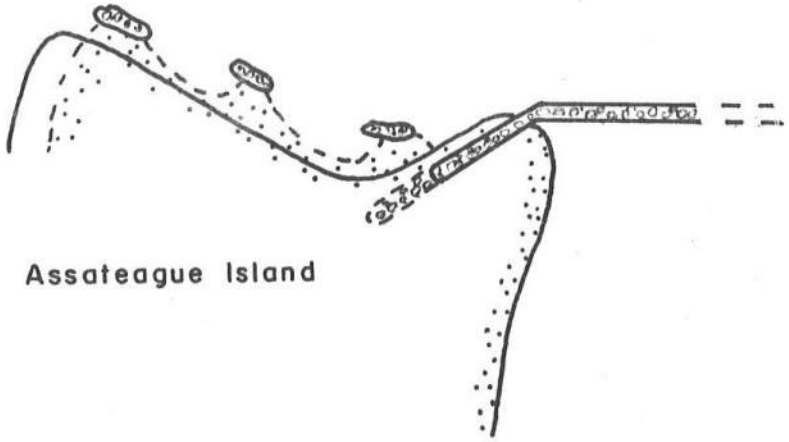

Figure 58a. Stabilization of North Shore by Shore-Parallel Structures to Form Crenulate Bays.

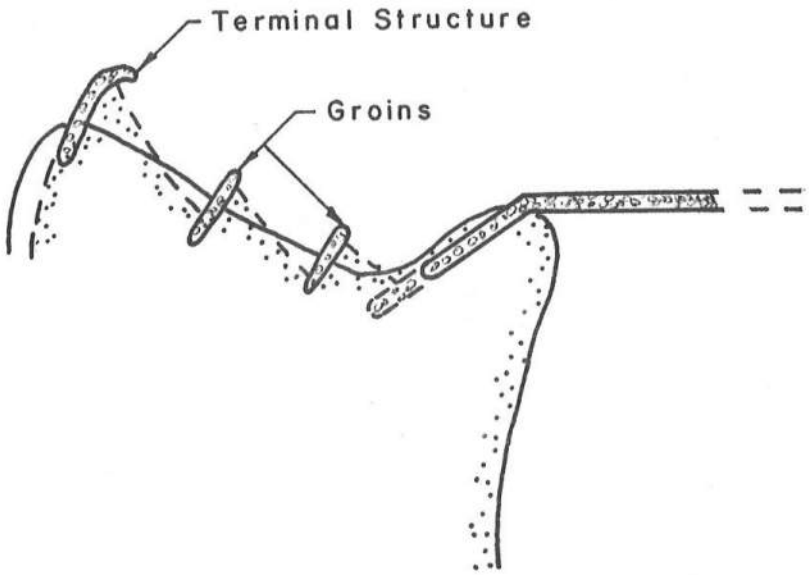

Figure 58b. Stabilization of North Shore by Terminal Structure and Intermediate Groins.

Figure 58. Options for Structural Stabilization of North Shore of Assateague Island.

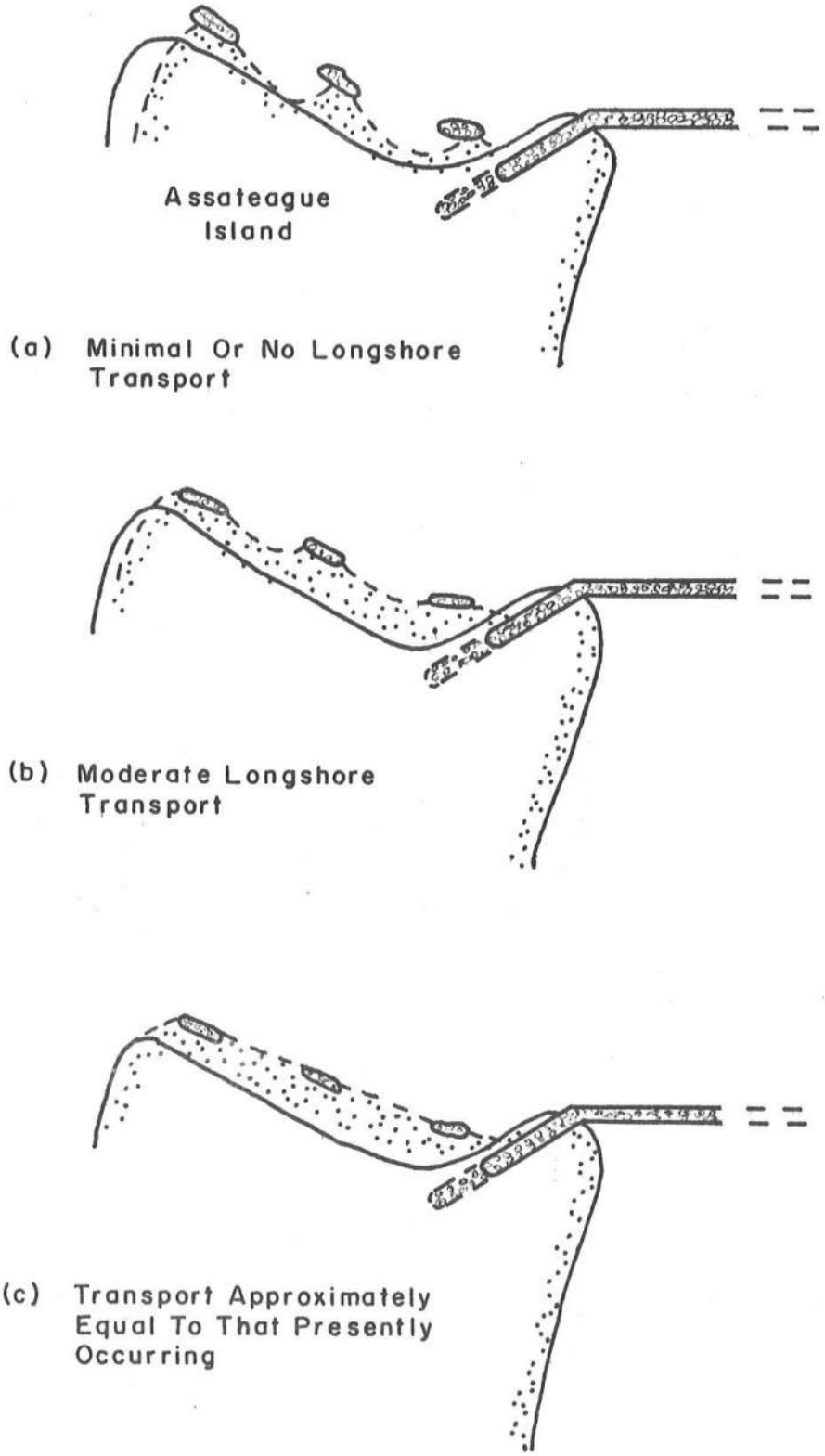

Figure 59. Equilibrium Crenulate Bay Shoreline Shapes For Various Amounts of Longshore Transport.

The crenulate bay approach is believed to be preferable although the terminal structure with intermediate groins should prove workable.

Revetment of North Shore of Assateague Island

This method of stabilization comprises the placement of a graded continuous revetment along the entire north shoreline of Assateague Island. Disadvantages include the relatively high cost and the high probability that with the reduction in sand supply, there will be very little beach remaining between the revetment and the inlet water line.

X. REFERENCES

1. Dean, R. G., and M. Perlin, "Coastal Engineering Study of Ocean City Inlet, Maryland", Proceedings, ASCE Specialty Conference "Coastal Sediments '77", Charleston, South Carolina, p. 520-542.

2. Hayes, M. O., "Morphology of Sand Accumulation in Estuaries: An Introduction to the Symposium", Vol. II, Estuarine Research, Academic Press, New York, p. 3-22.

3. Jarrett, J. T., "Tidal Prism - Inlet Area Relationship", Department of the Army, U. S. Army Corps of Engineers, GITI Report 3, February, 1976.

4. Kraft, J. C., "Sedimentary Facies Patterns and Geologic History of a Holocene Marine Transgression", Bulletin, Geological Society of America, Vol. 82, 1971, p. 2131-2158.

5. Maurmeyer, E. M., "Analysis of Short- and Long-Term Elements of Coastal Change in a Simple Spit System: Cape Henlopen, Delaware", M.S. Thesis, Department of Geology, University of Delaware, 1974.

6. O'Brien, M. P., "Equilibrium Flow Areas of Inlets on Sandy Coasts", J. Waterways, Harbors and Coastal Engineering Division, ASCE, Vol. 95, No. WW1, pp. 43-52, Feb., 1969.

7. U. S. Army Corps of Engineers, Baltimore District, "Ocean City Harbor and Inlet and Sinepuxent Bay, Maryland; Design Memorandum No. 1, Restoration of North Jetty", November, 1954.

8. U. S. Army Corps of Engineers, Baltimore District, "Disaster Recovery Operations From 6-8 March 1962 Storm", December, 1962.

9. U. S. Army Corps of Engineers, Baltimore District, "Ocean City Harbor and Inlet and Sinepuxent Bay, Maryland; Design Memorandum No. 2, Restoration of South Jetty", February, 1963.

10. U. S. Army Corps of Engineers, Philadelphia District, "Beach Erosion Control and Hurricane Protection Along the Delaware Coast", 1966.

11. U. S. Army Corps of Engineers, "Atlantic Coast of Maryland and Assateague Island, Virginia", Draft of Survey Report, February, 1972.

12. Wicker, C. F., "Report on Shoaling, Ocean City, Maryland to Commercial Fish Harbor", Report to the Baltimore District, U. S. Army Corps of Engineers, December, 1974.

APPENDIX I

OCEAN BASELINE AND BEACH PROFILES

ON ASSATEAGUE ISLAND

INTRODUCTION

This appendix presents, for reference purposes, the profiles measured on Assateague Island. The baseline for these profiles has been presented previously as Figure 38.

KEY

- - - - Profile of South Jetty Projected on a Line Normal to Main Beach Alignment.
— . — Beach Profile: September 1, 1976.
——— Beach Profile: February 19, 1977.
. - - . Beach Profile: June 1, 1977.

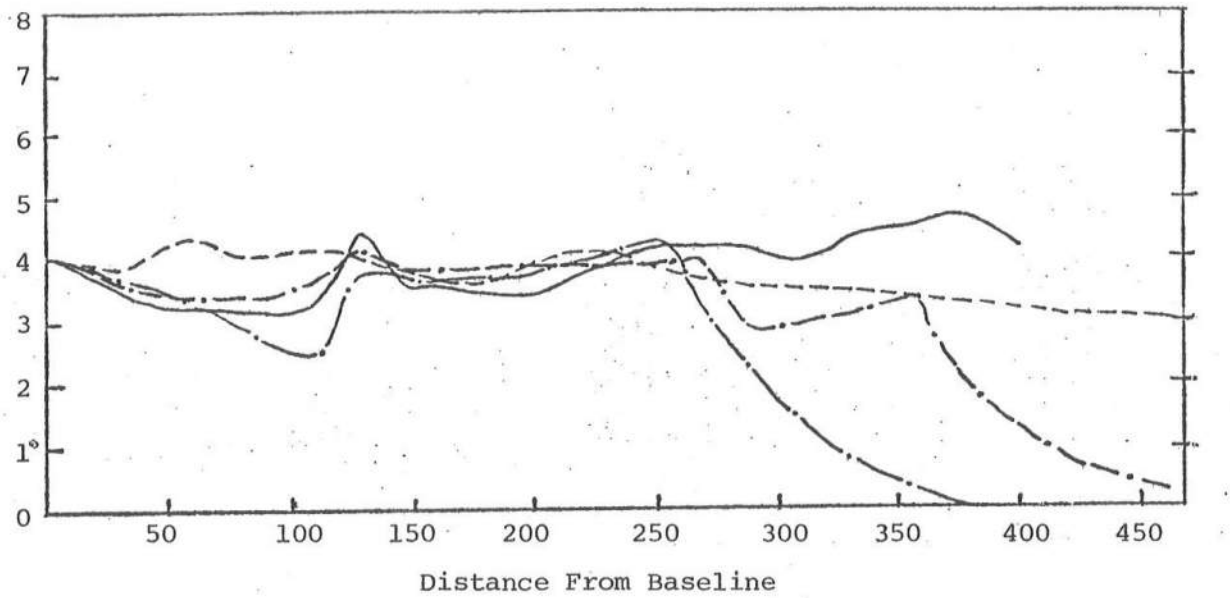

LINE 1-A

KEY

- - - - Profile of South Jetty Projected on a Line Normal to Main Beach Alignment.
— . — Beach Profile: September 1, 1976.
——— Beach Profile: February 19, 1977.
. - - . Beach Profile: June 1, 1977.

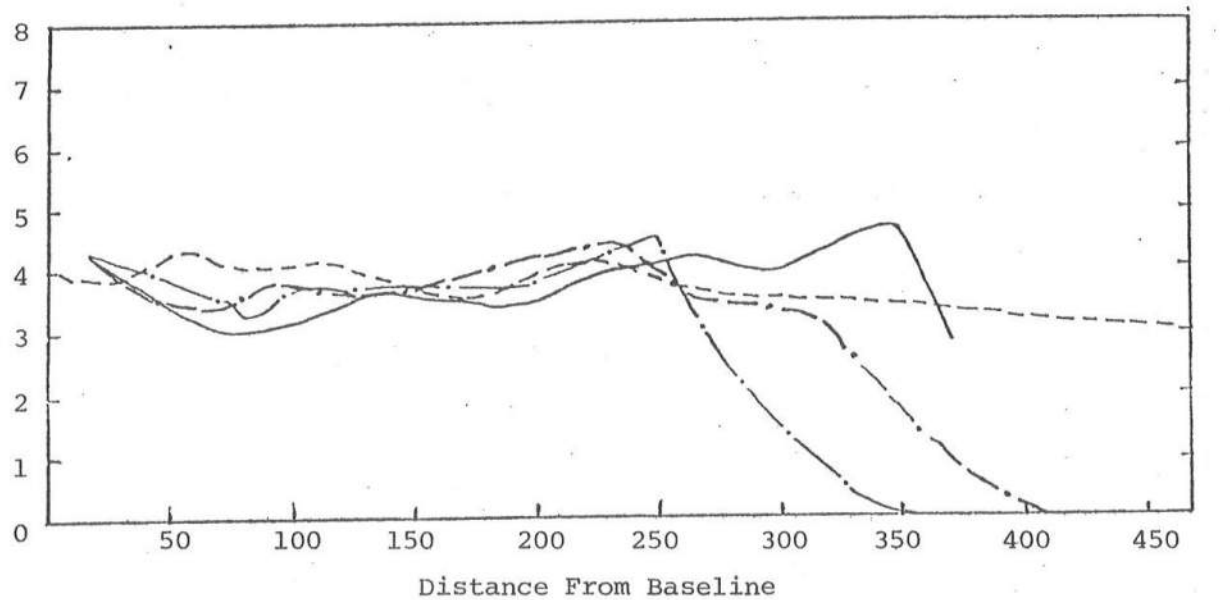

LINE 1-B

Figure I-1. Beach Profiles For Lines 1-A and 1-B, Assateague Island.

KEY

- - - - Profile of South Jetty Projected on a Line Normal to Main Beach Alignment.
— . — Beach Profile: September 1, 1976.
——— Beach Profile: February 19, 1977.

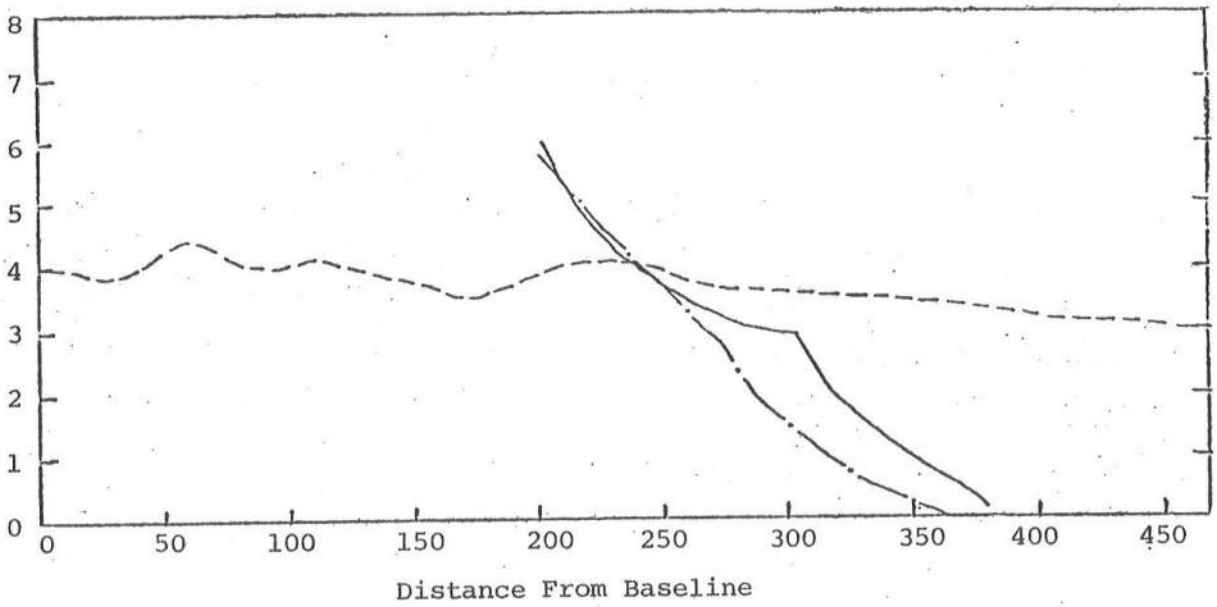

STATION 1

KEY

- - - - Profile of South Jetty Projected on a Line Normal to Main Beach Alignment.
— . — Beach Profile: September 1, 1976.
——— Beach Profile: February 19, 1977.

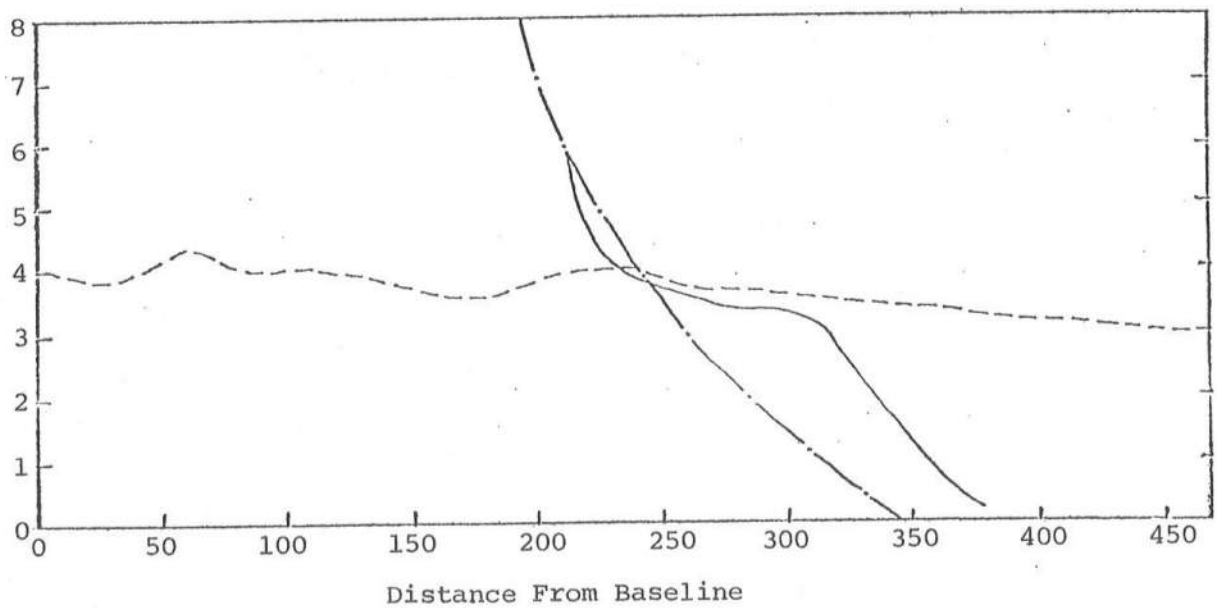

STATION 1-200

Figure I-2. Beach Profiles for Stations 1 and 1-200, Assateague Island.

KEY

- - - - Profile of South Jetty Projected on a Line Normal to Main Beach Alignment.
— . — Beach Profile: September 1, 1976.
——— Beach Profile: February 19, 1977.
. - - - . Beach Profile: March 19, 1977.
- - . - - Beach Profile: June 1, 1977.

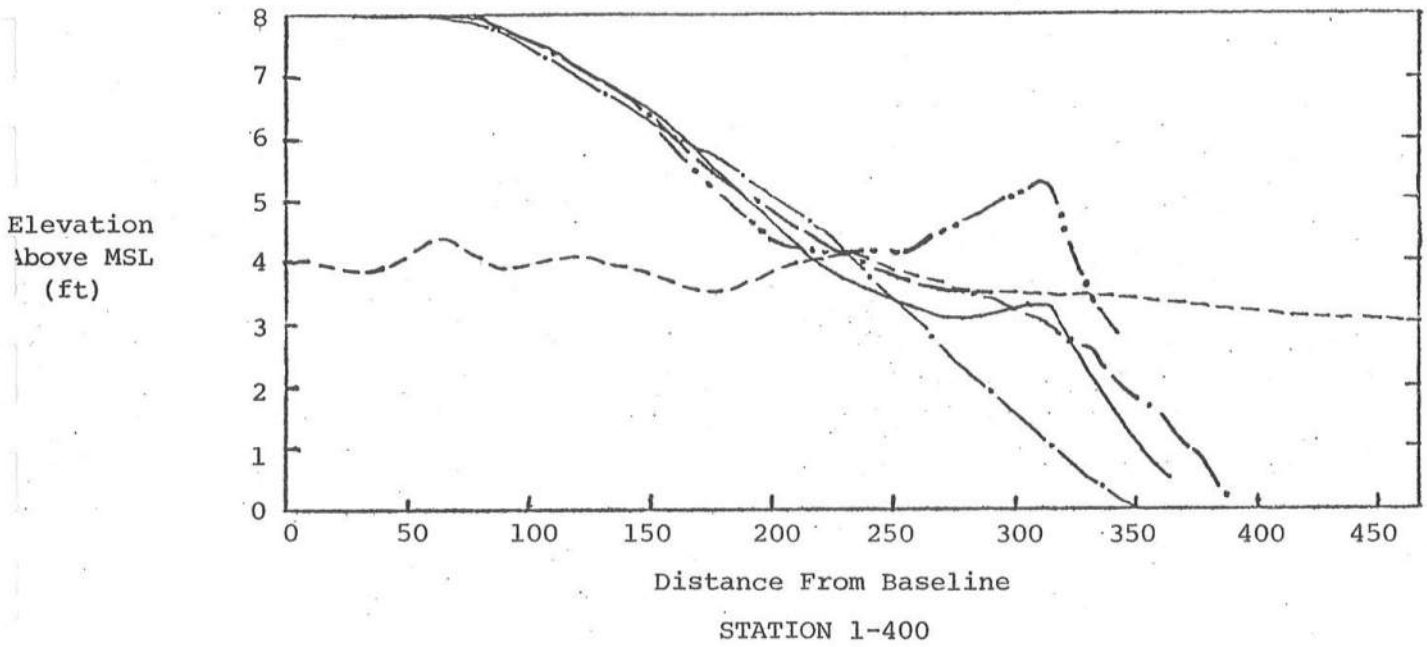

STATION 1-400

KEY

- - - - Profile of South Jetty Projected on a Line Normal to Main Beach Alignment.
— . — Beach Profile: September 1, 1976.
——— Beach Profile: March 1, 1977.

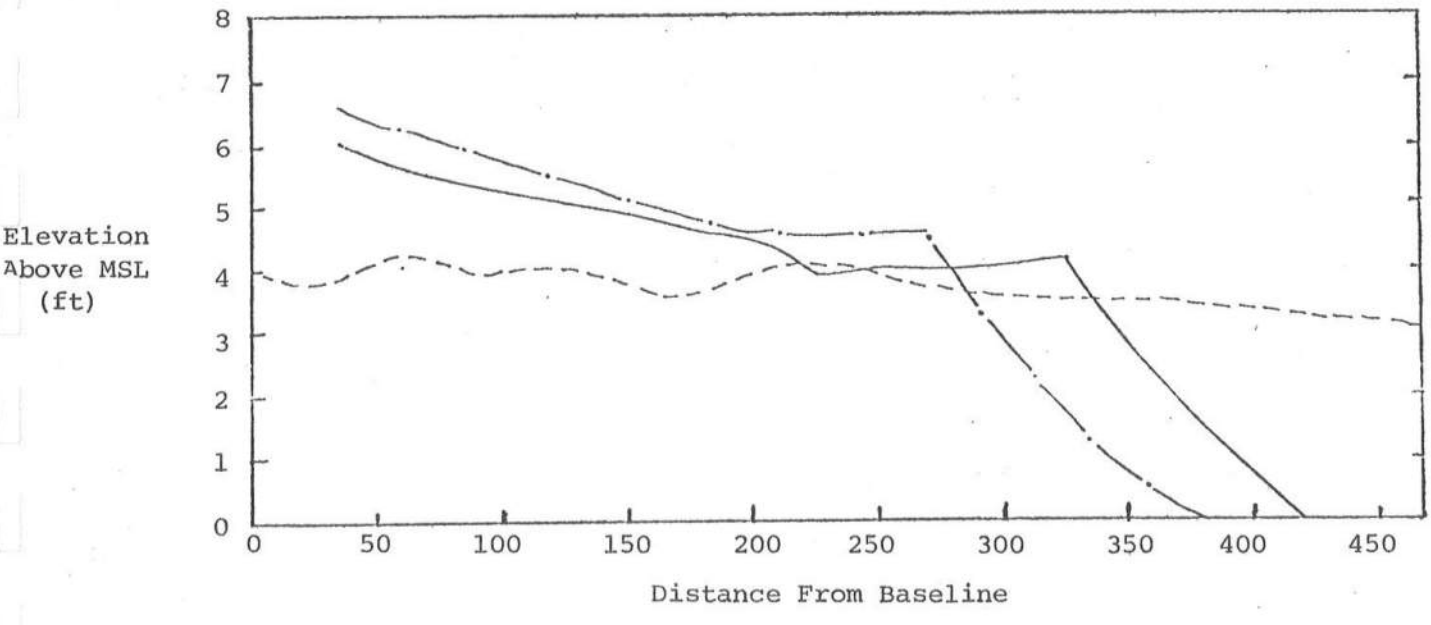

STATION 1-600

Figure I-3. Beach Profiles for Stations 1-400 and 1-600, Assateague Island.

KEY

- - - - Profile of South Jetty Projected on a Line Normal to Main Beach Alignment.
__ . __ Beach Profile: September 1, 1976.
_____ Beach Profile: March 19, 1977

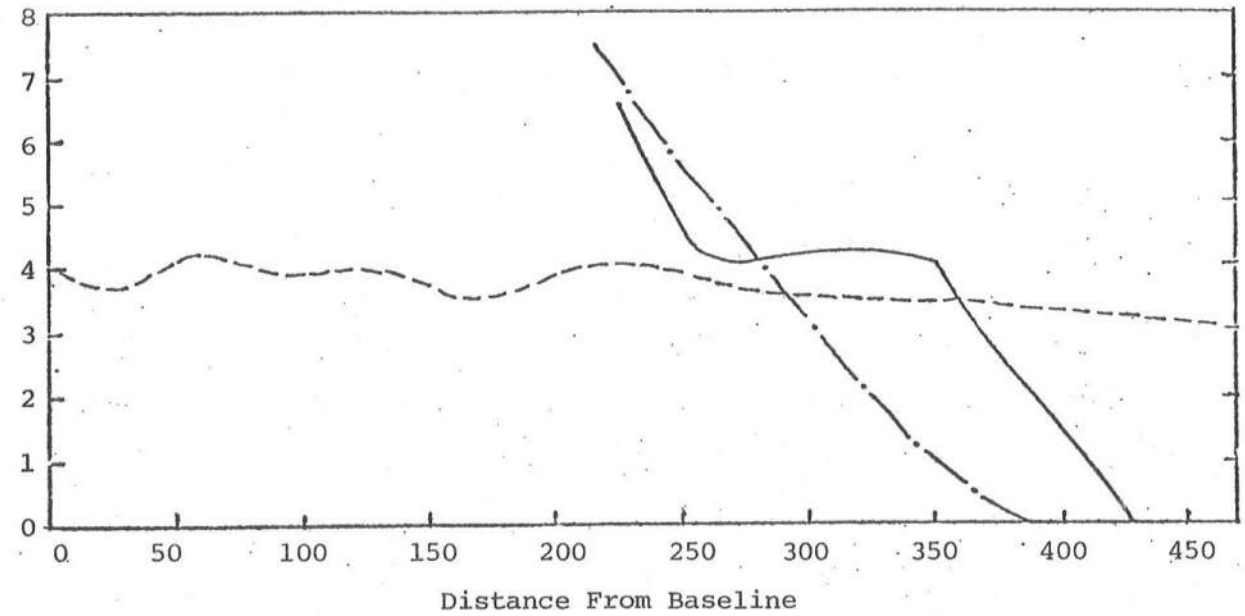

STATION 1-800

KEY

- - - - Profile of South Jetty Projected On a Line Normal to Main Beach Alignment.
__ . __ Beach Profile: September, 1976.
_____ Beach Profile: June 1, 1977.

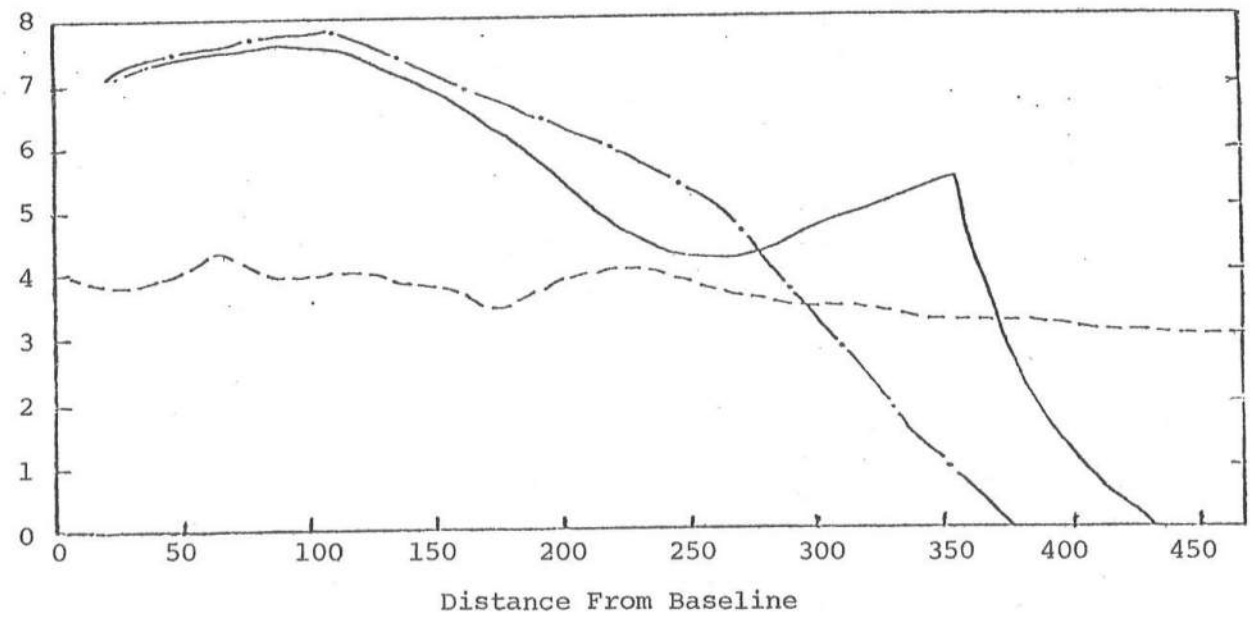

STATION 0

Figure I-4. Beach Profiles for Stations 1-800 and 0, Assateague Island.

KEY

- - - - Profile of South Jetty Projected on a Line Normal to Main Beach Alignment.
__ . __ Beach Profile: September 1, 1976.
_____ Beach Profile: June 1, 1977.

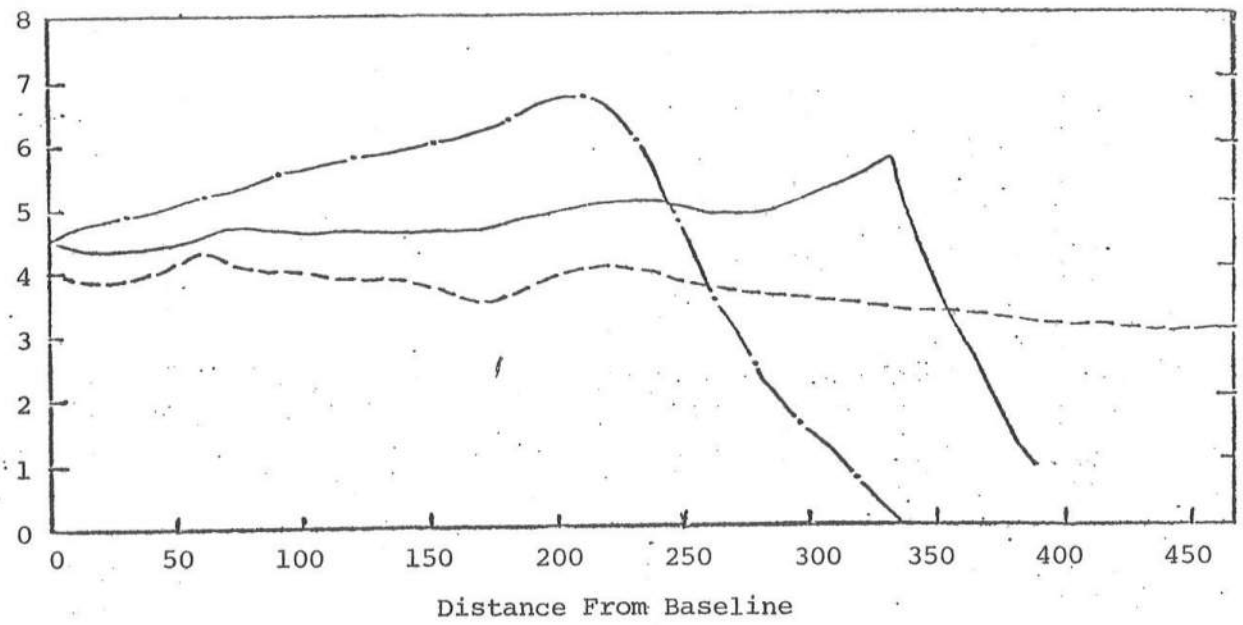

STATION 0-500

KEY

- - - - Profile of South Jetty Projected on a Line Normal to Main Beach Alignment.
__ . __ Beach Profile: September 1, 1976.
_____ Beach Profile: June 1, 1977.

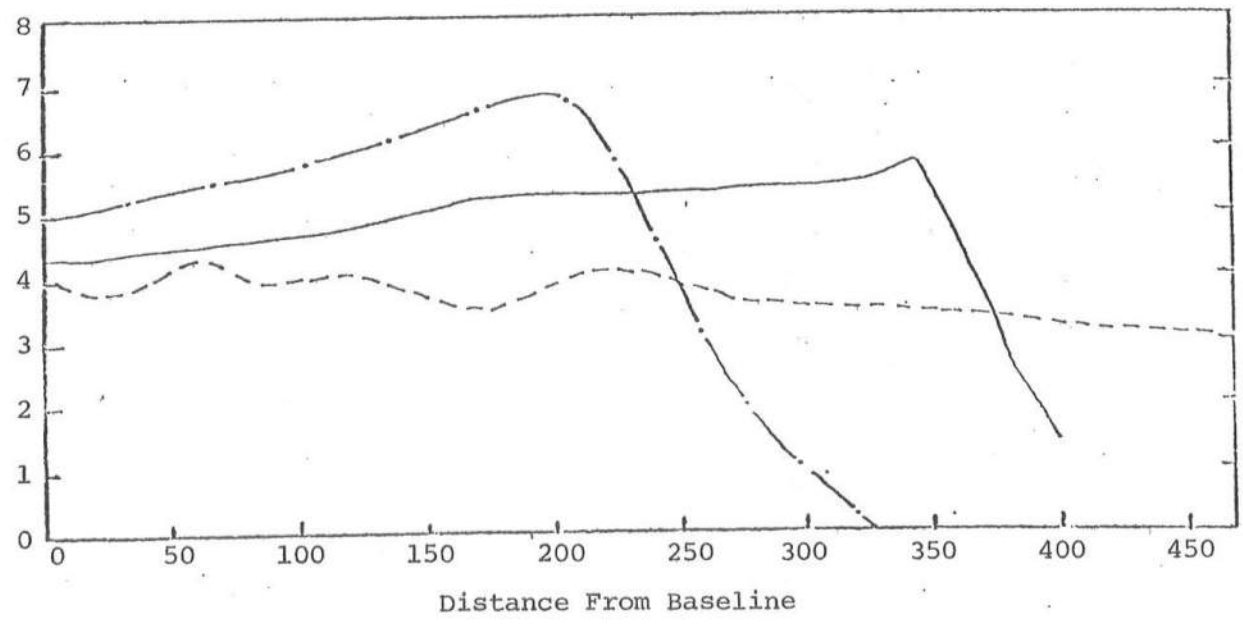

STATION 0-1000

Figure I-5. Beach Profiles for Stations 0-500 and 0-1000, Assateague Island.

KEY

- - - - Profile of South Jetty Projected on a Line Normal to Main Beach Alignment.
__ . __ Beach Profile: September 1, 1976.
_____ Beach Profile: June 1, 1977.

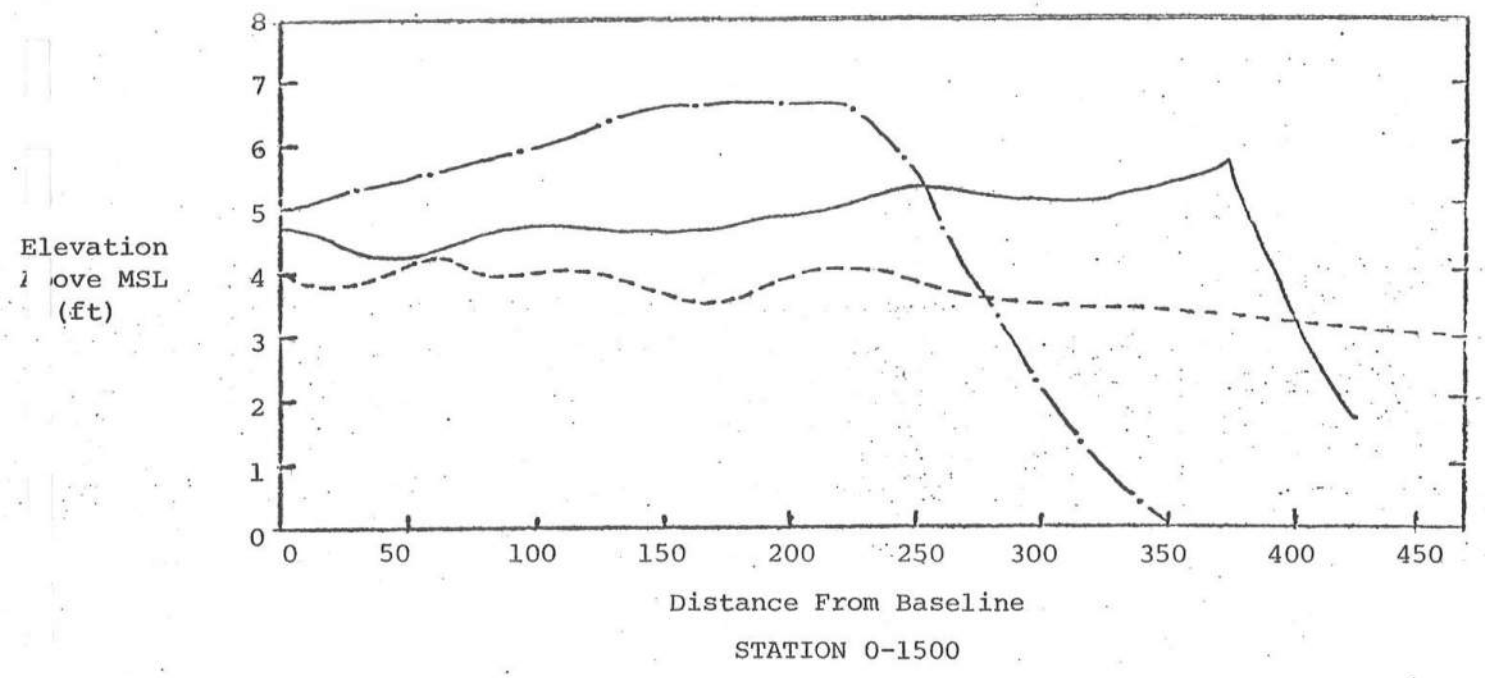

Figure I-6. Beach Profiles for Station 0-1500, Assateague Island.

APPENDIX II

NUMERICAL MODEL: DEVELOPMENT, CHARACTERISTICS AND RESULTS

APPENDIX II

NUMERICAL MODEL: DEVELOPMENT, CHARACTERISTICS AND RESULTS

Introduction

In order to obtain a complete description of the hydraulic characteristics of the inlet/bay system, a simple one-dimensional numerical model was developed, which calculates tidal elevations and discharges throughout the system. The purpose of the model is to demonstrate the overall flow characteristics of the inlet/bay system and in particular the distribution of flows through the inlet to Isle of Wight Bay to the north and Sinepuxent Bay to the south.

The following paragraphs present a description of the model, including the finite difference forms of the governing equations, the procedure used in the calibration of the model, and finally a discussion of the results of the model. The finite difference forms of the equations provide the basis for predicting the currents and tides over the entire system of interest. The model is then calibrated using the field data (currents and tides) obtained during the study. Once the calibration is complete, changes to the system could be introduced and their effects on the system approximated. Figure II-1 shows the system consisting of Isle of Wight Bay, Assawoman Bay, Sinepuxent Bay, and Ocean City Inlet, and the idealized one-dimensional representation of the various areas. The definitions of the locations of the tidal elevations, η, and conventions for discharge, Q, are presented for a typical segment in Figure II-2.

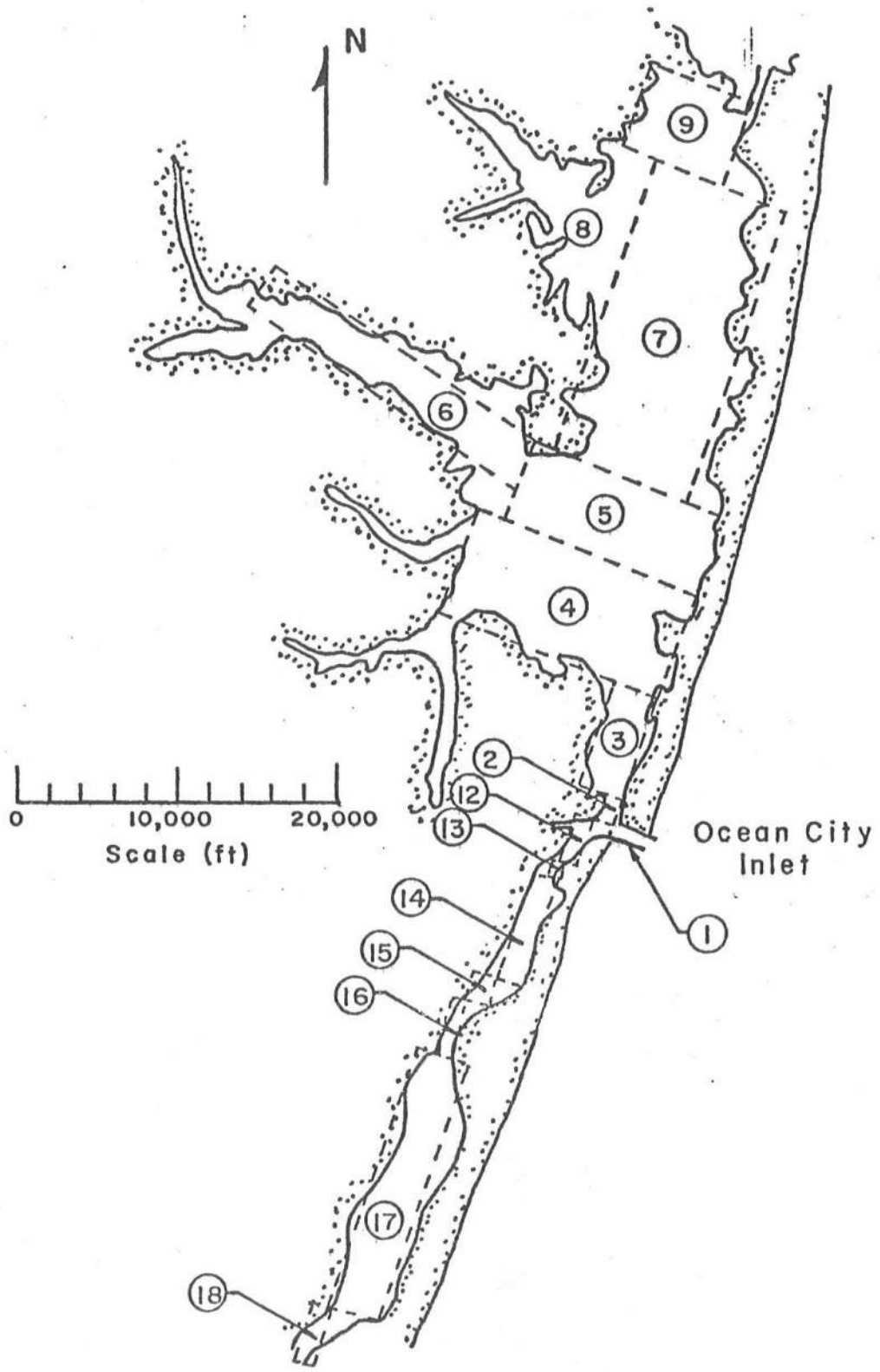

Figure II-1. Numerical Model Representation of Inlet/Bay System.

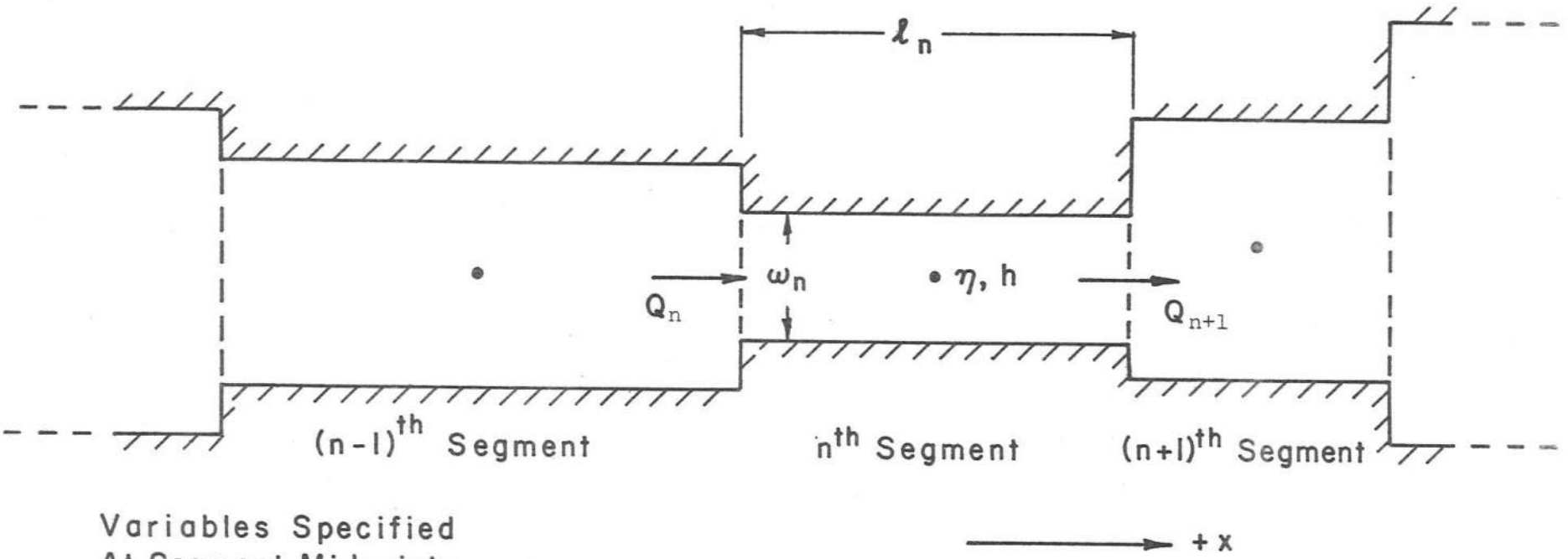

Figure II-2. Illustration of Bay Segment Representation.

Governing Differential Equations

Momentum Equation

The governing momentum equation for a one-dimensional flow can be expressed approximately as

$$\frac{\partial Q}{\partial t} + \frac{\partial (UQ)}{\partial x} = -gDw \frac{\partial \eta}{\partial x} + \frac{w}{\rho}(\tau_s - \tau_b) \qquad \text{(II-1)}$$

in which

Q = discharge in the positive flow direction (ft^3/sec)

t = time (sec)

U = average velocity (ft/sec)

x = horizontal distance coordinate aligned with the bay axis (ft)

ρ = mass density of sea water (= 1.99 $slugs/ft^3$)

g = gravitational constant (32.17 ft/sec^2)

D = total depth = $h + \eta$ (ft)

h = depth referenced to still water level (ft)

η = water surface displacement (ft)

w = width of bay (ft)

τ_s = wind stress in positive flow direction (lb/ft^2)

τ_b = bottom shear stress, positive direction opposite to positive flow direction (lb/ft^2)

The second term in Eq. (II-1) requires careful consideration in bay systems in which abrupt expansions are present. Eq. (II-1) would predict that the kinetic energy reduction is recovered as some other form of effective flow energy in such an expansion. It is well known in hydraulics that, to a good approximation, the kinetic energy reduction can be considered to be

lost to turbulent energy dissipation, hence, this will be represented in the model.

Continuity Equation

The one-dimensional depth integrated equation of continuity can be written in differential form as

$$\frac{\partial \eta}{\partial t} + \frac{1}{w}\frac{\partial Q}{\partial x} = 0 \qquad \text{(II-2)}$$

This equation ensures that the difference in inflow and outflow to a section over some time interval is accounted for by a proper change in water surface displacement, η.

Boundary and Initial Conditions

Flow Through the Inlet

The discharge through Ocean City Inlet is designated Q_1 and represents one boundary condition to the bay system. The discharge Q_1 can be represented in terms of the inlet geometry and frictional characteristics and the instantaneous tidal elevation in the ocean, η_1, and that in Segment 2, η_2, i.e.

$$Q_2 = \frac{A_1\sqrt{2g|\eta_1 - \eta_2|}}{\sqrt{K_{EN} + K_{EX} + K_B + \frac{f\ell}{4R}}} \text{ sign } (\eta_1 - \eta_2) \qquad \text{(II-3)}$$

in which A_1 represents the product of the inlet width and effective average depths in the inlet, i.e.

$$A_1 = w_1 \bar{D}_1 \tag{II-4}$$

and

$$\bar{D}_1 = [h_1 + 0.5\ (\eta_1 + \eta_2)] \tag{II-5}$$

The term "sign $(\eta_1 - \eta_2)$" simply means that the flow, Q_1, is positive if the ocean tidal elevation, η_1, is greater than η_2 and vice versa. The other terms in Equation (II-3) are:

K_{EN} = Entrance loss coefficient (taken as 0.3)

K_{EX} = Exit loss coefficient (taken as 1.0)

K_B = Bend loss coefficient (taken as 1.0)

f = Darcy Weisbach Friction Coefficient

ℓ = Effective length of inlet

R = Hydraulic radius = $A_1/(w_1 + 2\bar{D}_1)$

The model was programmed such that either a sinusoidal tide of constant tidal range could be specified or a tide with variable range could be imposed. This feature will be illustrated in a following section of this appendix.

North End of Assawoman Bay

Although there is some flow occurring into Assawoman Bay from Rehoboth Bay, this was neglected by requiring the discharge, Q_{10}, to be zero. Note that in this case, Segment 10, (see Figure II-1) is really a "dummy" segment employed for simplicity in applying this no-flow boundary condition.

South End of Model

One approach to defining a boundary condition at the south end of the model would simply have been to extend the model to Fishing Point and apply the ocean tide condition, treating this boundary as was described for Ocean City Inlet. In order to avoid a model extending the entire distance to Fishing Point, the last segment included in the numerical model was located some 6.4 miles south of Ocean City Inlet and the boundary condition was defined in accordance with the observed tidal characteristics at this location. The tide at the southern segment is η_{19} and is related to the ocean tide, η_1, as follows

$$\eta_{19}(t) = 0.160\ \eta_1(t - t_0) \qquad \text{(II-6)}$$

which means that the tide at Segment 19 is a damped and lagged version of the ocean tide. The lag, t_0, was found to be approximately 3 hours.

Initial Conditions

The most simple and direct initial condition is that all tidal response starts from a condition of no motion throughout the bay. There is a "start up" or transient time that is not representative of bay motions; however, it was found that the bay tidal ranges and lags stabilized for a constant ocean tidal range within approximately one tidal period after commencement.

Wind Stress

Although the numerical model included a capability to specify a uniform wind stress on the bay water area, this option was not exercised.

Bottom Shear Stress

The bottom shear stress, τ_b, is defined in terms of the Darcy Weisbach friction coefficient, f, as

$$\tau_b = \frac{\rho f |Q| Q}{8(wD)^2} \qquad \text{(II-7)}$$

Finite Difference Forms of the Governing Differential Equations

In describing the finite difference representations of Eqs. (II-1) and (II-2), it is helpful to refer to Figure II-2 which portrays the convention in the numerical model. The discharges are defined at the junctions of adjacent segments and Q_n represents the flow onto Segment n and is positive if flood velocities are occurring. The tidal displacement, η_n, is located at the center of the n^{th} segment. This space staggered geometric representation is well-suited for a time-staggered method of solution to be described later.

Equation of Motion

The finite-difference form of the equation of motion can be expressed approximately as

$$Q_n^{j+1} = \frac{1}{B_{3_n}}[Q_n^j - g\Delta t(\eta_n^{j+\frac{1}{2}} - \eta_{n-1}^{j+\frac{1}{2}})\bar{A}_{c_n} + \frac{\tau_{s_n}\bar{A}_{s_n}\Delta t}{\rho}] \qquad \text{(II-8)}$$

where

Δt = Time increment, $\Delta t = t_{j+1} - t_j$

Q_n^{j+1} = Discharge at the $(j+1)^{th}$ time value at the junction between the n^{th} and $(n-1)^{th}$ segments and is positive when onto the n^{th} segment.

Q_n^j = Same as above, except at the j^{th} time step.

$\eta_n^{j+\frac{1}{2}}$ = Tidal displacement at the $(j+\frac{1}{2})^{th}$ time value at the center of the n^{th} segment.

$\bar{A}_{c_n}$ = Effective cross-sectional area, defined as

$$A_{c_n} \equiv \frac{[D_n w_n \ell_n + D_{n-1} w_{n-1} \ell_{n-1}]}{\ell_n + \ell_{n-1}} \qquad \text{(II-9)}$$

$\bar{A}_{s_n}$ = Effective surface area, defined as

$$A_{s_n} \equiv \frac{w_n \ell_n + w_{n-1} \ell_{n-1}}{2} \qquad \text{(II-10)}$$

The quantity B_{3_n} is defined as

$$B_{3_n} = 1 + [K_n^j Q_n^j B_{1_n}^j + \frac{f|Q^j|}{8} B_{2_n}^j]\Delta t \qquad \text{(II-11)}$$

and

$$K_n^j = \begin{cases} 0 \text{ for an expanding cross-sectional area in the direction of flow} \\ 1 \text{ for a contracting cross-sectional area in the direction of flow} \end{cases}$$

$$B_{1_n}^{j} = \left[\frac{w_{n-1}D_{n-1} - w_n D_n}{w_{n-1}D_{n-1}w_n D_n}\right] \qquad \text{(II-12)}$$

$$B_{2_n}^{j} = \left[\frac{w_n \ell_n}{(w_n D_n)^2} + \frac{w_{n-1}\ell_{n-1}}{(w_{n-1}D_{n-1})^2}\right] \qquad \text{(II-13)}$$

Equation of Continuity

The finite-difference form of the equation of continuity is expressed as

$$\eta_n^{j+3/2} = \eta_n^{j+1/2} - \frac{\Delta t}{w_n \ell_n}[Q_n^{j+1} - Q_{n-1}^{j+1}] \qquad \text{(II-14)}$$

For the special case of "branching" flows for example from Segment 5, the appropriate equation is

$$\eta_5^{j+3/2} = \eta_5^{j+1/2} - \frac{\Delta t}{w_5 \ell_5}(Q_5^{j+1} - Q_6^{j+1} - Q_7^{j+1}) \qquad \text{(II-15)}$$

and similar equations are required for Segments 2 and 7. It is also noted that a trivial modification of the subscripts in Equation (II-14) is required when applied to Segments 7, 9, and 12 to account for the "upstream" segment number being different than implied by Equation (II-14).

Method of Solution of Finite Difference Equations

The method of solving Equations (II-8) and (II-14) is straightforward. The computations are started from a condition of zero flow and discharge throughout the bay system. The tide boundary conditions are then imposed on the system causing a flow into Segments 2 and 18 (see Equations (II-3) and (II-6)) and tidal elevations calculated throughout the bay by

Equation (II-14). Note however that for this first time step the tidal elevations will change only in Segments 2 and 18. The discharges throughout the bay system are then computed by Equation (II-8). This procedure is then repeated until the time interval of interest has been encompassed in the computations.

It may be helpful to consider the computational process as follows. The tide levels are considered fixed over the time interval t_j to t_{j+1} and the updated discharges computed by Equation (II-8). These discharges are considered to apply at t_{j+1}. The updated discharges are then considered fixed over the time interval, $t_{j+1/2}$ to $t_{j+3/2}$ and the updated tidal elevations computed by Equation (II-14). These elevations are considered to apply at $t_{j+3/2}$. This procedure is then repeated extending the computations into time. The process of calculating tidal elevations and discharges at different time levels gives rise to the "time-staggered" notation associated with this method. This procedure of calculating the tidal elevations and discharges at different time levels is also called an "explicit" scheme and has a maximum allowable time step for computational stability as

$$(\Delta t)_{max} < \frac{\ell}{\sqrt{gD}} \qquad \text{(II-16)}$$

In the present numerical model, the dimensions of the segments defined are such that the maximum allowable value of Δt is 59.5 seconds and for convenience, the time step used in the computations was taken to be 30 seconds.

Geometric Characteristics of Numerical Model

The Ocean City Inlet-Bay System of interest was approximated for computational purposes as shown in Figure II-1. The dimensions of the individual segments are presented in Table II-1. The effective dimensions of the inlet and other segments with considerable variability in depth and/or width were selected in accordance with accepted hydraulic principles.

Calibration of the Numerical Model

The bottom friction coefficient was the only characteristic of the numerical model that was adjusted to obtain approximate correspondence with the field measurements of tidal ranges and tidal lags. It was found that reasonably good agreement resulted for a friction coefficient, $f = 0.24$, which is approximately a factor of four to six higher than would be expected for channel cross-sections through which the flow velocity is uniform. The interpretation of this high friction coefficient is that for many of the segments the flow is significantly non-uniform. As an example, if the flow only occupies one half of the width of a segment, the required friction coefficient based on considerations of uniform flow across the entire width would be four times the actual value. Therefore, a two-dimensional model describing the flow distribution across each segment would probably "calibrate" with a more realistic value of the friction coefficient. The friction coefficient obtained by calibration should therefore be regarded as including an effect of representing the complex bay system by a one-dimensional representation.

TABLE II-1

GEOMETRIC CHARACTERISTICS OF NUMERICAL MODEL
REPRESENTATION OF OCEAN CITY INLET/BAY SYSTEM

Segment No. n	Width, w_n (ft)	Length, ℓ_n (ft)	Depth Relative to Mean Low Water, h'_n (ft)
1	894	2,040	14.4
2	1,300	2,800	15.2
3	4,000	9,000	4.0
4	20,000	8,270	2.9
5	12,000	5,550	3.5
6	3,960	20,000	4.5
7	9,450	19,000	3.9
8	17,800	6,260	4.5
9	6,500	5,200	3.8
12	1,250	3,000	11.9
13	750	1,110	9.1
14	2,200	7,800	1.5
15	2,000	1,830	2.0
16	825	4,000	2.9
17	3,150	17,250	2.3
18	1,380	3,660	4.2
19	8,377	9,962	2.3

Notes: 1) Segment Number 1 is Ocean City Inlet.

2) Segment Numbers 10 and 11 are "Dummy" Segments.

3) Depths Relative to Mean Sea Level, h_n, are Determined by $h_n = h'_n + 1.7$.

The comparisons of the measured and calculated tidal range and tidal lag results have been presented previously as Figures 47, 48, 49 and 50. The computational results are considered to be in adequate agreement with the measurements for the purposes of this study.

For illustration purposes Figure II-3 presents, as a sample of results from the numerical model, tidal elevations for the ocean and in Segment 7 and flows into the inlet and onto Segment 7 for ocean tides starting on August 5 and extending into August 7, 1976.

Numerical Model Results Which are Relevant to This Study

The numerical model could be used for a variety of purposes including: water quality, effects of any contemplated changes to the bay system, etc. For purposes of the present study, the primary results were the determination of the total spring tidal prism (0.81×10^9 ft^3) passing through the inlet and the relative division of flow north into Isle of Wight Bay (85%) and south into Sinepuxent Bay (15%). These results aid in inferring and interpreting the dominant water and sand flow patterns, see Section VIII of this report.

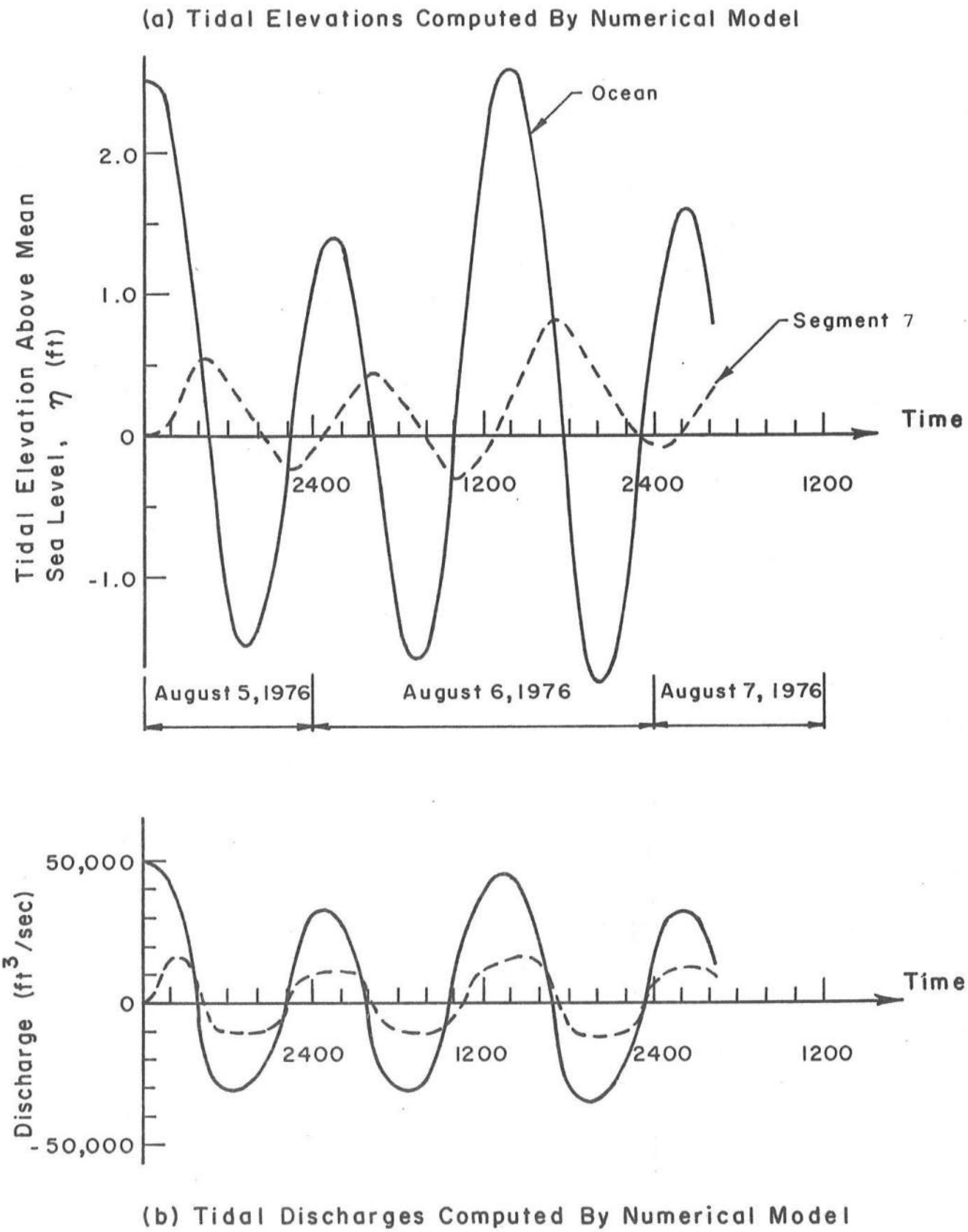

Figure II-3. Example Computations of Tidal Elevations and Discharges by Numerical Model. August 5, 6, 7, 1976.